



The Nuclear Legacy in Urbanized Areas: Generic Problems and the Moscow Case Study

Editor: Vladimir Novikov

RR-07-001
March 2007

The International Institute for Applied Systems Analysis

is an interdisciplinary, nongovernmental research institution founded in 1972 by leading scientific organizations in 12 countries. Situated near Vienna, in the center of Europe, IIASA has been producing valuable scientific research on economic, technological, and environmental issues for over three decades.

IIASA was one of the first international institutes to systematically study global issues of environment, technology, and development. IIASA's Governing Council states that the Institute's goal is: *to conduct international and interdisciplinary scientific studies to provide timely and relevant information and options, addressing critical issues of global environmental, economic, and social change, for the benefit of the public, the scientific community, and national and international institutions.* Research is organized around three central themes:

- Energy and Technology
- Environment and Natural Resources
- Population and Society

The Institute now has National Member Organizations in the following countries:

Austria

The Austrian Academy of Sciences

China

National Natural Science
Foundation of China

Czech Republic

The Academy of Sciences of the
Czech Republic

Egypt

Academy of Scientific Research and
Technology (ASRT)

Estonia

Estonian Association for
Systems Analysis

Finland

The Finnish Committee for IIASA

Germany

The Association for the Advancement
of IIASA

Hungary

The Hungarian Committee for Applied
Systems Analysis

India

Technology Information Forecasting
and Assessment Council (TIFAC)

Japan

The Japan Committee for IIASA

Netherlands

The Netherlands Organization for
Scientific Research (NWO)

Norway

The Research Council of Norway

Pakistan

The Pakistan Academy of Sciences

Poland

The Polish Academy of Sciences

Russian Federation

The Russian Academy of Sciences

Sweden

The Swedish Research Council for
Environment, Agricultural Sciences
and Spatial Planning (FORMAS)

Ukraine

The Ukrainian Academy of Sciences

United States of America

The National Academy of
Sciences

The Nuclear Legacy in Urbanized Areas: Generic Problems and the Moscow Case Study

Editor:

Vladimir Novikov

Contributors:

Rustam Churaev

Yury Gorlinsky

Vladimir Kutepov

Tamara Kuznetsova

Viktor Lagutov

Victor Malkovsky

Oleg Nikolsky

Vladimir Novikov

Frank Parker

Vitaliy Pavlenko

Alexander Pek

Nikolay Ponomarev-Stepnoy

Evgeniy Ryazantsev

Tatyana Sazikina

Vasiliy Velichkin

RR-07-001

March 2007



International Institute for Applied Systems Analysis
Laxenburg, Austria

International Standard Book Number 978-3-7045-0146-2

Research Reports, which record research conducted at IIASA, are independently reviewed before publication. Views or opinions expressed herein do not necessarily represent those of IIASA, its National Member Organizations, or other organizations supporting the work.

Copyright © 2007

International Institute for Applied Systems Analysis

ZVR-Nr: 524808900

All rights reserved. No part of this publication may be reproduced or transmitted in any form or by any means, electronic or mechanical, including photocopy, recording, or any information storage or retrieval system, without permission in writing from the copyright holder.

Printed by **Remaprint**, Vienna.

Contents

List of Figures	v
List of Tables	vii
Foreword	ix
Acknowledgments	x
Executive Summary	xi
1 Generic Problems of the Nuclear Legacy in Urbanized Areas	1
1.1 Growing urbanization and waste disposal facilities	1
1.2 Radioactive waste in urban environments as a part of the global nuclear legacy	1
1.3 Why radioactive waste in urban environments is a serious problem	3
1.4 General threat from residual radioactive waste in urbanized areas .	3
1.5 The nuclear and/or radiation threat from terrorism	4
1.6 World statistics on nuclear research reactors	5
1.7 Specific problems of decommissioning research reactors	7
2 Nuclear Facilities in the Moscow Megalopolis	9
2.1 General review	9
2.2 Research reactors in the Russian Research Center-Kurchatov Institute	15
3 The Moscow Case Study of the Nuclear Legacy	22
3.1 Study background, statement of needs, and goals	22
3.2 The nuclear legacy of RRC-KI	25
3.3 Environmental characteristics of the radioactive waste storage site	38
3.4 Human patterns near to RRC-KI	53
3.5 Run-off modeling	58
4 Conclusions and Recommendations	98

Appendix: Initial Code for the Radionuclide Redistribution	106
-------------------------------------------------------------------	------------

References	121
-------------------	------------

List of Figures

1.1	World's research reactors that are operational.	5
1.2	Power distribution of the world's research reactors.	6
1.3	Age of the world's research reactors.	6
1.4	World's research reactors that are shut down but not decommissioned.	7
2.1	RFT reactor.	15
2.2	MR reactor.	17
2.3	WWR-2 reactor.	19
2.4	Romashka reactor.	20
2.5	Yenisey space nuclear power reactor.	21
2.6	Gamma reactor.	21
3.1	Location of RRC-KI in the Schukino municipality.	23
3.2	Location of RRC-KI in Moscow.	24
3.3	Spent nuclear fuel storage at the MR reactor site.	26
3.4	Sobolevsky Creek.	28
3.5	Bird's-eye view of the RRC-KI radioactive waste storage site, winter 2003	28
3.6	Location of the storage tanks (repositories) at the radioactive waste (RW) storage site.	29
3.7	IIASA RAD project team at the RRC-KI radioactive waste storage site, winter 2002.	30
3.8	Exposure dose rate at the RRC-KI radioactive waste storage site.	33
3.9	Volumetric concentration as a function of the radius of a disk.	34
3.10	Volumetric concentration as a function of disk thickness.	34
3.11	Initial ^{137}Cs contamination of the site in kBq/m^2	36
3.12	Initial ^{90}Sr contamination of the site in kBq/m^2	36
3.13	Distribution of ^{137}Cs and ^{90}Sr against depth of sampling	38
3.14	General view of the radioactive waste storage site and its municipal surroundings.	39
3.15	Vertical cross-sections 1-1 and 1-2 around the inner concrete wall of the storage site.	40

3.16	Vertical cross-sections 3-3 and 4-4 around the inner wall of the storage site.	40
3.17	Area of the waste storage site of RRC-KI and its neighborhood. . . .	41
3.18	Relief of the RRC-KI radioactive waste storage site and adjacent area, and contours of the inner and the outer walls.	42
3.19	Isometric drawing of the digital elevation map, showing walls, buildings, and other constructions.	42
3.20	A diagrammatic geological section of the site.	48
3.21	Position of the nearest observation wells of the federal system for groundwater monitoring.	50
3.22	Variation in groundwater table in two federal monitoring wells near the site.	51
3.23	Rose diagram of wind patterns in Moscow (% of total observations).	52
3.24	Age distribution of the local population.	57
3.25	Storm-water run-off field for the waste storage site of RRC-KI and its surroundings.	61
3.26	Water run-off fields over the digital elevation map.	62
3.27	Illustration for chosen modeling scenarios.	62
3.28	Simplified flowchart of LISEM (Jetten, 2002).	66
3.29	Overland and channel flow in LISEM based on the local drain-direction structure.	68
3.30	Time-series for rainfall intensities for two scenarios.	74
3.31	The radionuclide washout path for the “No hole” scenario.	77
3.32	¹³⁷ Cs redistribution for the “No hole” scenario.	78
3.33	¹³⁷ Cs redistribution with rain intensity 100 mm/hour for scenario “K”.	78
3.34	¹³⁷ Cs redistribution with rain intensity 35 mm/hour for scenario “K”.	79
3.35	Radionuclide redistribution path for scenario “I”.	80
3.36	¹³⁷ Cs redistribution for scenario “I”.	80
3.37	¹³⁷ Cs redistribution for the “No fence” scenario.	81
3.38	⁹⁰ Sr redistribution for the “No fence” scenario.	81
3.39	Comparison of water discharges through the hole in the inner wall for scenario “I.”	82
3.40	Rills network formed when it rains in the “No hole” scenario.	83
3.41	Rills network in scenario “K.”	83
3.42	Rills network in the “No fence” scenario.	84
3.43	Rills network in scenario “I.”	84
3.44	¹³⁷ Cs redistribution within the site for scenario “100, “I,” wet 40.”	85
3.45	Flooded area near to the boundaries of the RRC-KI radioactive waste storage site during downpours that occurred from 1998 to 2000. . . .	87

List of Tables

2.1	Research reactors in Moscow and the Moscow Region.	10
2.2	Basic characteristics of RFT reactor loops.	16
2.3	General characteristics of the MR loop installations.	18
3.1	Results of experiments to determine the partition coefficients of ¹³⁷ Cs and ⁹⁰ Sr.	37
3.2	Physical properties of the soil.	43
3.3	Granulometric structure of the soil.	44
3.4a	Infiltration rate from field and laboratory studies.	45
3.4b	Infiltration rate from literature search.	45
3.5	Variations in weather conditions, atmospheric stability, and velocity of wind.	53
3.6	Distribution of the population within a 5 km radius of RRC-KI. . . .	54
3.7	Time spent outdoors by age groups.	58
3.8	Parameters used to model the radioactive waste storage site.	70
3.9	Simulation results for radioactivity washout from the RRC-KI radioactive waste storage site.	76
3.10	The redistribution of radionuclides within the site for scenario “100, “I,” wet 40.”	85
3.11	Surface activity of radionuclides in some local areas contaminated by run-off from the RRC-KI radioactive waste site.	88
3.12	External exposure received by members of the public from groundshine in some local areas contaminated after run-off from the RRC-KI radioactive waste site.	90
3.13	Exposure received by members of the public from inhalation of resuspended radionuclides at the municipal car park.	93
3.14	Exposure received by members of the public from inhalation of resuspended radionuclides at the flooded area in the street adjacent to the outer wall of RRC-KI.	94
3.15	Annual doses received by the critical local groups of inhabitants from contact with the areas contaminated by run-off from the radioactive waste site of RRC-KI.	96

Foreword

This publication signals the closure of IIASA's "Radiation Safety of the Biosphere" Program that started in 1995. The goal of the Program was to assess the world radiation legacy after the end of the Cold War. As such, it was a typical IIASA program: interdisciplinary, independent, and involving East–West collaboration.

The Program aimed to investigate the accumulation over the past 50 years of vast quantities of radioactive waste and numerous radioactively contaminated sites resulting from the production and testing of nuclear weapons, as well as from nuclear accidents, in several countries, particularly Russia and the United States.

While it was not possible for the Program to provide a complete inventory of all sites and remediation options, it did select the most significant examples. Studies of Russian sites, a comparison of these to similar sites in the United States, and ongoing studies in China helped to provide a greater perspective on the problem.

The Program carried out one of the first unclassified studies of the local problems related to radioactive contamination in areas of the former Soviet Union. This led to the publication of the book *Radiation Legacy of the Soviet Nuclear Complex*, which presented the first authoritative and detailed information available outside the former Soviet Union about the nuclear inheritance of the past half-century.

The Radiation Safety of the Biosphere Program also attracted the attention of policy makers to the problem of the nuclear legacy in urban areas. The directorate of the Kurchatov Institute in Moscow requested IIASA to start an international study to assess the radiological risk and resulting public impact from past waste management practices at the Institute.

Responding to this request, the Radiation Program performed a scoping analysis of the environmental and social impacts of the radioactive waste disposal sites on the premises of the Kurchatov Institute which, because of the growth of the city of Moscow over the last 50 years, had actually become a part of downtown Moscow. This case study, which is reported in this Research Report, is an illustration of the general problem of the nuclear legacy in urban areas.

With this report IIASA finalizes a successful program, which was not only an example of the Institute's collaborative work across the East–West political divide but also of IIASA's commitment to addressing issues of global change.

Leen Hordijk
Director

Acknowledgments

The work is a joint undertaking on the part of: members of the Radiation Safety of the Biosphere (RAD) project at the International Institute for Applied Systems Analysis (IIASA), Laxenburg, Austria; the Central European University in Budapest, Hungary; Russian specialists from the Ministry of Atomic Energy, the Russian Academy of Sciences, and the Russian Research Center, “Kurchatov Institute” (RRC-KI); and the Scientific and Production Association, “Typhoon.”

Although this research report is published by IIASA, the work was a joint effort and would not have been possible without the contribution of scientists and administrators from the above institutions.

We are grateful to the many people who contributed to the development of this research, including Academician N.N. Ponomarev-Stepnoy who, on behalf of the RRC-KI directorate, asked the IIASA RAD project to launch an international study to assess the radiological risk and resulting public impact from past waste management practices at RRC-KI, Academician E.P. Velikhov, President of RRC-KI, for help in obtaining the necessary input data, Dr. E.P. Ryazantsev, Director of the Institute of Research Reactors, RRC-KI, for his contribution at the start of the RRC-KI study, Uwe Meyer, Deputy Director of the International Science and Technology Center (ISTC), Moscow, for his constant interest in the study, Heikki Reponen, Moscow Division of the TACIS-Bistro Program, for valuable discussions on run-off modeling, and many others who quickly responded to the project’s needs.

A special acknowledgment is due to Professor Leen Hordijk, Director of IIASA, for his constant interest in the study and partial financial support, to IIASA support staff, to the IIASA Office of Sponsored Research for taking care of the administrative issues, and to Mrs. Kira Novikova for assistance and technical support in preparing this report.

Financial support for the work described herein was provided by IIASA, the TACIS-Bistro Program within contract BIS/00/021/013-N, and ISTC Financial Support for Project No. 2290.

The views and opinions of the authors expressed here do not necessarily reflect those of the sponsoring agencies or their institutions.

Executive Summary

Introduction

Since the final quarter of the twentieth century there has been a significant growth in urbanization throughout the world. It is expected that by 2015 half of the world's population will live in big cities and about 0.5 billion will inhabit megacities, each of more than 10 million people. Such megacities will include Beijing, Buenos Aires, Cairo, Calcutta, Dacca, Lagos, Mexico City, Moscow, Mumbai, New York City, Shanghai, and Tokyo.

The expanding residential areas produced by this urbanization and by the growth of megacities have resulted in waste disposal facilities now being located in densely populated urban areas. This represents a global problem in that past waste management facilities and practices are a potentially serious threat to the public now and in the future. Such waste disposal sites can be of chemical, industrial, municipal, or mixed origin. Many sites are now obsolete, and in many cases waste is stored under inadequate conditions, with potentially negative consequences for people living close to the sites.

Obviously, there is a need not only to prevent any direct impact on those living in the immediate vicinity of a waste disposal site, but also to rehabilitate and make good areas that are of value to the city.

The location of radioactive waste storage sites in what are now urban areas is an extreme example of this phenomenon. There are a number of reasons why the nuclear legacy in the urban environment has only recently come to the attention of environmental specialists and to the population as a whole. The first reason is that the urban nuclear legacy in countries with developed nuclear industries is less than 1% of the total nuclear legacy. Moreover, it was natural, after the end of the Cold War, for studies of the global nuclear legacy to focus mainly on nuclear weapons production sites, which contain the vast majority of accumulated radioactive waste. As a rule, for secrecy reasons, these sites were commissioned in scarcely populated areas and most of them remain in areas of low population. Only later was it widely recognized that, although the nuclear legacy in the urban environment was a small fraction of the total, other factors, such as urban population density and proximity to operational or obsolete nuclear facilities, increase the importance of this legacy and perhaps even give it priority in terms of social considerations.

Results

Section 1, Generic Problems of the Nuclear Legacy in Urbanized Areas, can be considered as an extended introduction to the case study of Moscow.

It describes the nuclear legacy in the urban environment that was created mainly by nuclear facilities, such as experimental nuclear reactors for research and testing and educational centers, built between the 1940s and 1970s. Most of these nuclear centers were in the vicinity of big cities and are now within the city limits. After decades of operation the research reactors of the nuclear centers have produced millions of Curies of radioactivity in spent nuclear fuel and radioactive waste. As, in many cases, the spent fuel of the research reactors was “non-standard,” it could not be reprocessed by standard reprocessing technologies and even required special storage conditions. In some cases this spent nuclear fuel, or a substantial part of it, is stored at the nuclear center itself (i.e., in the host city).

An additional input to this legacy is the radioactive waste generated during the operation of research reactors, their decommissioning, etc. The radioactive waste was often put into so-called temporary storage at the nuclear center sites. The radiation protection norms when these storage sites were created were not always as strict as those in place now. Moreover, in many cases they were not even properly implemented, either because of the nuclear arms race or just through negligence.

Nuclear facilities in the urban environment are not only a source of radioactive waste, often stored under inadequate conditions at the facility site; they also create dangerous targets as they have no protection against possible plane crashes or missile attacks. Recent terrorist attacks in Russia, Spain, the United Kingdom, and the United States highlight the risk posed by/to urban facilities that contain radioactive waste or spent nuclear fuel and that may be damaged in accidents or targeted in attacks. This topic is receiving more and more attention from the nuclear scientific community.

The report analyzes world statistics concerning nuclear research reactors. It concludes that 60% of the world’s research reactors are more than 30 years old and that many are in, or rapidly approaching, crisis conditions. It states that there is a lack of attention to decommissioning by political decision makers. This often results in passive decommissioning strategies and, in the longer term, a variety of safety concerns.

The former practice of creating nuclear centers in or near large cities can easily be traced throughout the world. The French nuclear center Sacle is about 20 km from the center of Paris, and nuclear institutions in, for example, Berlin, Budapest, Grenoble, London, San Diego, and Sofia are in a similar situation. Nevertheless, the Moscow case seems to some extent to be extraordinary because of the rush nuclear program to achieve nuclear parity with the United States that began in the city after the nuclear bombing of Hiroshima.

Section 3, on the Moscow case study of the nuclear legacy, compiles and generalizes results from the Moscow case study carried out by the International Institute for Applied Systems Analysis (IIASA) and the Central European University, with the cooperation of Russian institutions of the Federal Agency for Atomic Energy, the Russian Academy of Sciences, and the Russian Research Center-Kurchatov Institute (RRC-KI).

As a result of the intensive development of nuclear science and technology in the former Soviet Union (FSU), Moscow and the Moscow Region have inherited several nuclear centers and institutions that possess nuclear installations, such as research reactors, radiochemical laboratories, and thousands of radiation sources, as well as—almost inevitably—sites for the temporary storage of spent fuel and/or radioactive waste.

Analysis of the statistics for nuclear facilities in Moscow and the Moscow Region shows that priority should be given to the nuclear legacy of RRC-KI because of the amount of radioactivity accumulated at the site and its proximity to the densely populated areas of downtown Moscow.

RRC-KI is the largest and oldest nuclear center in this megacity. Currently, it possesses more than nine research reactors (some of which are still in operation), 17 critical assemblies, a hot laboratory for materials testing, spent fuel storage sites, and, in particular, temporary radioactive waste storage sites, with the inevitable soil and groundwater contamination around them.

The RRC-KI directorate asked the IIASA Radiation Safety of the Biosphere (RAD) project to launch an international study to assess the radiological risk and resulting public impact from past waste management practices at RRC-KI. In response, IIASA asked the Technical Assistance for the Commonwealth of Independent States (TACIS) program of the European Commission to subsidize an IIASA study to evaluate information on the history of disposal at RRC-KI and to perform a scoping analyses of the environmental and social impacts of the radioactive waste disposal sites there (which have actually become part of downtown Moscow because of Moscow's growth in the past 50 years). In parallel, IIASA applied to the International Science and Technology Center (ISTC) in Moscow to subsidize the gathering of information needed to assess the actual and potential implications of that nuclear legacy.

In 2003 the project received a TACIS-Bistro grant to perform a study entitled "Impacts of Radioactive Waste Storage at the Territory of the RRC-Kurchatov Institute in Moscow," with a major focus on the evaluation of radioactivity migration from the storage site of RRC-KI via run-off water.

In parallel with the IIASA activity, in 2002 RRC-KI made the first practical steps toward rehabilitating contaminated objects within its grounds (the so-called Rehabilitation Project). Some of the results of this project were presented at the International Symposium on Radwaste Management '03.

Then, in 2004 IIASA proposed an International Workshop “Solutions to Security Concerns about the Radioactive Legacy of the Cold War that Remains in Urban Environments.” The workshop was held at the Vanderbilt University (Tennessee, United States), on 14–17 November 2004, and *inter alia* critically discussed the results of these Moscow studies.

Section 3, on the Moscow case study of the nuclear legacy, describes the materials collected within the studies listed above and summarizes the findings. Data on the nuclear facilities of RRC-KI responsible for the nuclear legacy have been collected. They show that spent nuclear fuel storage units now contain over 1,300 spent fuel assemblies of various designs, with a total radioactivity of about 2 MCi.

The spent fuel differs in terms of its chemical composition, its degree of uranium enrichment, and the protective cladding used. Moreover, being in many cases “non-standard,” it could not be reprocessed by standard reprocessing technology and even requires special storage conditions. Non-standard spent nuclear fuel constitutes 60% of the total amount, of which 10% is damaged to varying extents. The time required to transport the spent nuclear fuel of RRC-KI to the Urals or the Krasnoyarsk Mining and Chemical Combine in Siberia is estimated to be not less than seven years. This estimate relies on technical, financial, and political (decision-making) conditions all being favorable, which is highly questionable at the moment.

Another important component of the RRC-KI nuclear legacy is radioactive waste in temporary storage places. Most of this was stored in the 1950 and 1960s without due attention being given to the environmental consequences. The result is contamination of both the surface layer of the site and the groundwater under the site.

Living close to such “neighbors” inevitably gives Moscow’s inhabitants and visitors cause for concern about the environmental security of their living conditions. Indeed,

- The closest residential building area is only about 100 m from the RRC-KI radioactive waste storage site.
- The area between the inner concrete wall of the storage site and an adjacent section of the outer brick wall of RRC-KI is actually occupied by municipal car parking. Though access to it is limited to people parking their cars, public access is not really restricted.
- The municipal road along the outer wall of RRC-KI passes at a distance of several meters from the wall. In the rush hour up to 3,000 vehicles per hour use this road.

This report summarizes the results of the collection, analysis, and collation of currently available data regarding the radioactive source term at the radioactive waste

disposal area within the main boundaries of the Kurchatov Institute. It also gives the environmental characteristics and human patterns necessary to model radionuclide migration within and out of the site.

The basic information regarding surface contamination at the storage site used in the study is a gamma radiation survey of the site surface made in 10 m steps at a distance of 1–1.5 m from the surface. This provides a field of exposure dose rate that typically varies from 30 $\mu\text{R/h}$ to 3000 $\mu\text{R/h}$ and that in some places is even higher than 3000 $\mu\text{R/h}$.

The maps of surface contamination with ^{137}Cs and ^{90}Sr were created by a recalculation of the exposure dose rate. The procedure is based on 1) the measurement of ^{137}Cs concentration in samples taken from nine points at the site and 2) an average ratio of ^{137}Cs and ^{90}Sr concentrations measured in seven samples taken from different parts of the site. Although these statistics are not sufficient for a site with very heterogeneous contamination, they will serve as a first approximation.

Another uncertain parameter is the hydraulic conductivity of the soil. The range of values now available for this parameter is extremely wide. We emphasize that these data are based on different methodologies: laboratory sample testing, field study of water pumping from observation wells, rate of restoration of created depression zone, etc. No comparative analysis of these results was possible because of the limited information regarding measurement details. After careful discussion of this uncertainty, it was recommended that we use an expert judgment, namely, that the “urbanosem” soil type is, on average, similar to the soil at the site that is covered in grass.

In general, analysis of the data collected on the environmental and radiological characteristics of the site conclusively shows that these are far from being comprehensive. In these circumstances, run-off modeling was done to give a scoping analysis rather than a site-specific analysis. The scoping analysis focused on an evaluation of the scale of and possible limits to the redistribution and washout phenomena; it was done to provide an initial insight into the seriousness of the situation with regard to run-off transfer and to provide recommendations for further experimental studies needed to reduce the uncertainties. Consequently, the study, while hopefully scientifically rigorous, was based more upon consequence analysis and general principles than on very rigorous site-specific features.

The choice of run-off scenarios examined within the study was made on the basis of the analysis of three major factors with an impact on the outcome of the modeling, namely:

- Precipitation rate.
- Soil properties within the site.
- How good a mechanical barrier the inner wall of the site provides against run-off transfer to outside the radioactive waste storage site.

Variations of these factors and their combination are shown using 16 different scenarios. These considerations for the run-off scenarios were applied to simulate the run-off erosion. The Limburg Soil Erosion Model (LISEM), a physically based hydrologic and soil erosion model developed at Utrecht University (Netherlands) within the framework of the European Union (EU) Spartacus Project, was applied with small modifications to account for the peculiarities of the RRC-KI waste storage site.

There are different approaches to evaluating the risk of radioactivity transfer to outside the allotment area, for instance, a comparison with the acceptable annual dose limit currently fixed by the official legislative and/or normative documents, an estimate of the extra lifetime risk caused by exposure, etc. As indicated above, run-off modeling was done to provide a scoping analysis. We thus decided that it was not reasonable to discuss the various aspects of the criteria used in each case or whether the dose limit was likely to change in future, but chose instead the simplest approach: a comparison with the current official dose rate limit. The data presented in this report on radionuclide contamination allow specialists to recalculate the risk in other terms, if they wish.

Uncertainty about the dose calculation is predominantly caused by uncertainties in the run-off erosion calculation. The run-off model (LISEM) used in the study is a physically based simulation model. Of course, it does apply some empirical relationships to describing the physical processes that underlie the model. All the papers we referred to conclude that the LISEM discharge estimate agrees with that observed to within 15% and that the uncertainty in the input parameters is of greater importance in assessing the final results. That is why we give the results of modeling 16 different scenarios that include variations of the major parameters within their uncertainty limits, evaluated by expert judgment. Actually, these 16 scenarios constitute a kind of sensitivity analysis and must produce a feeling for the range of variations in output data. Therefore, the maximum calculated dose should be considered as an upper limit obtained within the scoping analysis. In other words, it demonstrates that the approach is intentionally skewed toward overstating exposure and dose.

Despite all the limitations that have been introduced into the modeling, the results definitely indicate that the potential implications of the run-off transfer of radioactivity from the RRC-KI waste storage site cannot be ignored for the following reasons:

- Given the current condition of the inner wall around the storage site, which acts as a physical barrier to the path of the run-off water, and given the lack of any specific drainage system at the site, the site topography does not prevent run-off washout from the site.

- Run-off modeling showed that under unfavorable meteorologic conditions (periods of lengthy drizzle followed by a downpour of the maximum intensity observed in Moscow), the run-off water could transfer contaminated soil particles outside the perimeter of the storage site and further down to the municipal car park located between the inner wall of the storage site and the adjacent section of the outer wall of RRC-KI. This results in surface contamination of dozens of kBq/m².
- Such radioactivity in the washout will not significantly increase the dose uptake by critical groups of the population. However, even for the most conservative scenario (up to 20% of the established dose limit), the increase in radiation background outside the RRC-KI boundaries may cause public anxiety, especially if washed-out radioactivity reaches the city street.
- Last, but not least, is the potential redistribution of soil contaminants within the area of the storage site (about 100 m² could have contamination twice that before the run-off event). This should be taken into account when planning the site rehabilitation program.

Conclusion

As the radiation background in areas adjacent to the RRC-KI radioactive waste storage site can be noticeably increased by the run-off events, the first conclusion is obvious: these local areas need to be under systematic dosimetric control.

Next, to reduce the uncertainty caused by incomplete source terms and environmental characteristics, further experimental study to enable site-specific modeling is advisable.

As for specific recommendations to reduce the potential run-off washout, the following points should be considered:

- First of all, the RRC-KI radioactive waste storage site should have a special drainage system, designed to intercept and control run-off waters at the site.
- Repair work to the inner wall around the RRC-KI radioactive waste storage site, if deemed necessary, should be carried out during the winter months.
- A number of potential mechanical methods to reduce the run-off transfer to outside the storage site should be carefully evaluated and the optimum method or methods to achieve this should be chosen. As an example we list the obvious ones below:
 - Compaction of the soil to reduce the erosion rate could be considered. There are a number of technical ways of accomplishing this.

- Chemical stabilization, in which chemicals like cement and polymers retain the soil particles in place, could be considered.
- The need to use international experience to solve technological problems caused by radioactive contamination is evident.

To cope with the social aspects of the problem, we recommend as a priority the setting up of “round table” meetings to improve the exchange of views between social groups living near RRC-KI and the RRC-KI administration. We also recommend that these meetings should include: 1) communication with international experts; 2) provision of up-to-date information about the situation; and 3) information on how other countries have coped with contamination caused by nuclear activities in the urban environment. Such comparisons could help to identify the common and different aspects of coping with the radiation legacy in big cities and to work out recommendations for further improvements.

Another recommendation is to evaluate the role of the gradual accumulation of radionuclides through repeated wash-off events over a long period of time. This point could be of specific importance in planning a remediation program, as it is virtually impossible and even less reasonable to remediate to a “zero” level of contamination. Thus, an acceptable level of residual contamination that should provide no “substantial” release from the site for a long period of time (say, hundreds of years) should be examined and defined. We therefore recommend that run-off studies be extended to evaluate the cumulative, long-term consequences of run-off transfer from a site with residual contamination.

The current study focused on run-off from natural events, but below the storage site is a complicated network of different pipelines, including a municipal rainwater pipe that carries rainwater accumulated from an area of about 400 ha (4×10^6 m²) to the Moscow River. This is why, in addition to the modeling performed, the effects of possible infrastructural accidents (e.g., heavy run-off resulting from a failure of the rainwater pipe and consequent dispersal of water on the site) are worthy of special study.

Besides natural run-off events, there are several pathways for radionuclide migration from the radioactive waste storage site to the city, namely, migration with groundwaters, direct resuspension of dust from the site, and air transfer by strong winds. The contribution of these processes to the exposure of critical groups of city people should be a subject of further analysis. Such a study is of particular importance as remediation measures at the site have already started, including excavation of the contaminated soil and its separation into fractions of different contamination levels. Such operations create the pressure to implement this further study without delay.

Other contaminated areas in RRC-KI not indicated by the Russian partner of this study, for example, the enclave located on the bank of the Moscow River, also deserve attention and analysis.

The report concludes that countries with similar problems of a nuclear legacy in the urban environment could benefit from sharing their experience and cooperating in this field.

1

Generic Problems of the Nuclear Legacy in Urbanized Areas

1.1 Growing urbanization and waste disposal facilities

In the last quarter of the twentieth century there was a significant growth in urbanization throughout the world. It is expected that by 2015 half of the world's population will live in big cities and about 0.5 billion in megacities, each with more than 10 million people. Such megacities will include Beijing, Buenos Aires, Cairo, Calcutta, Dacca, Lagos, Mexico City, Moscow, Mumbai, New York City, Shanghai, and Tokyo.

The growth that has taken place in Dacca is an extreme example of the development of a megacity. In 1950 its population was 0.4 million; in 2000 it was 12.5 million; by 2015 it is expected to be 17.3 million.

As a result of these expanding residential areas produced by urbanization and the growth of megacities, some facilities built years ago for the disposal of chemical, industrial, municipal, or mixed waste are now in densely populated urban areas. This represents a global problem in that past waste management practices could seriously affect current and future public health. Many of the sites are now obsolete, and in many cases waste is stored under inadequate conditions, with potentially negative consequences for those living close to the sites.

Obviously, there is a need not only to prevent any direct impact on people living in the direct vicinity of the waste disposal site but also to rehabilitate valuable land needed by the city.

The location of radioactive waste storage sites in what are now urban areas is an extreme example of this phenomenon.

1.2 Radioactive waste in urban environments as a part of the global nuclear legacy

The problem of radioactive waste storage has its genesis in the global nuclear legacy of the past 50 years and was created by the global nuclear industry. Until now,

assessments of the global nuclear legacy focused mainly on nuclear weapons production sites, as they contain the vast majority of accumulated radioactive waste. As a rule, these sites were commissioned in scarcely populated areas for secrecy reasons, and most remain in areas of low population.

This part of the world's nuclear legacy was the subject of a rather detailed examination after the end of the Cold War. Summaries of these studies are presented in US Department of Energy (1997) for US legacies, Egorov *et al.* (2000) for those in the former Soviet Union (FSU), and in Pan Ziqiang *et al.* (1996) for those in China.

The nuclear legacy in urban environments and densely populated areas results mainly from nuclear research, testing, and educational centers created between the 1940s and 1970s in the vicinity of big cities. The centers provided a scientific and technological base for the development of nuclear power and the nuclear industry. For countries in the nuclear club, these centers mainly worked to develop a nuclear weapons program. They have (or had) nuclear research reactors, which were the main engines driving the development of nuclear power, basic nuclear science, materials development, radioisotope production for medicine and industry, and the education and training of scientists and engineers.

Initially located in the suburbs of cities, they became a part of downtown areas as a result of growing urbanization. After decades of operation the research reactors of the nuclear centers produced millions of Curies of radioactivity in spent nuclear fuel and radioactive waste. Being, in many cases, "non-standard," the spent fuel of the research reactors could not be reprocessed by standard reprocessing technologies and even required special storage conditions. As a result, the spent nuclear fuel from research reactors was often stored at the nuclear center site (e.g., in the host city). Naturally, some research reactors used to test new types of fuel, coolant, and other reactor innovations had operational problems which frequently produced high-level radioactive waste containing fission products and also resulted in radioactivity being deposited on construction materials. At the beginning of the nuclear era (say, the 1950s and 1960s), these radioactive wastes were often kept at the nuclear center sites, in so-called temporary radioactive waste storage. Needless to say, the radiation protection norms at that time were not as strict as those in place now and, in many cases, were not even properly implemented, either because of the rush to win the nuclear arms race or just negligence.

This legacy has only recently come to the attention of environmental specialists and the population in general.

1.3 Why radioactive waste in urban environments is a serious problem

The radioactive waste generated by research reactors is only a small fraction of the total amount of radioactive waste generated by the nuclear industry. This is true at least in the countries of the nuclear club. For instance, in Russia this fraction is about 1% (Egorov *et al.*, 2000). This is perhaps why the nuclear legacy of research reactors in the urban environment has not as yet received the attention it deserves.

However, even a preliminary look at the problem indicates the possibly serious impact of radioactive waste storage in an urban environment because of the proximity—in some cases, about 100 m—of nearby residential areas (Novikov *et al.*, 2003).

Indeed, the collective radiation dose caused by a hypothetical accident with a radioactive source term is proportional to the product of the quantity of the source term and the population density of the area over which the radioactivity spreads. Thus, in an urban environment with a population density of about 10^2 that of a rural area, a source term that is only 1% that of the rural area will have the same impact. The figures are even more impressive for individual radiation doses.

The distance from the radioactive source term in urban areas might be hundreds of meters, while the distance of a safe protective zone around plutonium production sites or spent nuclear fuel reprocessing facilities (where the majority of radioactive waste has been accumulated) is several kilometers. In the historical example of the Kystim accident in the Urals in 1957, when a tank with liquid radioactive waste exploded, 90% of all the radioactivity released fell in the vicinity of the tank, while only the remaining 10% formed a radioactive cloud that was responsible for long-distance transfer (see, for instance, IIASA, 1996).

In countries that have no developed nuclear industry, but have nuclear research centers with research reactors, the nuclear legacy associated with the research reactors is dominant.

In addition to this legacy, many radioactive sources from state and private industrial facilities that produce or use radioisotopes are in an urban environment where many orphan radioactive sources and contaminated spots have occurred. The location of these sources is frequently unknown.

1.4 General threat from residual radioactive waste in urbanized areas

In the same way that current nuclear use can cause the accidental release of radioactivity and result in environmental contamination, so residual radioactive waste

in urbanized areas poses a potential threat to the nearby population and environment. The pathways are actually the same (e.g., air transfer of radioactivity after atmospheric release, resuspension from contaminated soils into the atmosphere and further deposition, run-off from contaminated areas, and surface water and groundwater contamination). Natural events (for example, earthquakes, tornado, flooding) could also initiate an accidental release, as could the degradation of engineering barriers that protect the environment from contact with residual radioactive waste.

A specific threat may emerge because of orphan radioactive sources and contaminated spots in the urban environment. If laypeople occasionally obtain such sources and misuse them, as happened in the 1990s in Brazil, the consequences can be serious.

1.5 The nuclear and/or radiation threat from terrorism

Nuclear facilities in urban environments not only represent a source of radioactive waste which is often stored under inadequate conditions at the facility site; they are also potentially dangerous targets as they have no protection against plane crashes or missile attacks. Recent terrorist attacks in Russia, Spain, the United Kingdom, and United States highlight the risk of urban facilities containing radioactive waste or spent nuclear fuel being targeted in attacks. This topic has already come to the attention of the nuclear scientific community. Currently, the following specific four aspects of such terrorism are considered in the open literature (see, for instance, Ferguson *et al.*, 2003).

- Theft and subsequent detonation of an intact nuclear device;
- Theft of fissile material and detonation of an improvised nuclear device;
- Sabotage of nuclear facility;
- Theft of nuclear material or waste and its use in a radiological dispersal device.

The nuclear legacy in the urban environment may be most “useful” as a source for the last two aspects. International terrorists can bring radiological dispersal devices into different countries by multiple routes and methods; and, of course, an insider could attempt to acquire nuclear materials to use in radiological dispersal devices or sabotage a nuclear facility in the urban environment. For instance, research reactors in universities and other civilian institutions might be targeted. The readiness of terrorists to give up their lives in order to conduct terrorist acts must change our approaches to countermeasures.

As for the second aspect listed above (theft of fissile material), it was realized only recently that research reactors using highly enriched uranium are of special concern in the light of terrorist activity and non-proliferation efforts. Many have

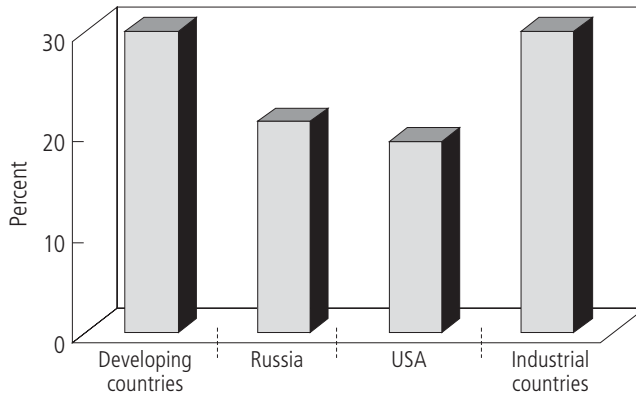


Figure 1.1. World’s research reactors that are operational.

appealed for a high priority to be placed on the full decommissioning of such facilities or at least that they be converted into reactors that use low-enriched uranium as fuel. In some cases there is a noticeable reluctance to follow this path. For instance, if such reactors are used within a research program to develop fast-breeder reactors, decommissioning might threaten the program, even if the reactors with highly enriched uranium are converted to low-enriched-uranium mode.

In November 2004 the International Institute for Applied Systems Analysis (IIASA), the International Science and Technology Center (ISTC), and Vanderbilt University conducted the workshop “Urban Radiological Security” (Kosson *et al.*, 2004). The workshop emphasized, inter alia, the need for an internationally coherent and comprehensive analysis of this phenomenon.

1.6 World statistics on nuclear research reactors

The total number of nuclear research reactors commissioned throughout the world during the second half of the twentieth century is about 650 (IAEA Database, 2004). Of this number, half are still operational in 58 countries. Russia and the United States have about 20% each, 30% are in industrial countries, and the remaining 30% are in the developing world (see *Figure 1.1*).

As can be seen in *Figure 1.2*, one-third of operational research reactors have more than 1 MW of power, and 4% have power comparable, for instance, with that of a nuclear submarine.

Figure 1.3 illustrates the age distribution of the research reactors in operation. It can be seen that 60% are more than 30 years old, of which one-third are 40–50 years old. Such statistics certainly give cause for safety concerns.

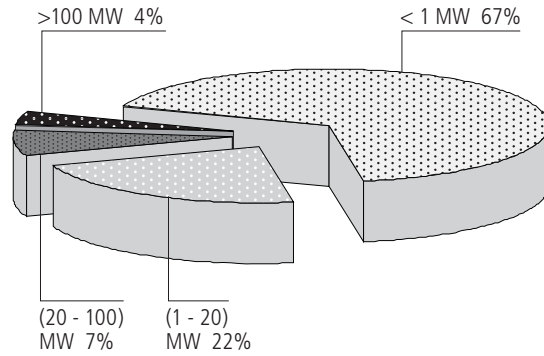


Figure 1.2. Power distribution of the world's research reactors.

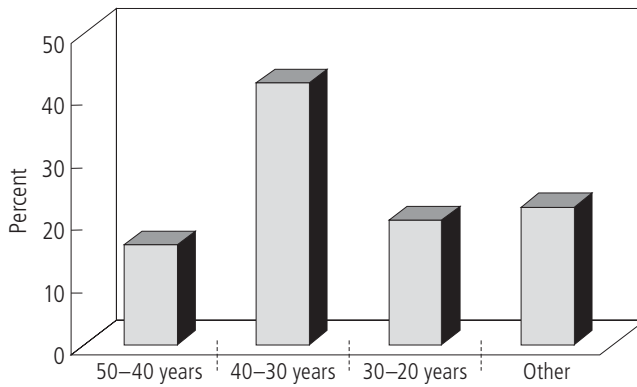


Figure 1.3. Age of the world's research reactors.

In recent years the original mission of some nuclear facilities has been accomplished or has become obsolete. Tight budgets and changing priorities have caused some governments to cut back on baseline support. Moreover, the stagnation or even decline of nuclear power use in many industrialized countries has reduced the demand for nuclear education and training. Furthermore, worldwide computerization has opened the door to the wide application of simulators for some of the training of nuclear power plant operators that was previously provided by research reactors. Thus, the large number of research reactors currently in operation clearly exceeds the worldwide demand for nuclear science research, reactor services, and training. Old research reactors will therefore continue to be shut down in increased numbers. As for those research reactors that it is planned to continue operating, a strategy must be worked out for their long-term sustainability, in terms of both finding customers for their services and providing an acceptable level of safety.

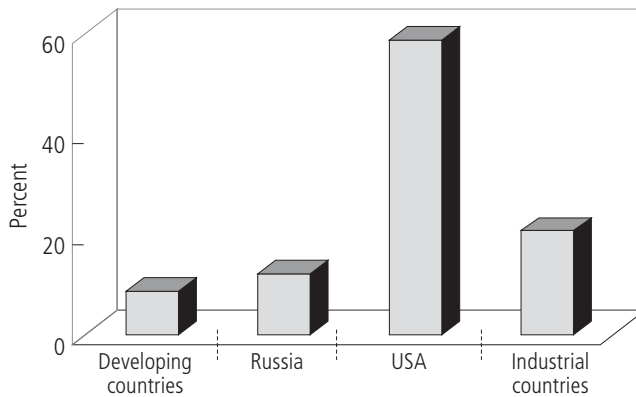


Figure 1.4. World's research reactors that are shut down but not decommissioned.

More of these shut-down reactors have to be decommissioned. As *Figure 1.4* shows, there are greater delays in decommissioning shut-down reactors than in the shutdown process itself. The reason seems, in some cases, to be the lack of required infrastructure, as little attention was given in early planning to the decommissioning of research reactors.

1.7 Specific problems of decommissioning research reactors

Unlike nuclear power plant reactors, research reactors come in a large variety of designs. The main difference is that the fuel elements of research reactors were specially designed and manufactured to explore the different conceptual approaches that emerged during the first decades of the nuclear era. Some research reactors were even designed to include such exotic fuels as liquid nuclear fuel—for instance, water solution, micro-particle suspension, or molten salt (Novikov *et al.*, 1990), or gas fuel in the form of UF_6 (Kikoin *et al.*, 1958). As for solid fuel elements, these differ in terms of their chemical compounds, the degree of uranium enrichment, their cladding material, geometry, etc. The fuel elements of nuclear power plants, unlike those of research reactors, were manufactured for only a number of selected approaches.

The variety of designs for research reactors poses special challenges for decommissioning that require specific techniques and infrastructure. Furthermore, research reactors present particular difficulties at the back end of the fuel cycle. These include the need for the special management of experimental and exotic fuel elements with no reprocessing routes, fuel elements that failed during irradiation in reactors, and fuel assemblies that subsequently corroded in wet storage. In some of

the worst cases, fuel assemblies completely disintegrated during experiments and the circulating coolant spread fission products to the corresponding loops with deposition on the inner surface of the confinement. This produced radioactive waste that was frequently stored either at the site of the research reactor or at a special storage site within the research center.

Nuclear Facilities in the Moscow Megalopolis

This section summarizes data on the nuclear facilities in Moscow and the Moscow Region and illustrates how many and what kind of nuclear facilities there are. Such facilities created the nuclear legacy in the Moscow megalopolis and in some cases are also part of this legacy. More specific attention is given to research reactors in the Russian Research Center-Kurchatov Institute (RRC-KI), the biggest nuclear enterprise in the area.

2.1 General review

The nuclear research centers of the FSU are used for studies in the fields of nuclear physics, solid state physics, radiation materials science, radioisotope production, and other tasks. Most were constructed in the 1940s and 1950s, and the main facilities became operational in the late 1960s. As a rule, these centers were complex systems; that is, they involved not only the research reactors, but also “hot” cells for materials tests, research laboratories, radwaste handling facilities, etc. The research reactors installed in the nuclear centers are very diverse in their design, power level, materials used, and operation mode. Brief characteristics of the research reactors are given in *Table 2.1* (Egorov *et al.*, 2000).

In addition to research reactors as generators of radioactive waste, thousands of orphan radioactive sources and contaminated spots, originating from state industrial facilities that produced or used radioisotopes, occur in the Moscow urban environment. The location of these sources is frequently unknown. For instance, the Chief of the Moscow Division of the Ministry of Emergency Situations reported at the Vanderbilt workshop (Kosson *et al.*, 2004) that 1,500 previously unknown contaminated spots have been discovered in Moscow and that the rate of “discovery” (currently, about 90 spots per year) is proportional to the efforts to find them (i.e., discovery is far from complete).

Table 2.1a. Research reactors in Moscow and the Moscow Region.

Location, Owner, Department	Reactor type	Fuel type (enrichment, composition, form)	Date of reaching criticality and shut- down	Power (MW)		Application
				Design	After recon- struction	
Russian Research Center- Kurchatov Institute ^a	F-1 (uranium-graphite)	Natural uranium (metal, UO ₂ and U ₂ O ₈) Uranium of 2% enrichment	1946	0.024		Calibration of neutron detectors, testing of new ionization chambers (ICs), Investigation of IC characteristics, Certification of neutron detectors
	VVR-2 (tank type, water-water)	Uranium of 2% enrich- ment, UO ₂ + Al Uranium of 36% enrich- ment, UAl alloy 10 mm diameter rods	1954 (1983)	0.3	3	Nuclear physics investigations
	RTF (channel-type graphite moderator)	Uranium of 10–90% enrichment U + Mg, UO ₂ + Mg, UO ₂ + Al, tubes	1952 (1962)	10	20	Tests of reactor materials, fuel rods, and fuel assemblies for power and research reactors Nuclear physics investigations
	IRT (pool-type)	Uranium of 10–90% enrichment UO ₂ + Al, UAl alloy, pipes	1957 (1979)	2	8	Nuclear physics Physics of solid-state studies Neutron-activation analysis Isotope production
	IIN-3M Gidra (homogeneous water solution)	Uranium of 90% enrichment Water solution of UO ₂ SO ₄	1972	0.01	–	Nuclear physics investigations Neutron activation analysis Fuel rod testing under non-stationary conditions

impulse

Table 2.1b. Research reactors in Moscow and the Moscow Region (continued).

Location, Owner, Department	Reactor type	Fuel type (enrichment, composition, form)	Date of reaching criticality and shut- down	Power (MW)		Application
				Design	After recon- struction	
Russian Research Center-	Argus (homogeneous water solution)	Uranium of 90% enrich- richment (water solution of UO_2SO_4)	1981	0.02	–	Neutron radiography Neutron activation analysis
Kurchatov Institute (cont'd)	OR (tank-type, water–water)	Uranium of 10% enrich- ment ($UO_2 + Al$) Uranium of 36% enrich- ment (UAl alloy)	1989	0.3	–	Production of isotopes and nuclear filters Investigations and tests of neutron and gamma radiation shields Testing of radiation stability of equipment for nuclear installations
	Romashka (homogeneous)	Uranium of 90% enrich- ment (UC_2)	1964 (1966)	0.04	–	Investigation of nuclear power units for direct energy conversion
	Topaz-2 (channel-type, $U-Zr$ hydride)	Uranium of 90% enrich- ment (UO_2)	1973 (1986)	0.1	–	Investigation of space nuclear power units
	SF-1 Critical test facility (uranium–water)	–	1972	100 W	–	Investigation of neutron physics of water–water reactor core
	SF-3 Critical test facility (uranium–water)	Uranium of 90% enrich- ment (UZr alloy) Uranium of 21% enrich- ment (UO_2)	1979	100 W	–	Investigation of neutron physics of water–water reactor core
	SF-5 Critical test facility ($U-Zr$ hydride)	Uranium of 25% and 36% enrichment (inter- metallic composition)	1990	100 W	–	Studies of reactor physics of uranium hydride–zirconium fuel

Table 2.1c. Research reactors in Moscow and the Moscow Region (continued).

Location, Owner, Department	Reactor type	Fuel type (enrichment, composition, form)	Date of reaching criticality and shut- down	Power (MW)		Application
				Design	After recon- struction	
Russian Research Center-	Kvant Critical test facility (uranium-water)	Uranium of 90% enrich- ment (uranium inter- metallic composition)	1990	1000 W	-	Investigation of neutron physics of water-water reactor cores
Kurchatov Institute (cont'd)	Critical test facility modeling of the MR reactor (water-beryllium)	Uranium of 90% enrich- richment (UAI alloy)	1971	100 W	-	Simulation of and critical experiments with MR reactor core Investigation of reactor loop experiment parameters
	UG Critical test facility (channel type, uranium-graphite)	Uranium of 2% enrich- ment (UO ₂)	1965	-	-	Critical experiment and physical studies of uranium-graphite channel-type reactor core
	Critical test facility of RBMK reactor (channel-type, uranium-graphite)	Uranium of 2% enrich- ment (UO ₂)	1981	25 W	-	Critical experiments and physics study of RBMK core
	ASTRA Critical test facility (uranium-graphite)	Uranium of 21% enrich- ment (UO ₂)	1981	100 W	-	Critical experiments and physics study of uranium-graphite reactor core
	EFIR-2M Critical test facility (uranium-water)	Uranium of 90% enrich- ment (UO ₂ + Al)	1973	100 W	-	Critical experiments and neutron physics study of water-water reactor core
	MAYAK Critical test facility (uranium-water)	UAI alloy	1967	10 W	-	Critical experiments and neutron physics study of water-water reactor core

Table 2.1d. Research reactors in Moscow and the Moscow Region (continued).

Location, Owner, Department	Reactor type	Fuel type (enrichment, composition, form)	Date of reaching criticality and shut- down	Power (MW)		Application
				Design	After recon- struction	
Russian Research Center-	NARCIS M2 (U-Zr hydrides)	Uranium of 96% enrich- ment (UO ₂)	1983	10 W	–	Critical experiments and neutron physics study of reactor with U-Zr hydrides fuel
Kurchatov Institute (cont'd)	GROG Critical test facility (uranium-graphite)	Uranium of 7% and 10% enrichment (UO ₂)	1980	100 W	–	Critical experiments and neutron physics study of uranium-graphite reactor core
	P Critical test facility (uranium-water)	Uranium of 2.0, 2.4, 3, 3.6, 4.4, 6.5, and 10% enrichment (UO ₂)	1987	200 W	–	Critical experiments and neutron physics study of water-water reactor core
	ISKRA Critical test facility (uranium-water)	Uranium of 90% enrich- richment (UAl alloy, uranium nitride)	1996	199 W	–	Critical experiments and neutron physics study of reactor cores of different composition
Institute of Theoretical and Experimental Physics ^b	TVR (heavy water reactor)	Uranium of 80% enrich- ment (UO ₂ + Al, tubes)	1949 (1986)	0.5	2.5	Nuclear and solid state physics studies Neutron physics Isotope production Experiments on neutron scattering Radiation tests
	Critical test facility (uranium-heavy water)	Natural uranium	1976	1000 W	–	Critical experiments and neutron physics study of heavy-water- moderated and cooled reactor core

Table 2.1e. Research reactors in Moscow and the Moscow Region (continued).

Location, Owner, Department	Reactor type	Fuel type (enrichment, composition, form)	Date of reaching criticality and shut- down	Power (MW)		Application
				Design	After recon- struction	
Moscow Institute for Engineering Physics ^c	IRT (pool-type)	Uranium of 90% enrich- ment (UO ₂ + Al)	1967	2	2.5	Reactor physics and engineering studies of solid state physics Material irradiation Radiation physics of semi- conductors and dielectrics Nuclear spectrometry
Research Instrumentation Institute (NIIP) ^d	IRV-M1 (pool-type)	Uranium of 90% enrich- ment (UAl alloys, tubes)	1974 1990	2		Radiation testing of electronic devices

^aRussian Research Center-Kurchatov Institute, Kurchatov Square, Moscow, 123182, Russian Federation.

^bInstitute of Theoretical and Experimental Physics, Federal Agency for Atomic Energy, B.Cheryomu-shkinskaya, 25, Moscow, 117259, Russian Federation.

^cMoscow Institute for Engineering Physics, Ministry for General and Professional Education, Kashirskoye-shosse, 31, Moscow, 115409, Russian Federa-
tion.

^dResearch Instrumentation Institute (NIIP), Federal Agency for Atomic Energy, Lytkarino, Moscow Region, 140061, Russian Federation.

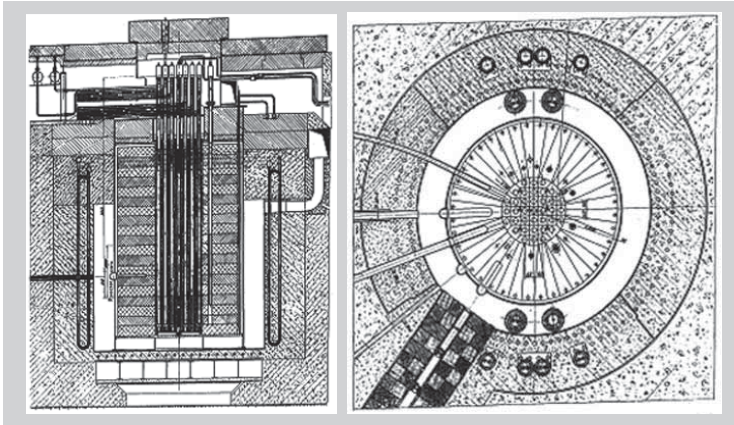


Figure 2.1. RFT reactor. Left: longitudinal section. Right: cross-section.

2.2 Research reactors in the Russian Research Center-Kurchatov Institute

It is clear from *Table 2.1* that the majority of the nuclear installations in Moscow and the Moscow Region were at RRC-KI. This section summarizes details of the most important research reactors in RRC-KI, the full list of which is given in the previous section (for further details, see Goncharov, 1986).

2.2.1 RFT reactor

The 10 MW RFT reactor was put into operation in April 1952 as part of the first experimental materials-testing complex constructed in the FSU (Kruzhilin, 1955; Kurchatov *et al.*, 1955). The RFT was the first Russian research reactor using enriched uranium intended for materials-testing research (*Figure 2.1*). It was equipped with five loop installations, which allowed constructional and fuel materials to be tested in conditions similar to those in power reactors. At the initial stage of nuclear power engineering (from 1952), it was used to test the fuel elements of practically all reactor projects, to search for the best fuel element designs and fuel compositions, and to explore their operational reliability.

After reconstruction in 1957, the power of the reactor was increased to 20 MW through the use of better fuel assemblies. The reactor coolant system was supplemented by a third circuit. As a result of this reconstruction, the maximum flux density of thermal neutrons in the reactor core increased from 8×10^{13} n/cm²s to 1.8×10^{14} n/cm²s.

In the structure of the reactor there were three water coolant loops (PVO, PE, and PVK), one (PG) with a gaseous heat-carrier, and another (PM) with a liquid

Table 2.2. Basic characteristics of RFT reactor loops.

Nickname of loop	Coolant	Thermal power (kW)	Working pressure (MPa)	Flow rate of the coolant (m ³ /h)	Max. temp of the coolant (°C)	Max. temp. of fuel element surface (°C)	Max. number of canals in the loop
PVO	Water	1200	20	25	330	360	3
PVK	Water, water-steam emulsion	1000	10	25	310	325	3
PE	Water	1000	10	25	300	325	3
PG	Helium, CO ₂	25	9	1.1 (t/h)	500	–	1
PM	Lead-bismuth	1000	0.5	2.5	up to 620	–	1

Note: The abbreviations shown are of the Russian names.

metal heat-carrier (Amaev *et al.*, 1966). Each of the loops represented an analog of nuclear reactors designed for different applications (*Table 2.2*). Up to 15 loop-type experimental canals for testing fuel elements and materials were arranged in the reactor core and the reflector.

In 1962, after 10 years of intensive operation, the reactor was shut down and partly dismantled, and near to it, in the same building, the more powerful MR loop reactor (see next section) was constructed. The undismantled part of the reactor, namely, the graphite from the core of the reactor and the reflector, has remained in its regular steel case. Concrete was laid on top of the case and steel plates placed above the concrete.

Importantly, some fuel-element cladding failed during testing at the RFT reactor (especially from 1953 to 1957). In some cases these failures were aggravated by fusion taking place in the claddings and the destruction of the loop and/or working channels, with fuel being washed out and fission products, even actinides, being released into the coolant of the cooling system and the graphite stack (so-called wet accidents).

Analysis of the operational reliability of working fuel elements for the 10 years in which the reactor ran shows that one-third of them were removed from the reactor because of damage that occurred during irradiation. Clearly, then, the reactor operation was accompanied by the generation of a great deal of radioactive waste. This waste can be divided into two groups: 1) the equipment of the reactor and the loop installations disassembled during decommissioning and 2) the “operational” radioactive waste.

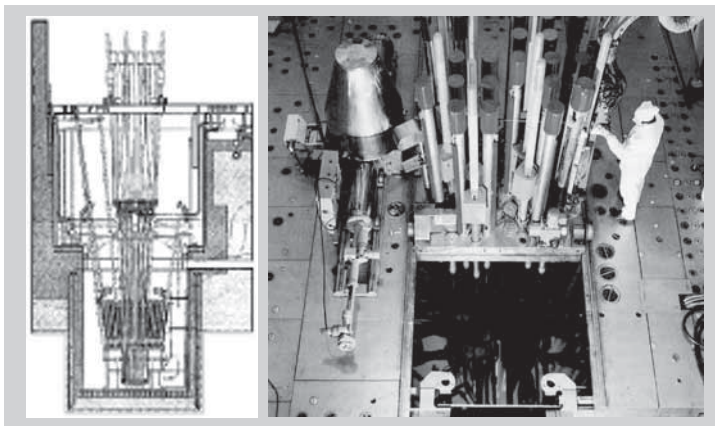


Figure 2.2. MR reactor.

A database of the component composition of both types of radioactive waste has been developed and includes both historical records and reconstruction results. Some details of the database are presented in the final report of ISTC project No. 2290 (2004). Data analysis shows that the weight and dimensional characteristics of the second type of radioactive waste are comparable with those of the first. The total mass of the disassembled equipment and the “operational” radioactive waste is about 200 tons.

2.2.2 MR reactor

The MR reactor, a multiloop channel-type research reactor immersed in a swimming pool filled with water (*Figure 2.2*), began operation in 1964 (Goncharov *et al.*, 1965). The thermal power of the reactor with loop-back installations is 50 MW. The maximum flux density of thermal neutrons in the nuclear core reached 5×10^{14} n/cm²s (Ryazantsev *et al.*, 1999a).

As a successor to the decommissioned RFT reactor, the MR reactor specialized in testing fuel elements and construction materials, but on a much wider scale. It was also used to produce radioactive isotopes for medical applications. The reactor was equipped with nine loop-type installations (*Table 2.3*).

It was the comprehensive program of nuclear materials testing performed in the 1953–1993 period with the help of the RFT and MR reactors and the “hot” radiochemical laboratories attached to them that enabled the certification of fuel elements and structural materials for practically all the Soviet-made nuclear power plants.

Table 2.3. General characteristics of the MR loop installations.

Nickname of loop	Coolant	Thermal power (kW)	Coolant flow rate (MPa)	Coolant pressure (MPa)	Max. coolant temperature (°C)	Max. number of experimental channels
PVTs-1	Water and steam–water emulsion	3000	30	10.0	310	7
PVTs-2	As above	300	30	10.0	310	2
PVK	As above	300	150	20.0	330	6
PVU	As above	300	30	20.0	330	4
PVO	Water	2000	100	20.0	330	5
PV	Water	3000	30	20.0	330	2
POV	Water	1000	30	10.0	310	2
PVM	Pb–Bi	2000	2.5	0.5	620	1
PG	Helium	100	7	10	900	1

During reconstruction of the reactor, some of the constructional elements with a radiation source that had become exhausted were dismantled and placed in radioactive waste storage as high-activity waste. Beryllium blocks were also substituted for some of the reflector’s graphite blocks. Contaminated graphite blocks were unloaded and placed into the radioactive waste storage.

In 1973 the radioactive waste that had accumulated in storage at the MR reactor and hot laboratory since 1962 was transferred to the radioactive waste storage site within the grounds of RRC-KI. A major part of this radioactive waste is waste generated during investigations of fuel elements in “hot cells.” The high-activity operational waste of the reactor and other such wastes were buried in metal cases. Other parts (graphite blocks from the MR reactor, offcuts of canal tubes, etc.) were buried without cases (Ryazantsev *et al.*, 1999b).

2.2.3 WWR-2 reactor

The WWR-2 reactor, a heterogeneous thermal research reactor, began operation in 1954 (*Figure 2.3*). Modernization in 1957 raised its thermal capacity to 3 MW. Distilled water was used as coolant, moderator, and also top protector.

The reactor was used to examine design problems in propulsion nuclear power reactors, such as the radiation impact on isolation, organic and semi-conductor materials, and also the efficiency of radiation protection.

In 1983 the reactor was shut down and dismantled. Currently, the unloaded fuel and accumulated radioactive waste are in temporary storage units at the reactor site.

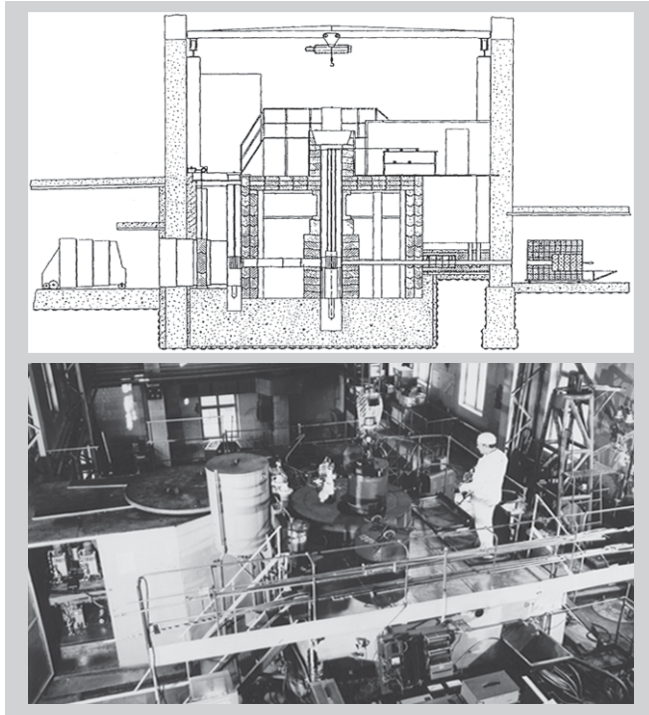


Figure 2.3. WWR-2 reactor.

2.2.4 R reactor complex

From 1963 to 1986 small research reactors were operated to investigate the space applications of the Romashka and Yenisey series.

2.2.5 Romashka reactor

The Romashka reactor–converter (40 kW) is the prototype for a nuclear power facility with direct thermoelectric conversion (*Figure 2.4*). Fuel rods based on UC_2 were used (Ponomarev-Stepnoy and Kukharkin, 2000).

In 1969, after the implementation of the research program, the Romashka reactor was shut down and dismantled. Premises at the R complex were reconstructed for ground tests of the Topaz space nuclear facility with the Yenisey reactor.

2.2.6 Yenisey reactor

The Yenisey reactor is the prototype for a space nuclear power facility with thermionic conversion of thermal energy into electricity (*Figure 2.5*). The ther-

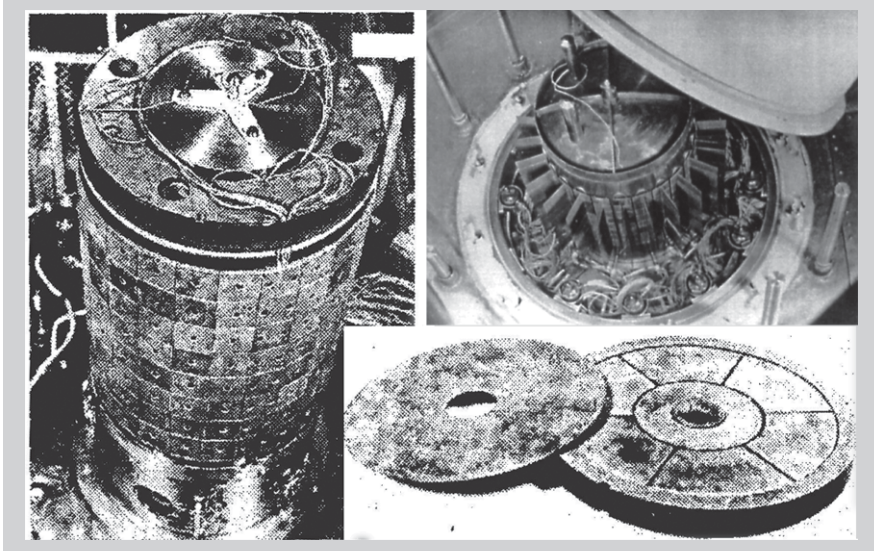


Figure 2.4. Romashka reactor.

mal capacity of the reactor is 100 kW, and the electrical capacity is 5 kW. A liquid metal eutectic alloy of sodium and potassium was used as coolant.

Four installations were examined between 1973 and 1986. At the end of the tests they were dismantled, and both fuel and accumulated radioactive waste are stored at the complex.

2.2.7 Gamma reactor

The Gamma research reactor with a thermal capacity of 220 kW was put into operation in 1982. Its cooling system is water–water with natural circulation, and it is a thermoelectric converter of 6 kW electrical output (*Figure 2.6*).

The research program ended in 2003, and a decision was taken to decommission the reactor. Now the installation is in shutdown mode with surveillance. Fuel is still in the active zone of the reactor.

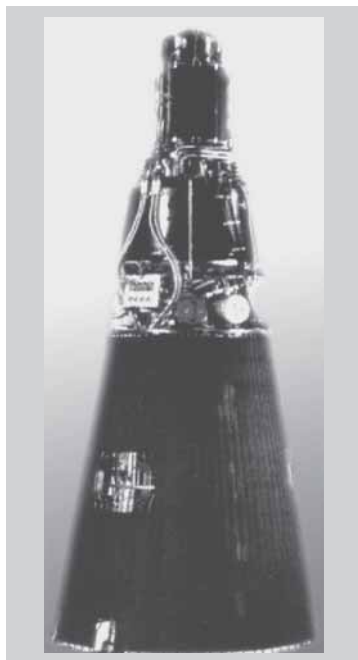


Figure 2.5. Yenisey space nuclear power reactor.



Figure 2.6. Gamma reactor.

The Moscow Case Study of the Nuclear Legacy

3.1 Study background, statement of needs, and goals

In the second half of the 1990s IIASA's "Radiation Safety of the Biosphere" (RAD) project conducted studies on general aspects of the radiation legacy from the Cold War period. Priority was given to gaining an overview of the radiation legacy of the FSU and, more specifically, of related problems within the Russian Federation. The initial funding for the Russian networking institutions to gather domestic information was provided by the European Union. The results are published in the IIASA report, *Radiation Inheritance of the Former USSR: Analytical Overview*, which presents a comprehensive picture of the characteristics of accumulated radioactive materials and radioactive waste for each sector of the nuclear complex of the FSU, in total and by individual enterprise. The preparation of the report was funded by the US Department of Energy. The report was also published in 2000 by Earthscan Press as a book entitled *Radiation Legacy of the Soviet Nuclear Complex* (Egorov *et al.*, 2000).

In the report particular attention was drawn to the fact that, as a result of the intensive development of nuclear science and technology in the FSU, Moscow and the Moscow Region had accumulated dozens of nuclear centers and institutions. These possessed nuclear installations such as research reactors, radiochemical laboratories, thousands of radiation sources, and also temporary storage units both for spent fuel and radioactive waste. Details are presented in the next section.

The major contribution to this inheritance is from RRC-KI, the biggest and oldest nuclear center in this megacity. It was created in 1943 as the leading institute of the nuclear program in the FSU. RRC-KI not only played a crucial role in the development of the first FSU nuclear bombs, but also performed numerous scientific investigations that substantiated technical decisions on nuclear power and nuclear industry development in the FSU and Russia. Today, it continues to play a leading role in nuclear science and technology.

Currently, RRC-KI possesses more than nine research reactors, some of which are still in operation, 17 critical assemblies, a hot laboratory for materials testing, spent fuel storage sites, and (particularly) temporary storage sites of radioactive

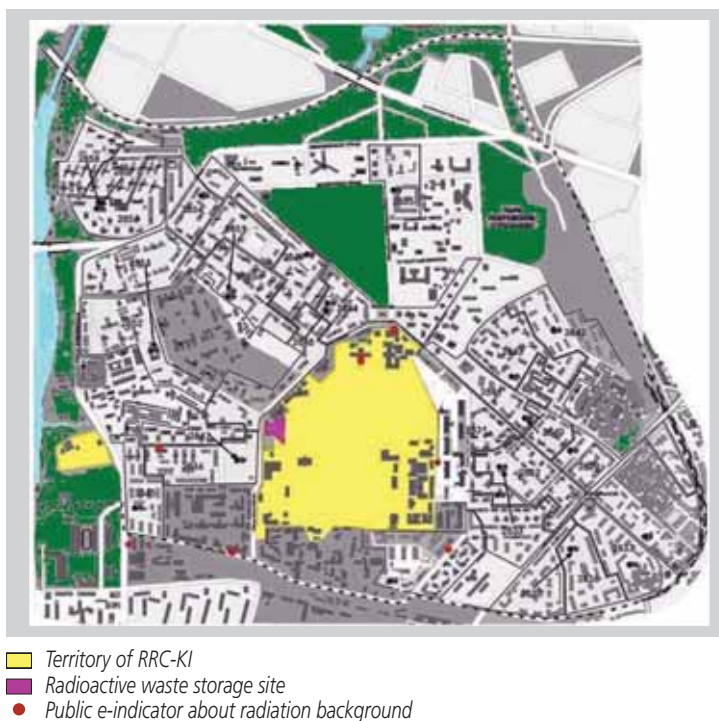


Figure 3.1. Location of RRC-KI in the Schukino municipality.

waste, with the inevitable soil contamination around them (Ryazantsev *et al.*, 2000, Ponomarev-Stepnoy *et al.*, 2002a). When founded, RRC-KI was located in an outlying part of Moscow. The FSU government decision allotted an area of about 100 ha (10^6 m²) for RRC-KI nuclear facilities, including a 4 ha enclave located on the bank of the Moscow River (*Figure 3.1*). During more than a half century of operation of nuclear facilities, huge amounts of radioactive waste were generated, some of which were stored within the boundaries of RRC-KI. The urbanization that has occurred during the past 50 years means that the boundaries of the Institute are today surrounded by densely populated residential and business districts, now part of the Moscow downtown area (*Figure 3.2*). Living close to such a “neighbor” inevitably causes Moscow’s inhabitants and visitors concerns about their environmental security.

The RRC-KI directorate asked IIASA’s RAD project to launch an international study to assess the radiological risk and resulting public impact of past waste management practices at RRC-KI. In response, IIASA asked the TACIS program to subsidize an IIASA study to evaluate both the information available on the history of radioactive waste disposal and the environmental and social impacts of the radioactive waste disposal sites in RRC-KI. In parallel, IIASA applied to the ISTC in

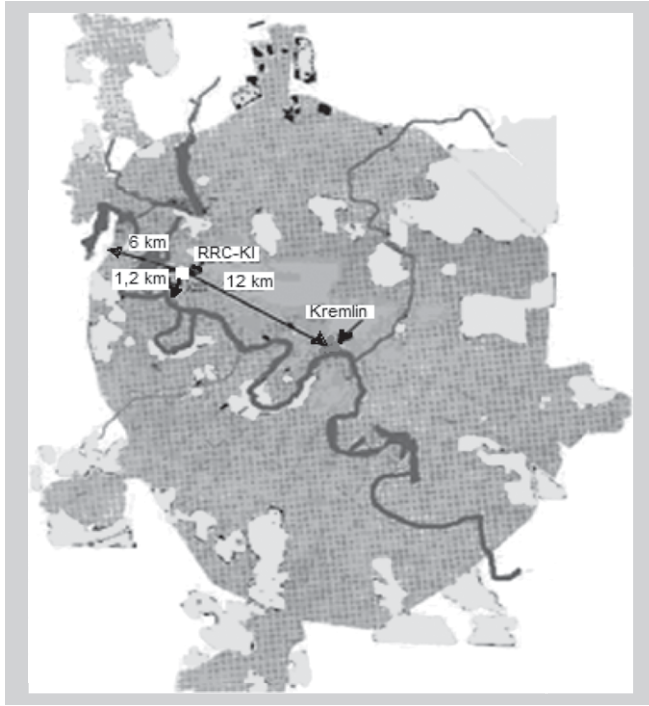


Figure 3.2. Location of RRC-KI in Moscow (12 km northwest of the Kremlin).

Moscow for funding to cover the gathering of the information needed to assess the actual and potential implications of this nuclear legacy.

In 2003 the project received a TACIS-Bistro grant for a study entitled “Impacts of Radioactive Waste Storage at the Territory of the RRC-Kurchatov Institute in Moscow,” with a major focus on the evaluation of the migration of radioactivity from the storage site of RRC-KI via run-off water. Simultaneously, ISTC approved the Russian application and Project #2290 “The Analysis of Burials of Radioactive Waste in the Territory of the Russian Research Center Kurchatov Institute in Moscow and Paths of Supposed Radionuclide Migration in the Environment” then began. IIASA was a foreign collaborator in this project and used its findings to model the environmental impacts.

In parallel with the IIASA activity, in 2002 RRC-KI made its first practical steps toward rehabilitating contaminated objects within its grounds (the Rehabilitation Project). Some results of this project were presented at WM’03 (Ponomarev-Stepnoy *et al.*, 2002b).

Then, in 2004 IIASA organized the International Workshop “Solutions to Security Concerns about the Radioactive Legacy of the Cold War that Remain in Urban Environments.” The workshop, held at Vanderbilt University (Tennessee, United

States) from 14 to 17 November 2004, inter alia critically discussed the results of these Moscow case studies. It was emphasized that the establishment of nuclear centers in or around big cities throughout the world could be easily traced. The French nuclear center “Saclay,” for example, is about 20 km from the center of Paris, and a similar situation exists with respect to nuclear institutions in Berlin, Budapest, Grenoble, London, San Diego, Sofia, etc. Thus, the case study of the specific problems in Moscow could serve as an introduction to a more general and systematic assessment of the potential impact of hazardous radioactive materials and chemicals in urban settings in many countries.

This section of the paper comprises materials collected within the studies listed above and summarizes the findings.

3.2 The nuclear legacy of RRC-KI

The nuclear legacy of RRC-KI mainly results from nuclear research and testing reactors created from the 1940s to the 1970s. These nuclear research reactors were the main engines in the FSU of progress in the development of nuclear power, basic nuclear science, materials development, radioactive isotope production for medicine and industry, and the education and training of scientists and engineers. They played a crucial role in the provision of a scientific and technological base for the development of the nuclear industry in the FSU and later in Russia. As a result of more than half a century of operations, a huge amount of radioactive waste has been generated and stored within RRC-KI’s boundaries. The total radioactivity of the spent fuel stored there is estimated to be 2 MCi, and the total radioactivity of radioactive waste at the temporary storage sites is about 0.1 MCi (Ryazantsev *et al.*, 2000; Ponomarev-Stepnoy *et al.*, 2002a).

3.2.1 Spent nuclear fuel at RRC-KI

Today, spent nuclear fuel storage units contain over 1,300 spent fuel assemblies of various designs. The spent nuclear fuels differ in terms of chemical composition, the degree of uranium enrichment, and the protective cladding used. It is important to note that as the spent nuclear fuel from the research reactors is, in many cases “non-standard,” it cannot be reprocessed using standard reprocessing technology—this fuel even requires special storage conditions. It was for this reason that most of the spent nuclear fuel was not transported to the RT-1 reprocessing plant at the Mayak, Russian nuclear center in the Urals (where spent nuclear fuel from nuclear power plants and nuclear submarines was routed) but stored instead on the premises of the research reactors where it still awaits final disposal.

Another important feature of the spent nuclear fuel of research reactors is that a high fraction of the experimental fuel elements were damaged during testing.

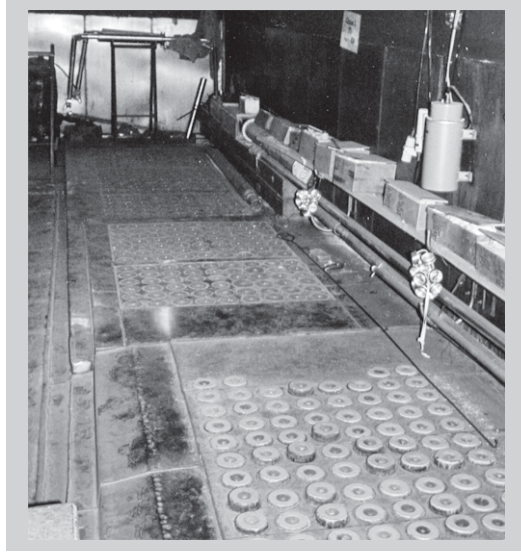


Figure 3.3. Spent nuclear fuel storage at the MR reactor site.

This also meant that this spent nuclear fuel could not be reprocessed at the existing reprocessing plant.

According to Ponomarev-Stepnoy and Gorlinsky (2004) non-standard spent nuclear fuel constitutes 60% of the total amount, while 10% has suffered varying degrees of damage. It is expected that, subject to allocation of the necessary resources, the spent nuclear fuel that can be reprocessed at the RT-1 factory will be transported to Mayak, and the spent nuclear fuel with no reprocessing route (non-standard and damaged) will be packed into tight cases and transported to the Mining Chemical Combine in Krasnoyarsk for long-term storage. The time necessary to transport the spent nuclear fuel from RRC-KI is estimated to be a minimum of seven years, assuming that all the conditions at Mayak and the Mining Chemical Combine are favorable (Ryazantsev *et al.*, 2000).

The MR reactor, which was the most powerful installation at RRC-KI, produced most of the spent nuclear fuel now kept in the dry storage site on the MR reactor premises (*Figure 3.3*). In addition to the spent nuclear fuel from the core of the MR reactor, spent nuclear fuel from the RFT reactor and experimental spent fuel assemblies examined for the WWR and RBMK reactor designs and for the navy ice-breaker and submarine propulsion nuclear reactors are also stored there. This location accounts for 70% of all spent nuclear fuel stored on RRC-KI territory.

The rest of the spent nuclear fuels are stored:

- In the pool storage at reactor IR-8 (about 50 spent fuel assemblies).

- At the site of the WWR-2 reactor, located in the RRC-KI enclave on the bank of the Moscow River (the so-called Gas Factory; see *Figure 3.1*). The storage unit contains about 300 spent fuel assemblies.
- In dry storage at the R reactor complex, there are about 200 kg of spent fuel assemblies from the Romashka reactor and 200 spent fuel assemblies from the Yenisey reactor.
- In the active zone of the Gamma reactor, there are 69 fuel assemblies with a fuel composition based on UAl alloy.

3.2.2 Radioactive waste storage site at RRC-KI

Short history of the site

Research reactors used to test new types of fuel, new types of coolant, and other reactor innovations naturally face some operational problems. Such problems frequently produce high-level radioactive waste containing fission products and also induce radioactivity in construction materials.

Initially, nuclear weapons production in the FSU, as in all nuclear club countries, was developed in a rush to win the nuclear arms race, and there was insufficient knowledge of the environmental consequences of radiation. At the beginning of the nuclear era this radioactive waste was often placed in so-called temporary storage. Radiation protection norms worldwide at that time were not as strict as they are now and, in many cases, they were not even properly implemented for the reasons given above.

Before the creation of a specialized enterprise for radioactive waste management (Radon) in 1965, all the radioactive waste generated during the operation of nuclear facilities at RRC-KI was stored in so-called temporary burial sites within the boundaries of RRC-KI.

Until 1955 solid radioactive waste was put into a natural ravine in the Sobolevsky Creek, which was in the western part of the RRC-KI grounds, very close to the Kurchatov Institute's brick perimeter wall (*Figure 3.4*). The ravine was 9 m deep with a general slope to the RRC-KI perimeter. The waste was dumped in the shallow, sandy horizon of the Quaternary sediments.

Dumped wastes were mixed and filled in with soil or construction rubbish, so there were no actual mechanical barriers between the radioactivity it contained and the biosphere. Now the ravine is completely filled in.

Figure 3.5 illustrates a general view of the area of the site, which was about 2 ha (2×10^4 m²).



Figure 3.4. Sobolevsky Creek.



Figure 3.5. Bird's-eye view of the RRC-KI radioactive waste storage site, winter 2003.

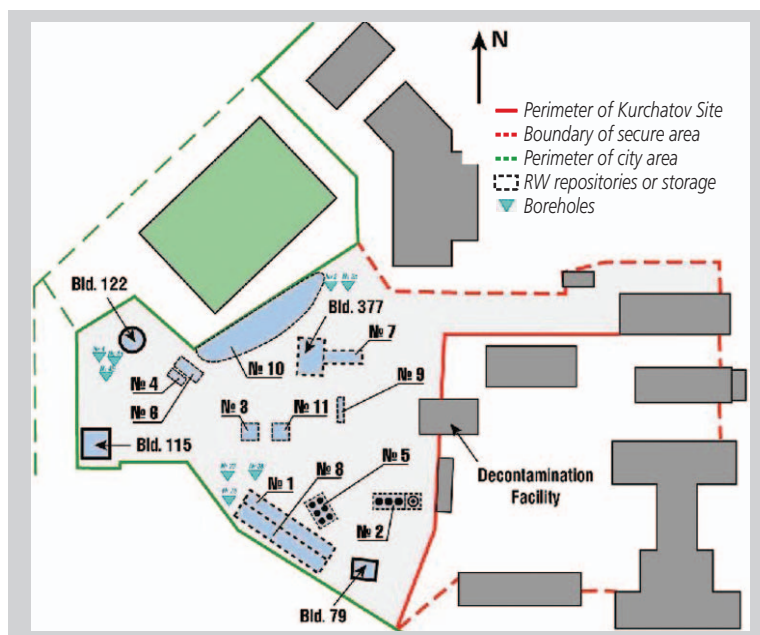


Figure 3.6. Location of the storage tanks (repositories) at the radioactive waste (RW) storage site.

After 1955, 11 concrete or brick tanks were commissioned for the storage of radioactive waste at the site. The location of these repositories is shown in *Figure 3.6*. Today, only one remains in operation.

In 1973 high-level radioactive waste that had accumulated at the premises of both the MR reactor and the hot laboratory had to be placed in tanks 4 and 6. High-level operational wastes were buried in metal cases. Other waste (contaminated graphite blocks from the MR reactor, channel tube offcuts, etc.) was buried without cases. In the same year, after additional radioactive waste was buried, the tanks were filled with cement slurry.

Potential pathways of radioactivity from the site

Before 1955 radioactive waste was buried in an open-trench system. This, together with leakages from the tanks, resulted in contamination of the surface layer soil and also of the water-bearing horizon.

The surface of the storage site showed an increased level of radiation. The exposure dose rate is up to 3000 microR/h at 1 m distance from the surface. In most of the area adjacent to the storage site, the exposure dose rate is at least twice the background rate at the rest of the Institute.



Figure 3.7. IIASA RAD project team at the RRC-KI radioactive waste storage site, winter 2002.

Thus, in the near-term perspective, under unfavorable meteorological conditions, the contaminated soil could be exposed to erosion transfer by surface water and to wind transfer in the direction of the nearest residential buildings, which are only 100 m from the radioactive waste burial site (*Figure 3.7*).

Sampling from the observation wells showed that soil contaminated by ^{60}Co , ^{134}Cs , ^{137}Cs , ^{90}Sr , ^{152}Eu , ^{241}Am , etc., was observed in water-bearing horizons in the area of the former trenches (Ryazantsev *et al.*, 2000).

Though most of the radioactive waste stored at the site is in repositories with concrete or brick walls, even this waste poses a threat of further propagation of the radioactivity. This is because the bases of some of the tanks are below the groundwater water table; mechanical degradation of the walls could also create a pathway for radioactivity from the storage facility. Thus, the threat that radioactivity leaching from the solid waste could be transferred by groundwater beyond the RRC-KI site should also be examined.

An important point is that the underground medium of the site was disturbed during building works carried out in this area during urbanization. In the 1960s an underground heating pipe crossed the site, but is now out of operation. The pipe that transmits rainwater accumulated from about 400 ha ($4 \times 10^6 \text{ m}^2$) of the surrounding area to the Moscow River is constructed in the lowest part of the Sobolevsky Creek (see *Figure 3.4*) and crosses the middle of the site from east to west. The pipe's

source is located 1.5 km to the east of the site and its outflow is 1.3 km to the west, on the bank of the Moscow River. The elevation drop of the rainwater pipe is 6 m. The pipe is enclosed by concrete shielding that has a cross-section at the site of 2.5 × 2.1 m. Failure of the rainwater pipe at the site or below it while there is a high level of precipitation might cause flooding with a potential transfer of radioactive contaminants from the site.

Failure of these underground pipe systems is not the only concern. The pipes, which flow along and around the piping systems, could also act as conduits for contaminants.

Experimental work at RRC-KI requires plenty of water for technological purposes. This is taken from artesian wells located within its boundaries. A large water intake from the wells could result in a spatial depression, which, in turn, could lead to water being pumped from the upper horizon of the site to a deeper one and thus to the contamination of the lower horizon.

Uncertainties as to the amount and the physicochemical properties of the buried radioactive waste, uncertainties in the hydrogeological data, and the close location of the storage site to the residential area outside the Institute mean that the potential pathways of radioactivity from the site could become actual pathways in the short-term perspective. The implications of this for environmental security deserve a careful assessment to identify potential countermeasures, their cost, and how they could minimize any radiological impact on the population and on the personnel involved in the remediation and/or stabilization of the site.

Analytical studies performed within the TACIS and ISTC projects were oriented toward a scoping analysis of the different pathways. More specifically, it was stipulated that the studies would focus on:

- Collection, analysis, and collation of the currently available data regarding the radioactive source term and the environmental properties;
- Modeling of radionuclide migration as a result of erosion caused by surface (run-off) water and assessment of the radiological impact of radionuclide migration in terms of dose uptake by critical population groups and of a general reduction in environmental security;
- Scoping analysis and estimates of groundwater and atmospheric transfer.

We emphasize that the study was directed at the radioactive waste disposal area within the main area of RRC-KI, as indicated by the Russian partner in the IIASA study. Hence, the possible migration of radioactive contaminants from other points in the area has not been studied, including the detached area (enclave) located about 1 km from the main territory, on the bank of the Moscow River (see the main territory of RRC-KI and its enclave in *Figure 3.1*).

Surface contamination of the site

Radiation background on the perimeter of RRC-KI

The external gamma radiation background at the perimeter of the RRC-KI site has been monitored for a number of years. The average value for the dose rates of gamma radiation at 16 control points for the 1990–1998 period was $8.2 \mu\text{R/h}$, which does not differ from the general background in Moscow. Only near the radioactive waste storage site was the average dose rate over the 9-year period above this, at $13.7 \mu\text{R/h}$.

Thus, the contribution from that technogenic source of radiation to the dose rates near the site is $5.5 \mu\text{R/h}$ (Borohovich *et al.*, 1999).

Exposure dose rate over the site

Assessment of the contamination of the surface layer of the ground at the RRC-KI radioactive waste storage site was based on the data obtained by a gamma radiation survey of the site and reported in Ponomarev-Stepnoy *et al.* (2002b).

The gamma radiation survey of the site was carried out with the help of a portable radiometer—a dosimeter designed for radiation control at industrial enterprises. The detection block works on the basis of a microcrystalline organic scintillator (anthracene), placed as a thin layer on a light conductor made from organic glass shaped in the form of a truncated cone. Measurements were carried out in steps of 10 m to a distance of 1–1.5 m from the surface. The dosimeter can register a range of exposure dose rates from 10^{-2} to $3000 \mu\text{Sv/h}$, with a power range in gamma radiation from 0.125 to 1.25 MeV. The accuracy of the measurements is $\pm 20\%$.

Figure 3.8 illustrates the results of the gamma radiation survey.

Method used to derive the concentration of the major radionuclides

The maps of surface contamination by ^{137}Cs and ^{90}Sr were created by recalculating the exposure dose rate field, assuming a 15 cm local layer of homogeneously contaminated surface soil. The recalculation is based on:

- Comparison of the actual exposure dose rate measurements for nine random points at the site with the calculated values of exposure dose rate obtained from measurements of ^{137}Cs concentrations in samples taken from those nine points. This comparison showed reasonable agreement with the supposition that the exposure dose rate is mostly formed by ^{137}Cs contamination at the surface layer.

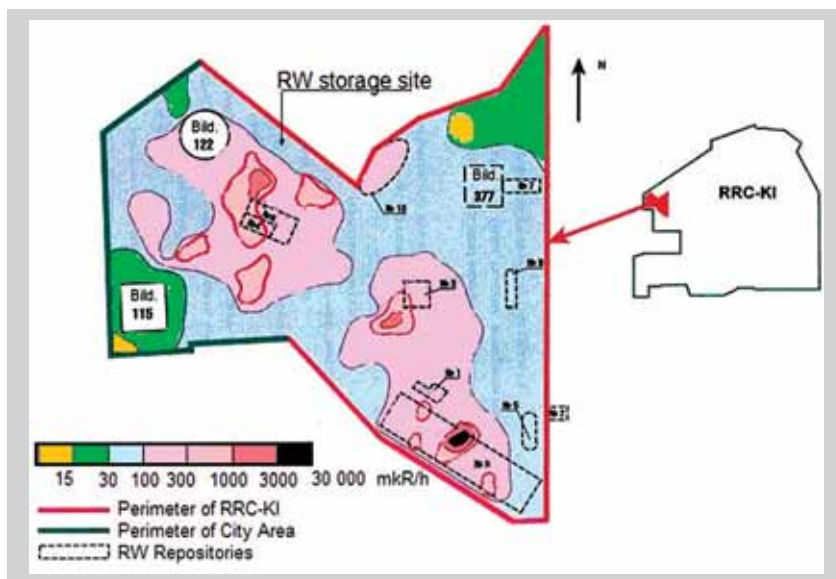


Figure 3.8. Exposure dose rate at the RRC-KI radioactive waste storage site (Ponomarev-Stepnoy *et al.*, 2002b).

- The average ratio between ^{137}Cs and ^{90}Sr concentrations measured in seven samples taken from different parts of the site. This ratio was used to create a ^{90}Sr contamination map.

Though the data are not sufficient for a very heterogeneously contaminated site, this method is still thought to be useful as a first approximation. Details of the methodology used are given below (Gorlinsky, 2003).

To find a correlation between contamination of the ground and an exposure dose rate of gamma radiation, the geometry of a volumetric source in the form of a disk was used. The calculation was carried out taking into account the self-absorption and multiple dispersion of gamma radiation in a source. Moreover, multiple dispersion of gamma radiation was incorporated with the help of a dose factor of accumulation, defined according to the model of Tailor (Gusev *et al.*, 1961).

Calculations for the various sizes of the disk were made, assuming that ^{137}Cs provides the basic contribution to the dose rate and is homogeneously distributed over the volume of the disk. Results of the calculations are given in *Figures 3.9* and *3.10*.

Figures 3.9 and *3.10* show that if the thickness of a layer of ground is 20 cm and the radius of the sector of polluted ground is 3 m, factor a , which reflects the

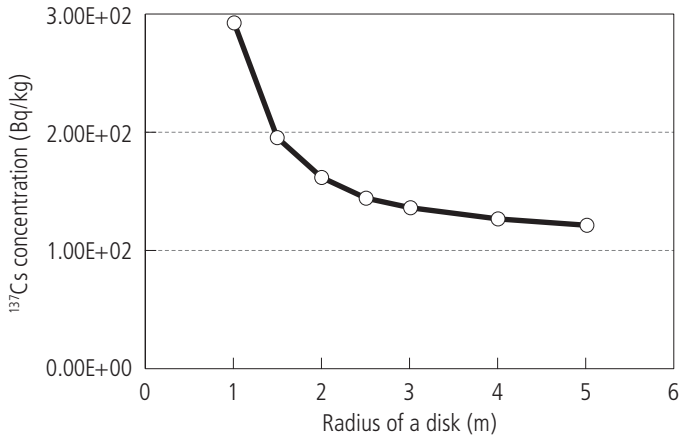


Figure 3.9. Volumetric concentration as a function of radius of a disk. The rate of gamma radiation from ¹³⁷Cs at a distance of 1 m along the axis of the disk is 1 μR/h (thickness of the disk is 20cm).

correlation between contamination of the ground by ¹³⁷Cs and the dose rate at the center of the polluted territory at a height of 1 m, is 135 (Bq/kg)/(μR/h). When the thickness of a layer is 10 cm, the error in the definition of factor *a* is about 20%, and when the thickness of a layer becomes more than 30 cm this error does not exceed 10%. When defining the value of *a*, the size of a sector of polluted ground becomes an important factor. *Figure 3.10* shows that the spread of values of *a* is

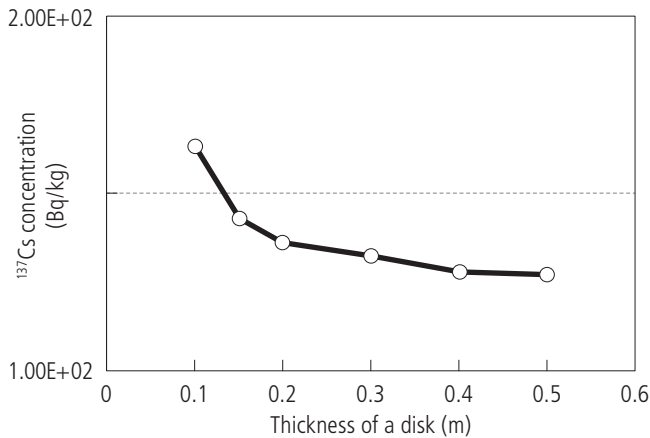


Figure 3.10. Volumetric concentration as a function of disk thickness. The rate of gamma radiation from ¹³⁷Cs at a distance of 1 m along the axis of the disk is 1 μR/h (radius of the disk is 3 m).

about $\pm 50\%$ when the radius of a sector of polluted ground varies from 1.5 to 5 m and more. Thus, the total error of definition of factor a is about $\pm 60\%$.

For comparison, let us consider the results of the experimental studies of polluted areas in the Kaluga region (Warner and Harrison, 1993; Petrov *et al.*, 1999). Contamination of both arable and non-arable lands was investigated. In samples of ground taken up to 1991, the composition of nuclides of Chernobyl origin was established as ^{137}Cs (88%), ^{134}Cs (10%), and ^{106}Ru (0.5%). It was noted that the concentration of ^{90}Sr is about 3% that of ^{137}Cs . It has been ascertained that the distribution of ^{137}Cs over cultivated lands is uniform down to a depth of 20 cm. At the same time, the distribution of ^{137}Cs over non-cultivated lands is described by an exponential law, basically, that it is in the top layer to a depth of about 5 cm. Strontium is distributed over non-cultivated lands exponentially, but with a flatter curve than for cesium. This shows that strontium has a better ground-penetrating ability. Based on a large amount of statistical material, a correlation between local ground contamination values and the dose rate of gamma radiation of radionuclides was calculated. For arable lands, this factor a was $2.5 (\mu\text{R/h})/(\text{Ci}/\text{km}^2)$ or, expressing it in the units used above (for a soil density of $2.0 \text{ g}/\text{cm}^3$), $150 (\text{Bq}/\text{kg})/(\mu\text{R}/\text{h})$. The factor a for a 20 cm layer of polluted ground, as *Figures 3.9* and *3.10* show, is $135 (\text{Bq}/\text{kg})/(\mu\text{R}/\text{h})$. Thus, the calculated and experimental values of factor a are in close agreement. This shows that there is sufficient reliability in the calculated value of factor $a = 135 (\text{Bq}/\text{kg})/(\mu\text{R}/\text{h})$ for it to be used to describe the surface contamination at the RRC-KI radioactive waste storage site.

Maps of the surface contamination by ^{137}Cs and ^{90}Sr

The contamination map required as input to the model should contain the levels in Bq/m^2 . However, this map was derived from the original contamination map (which indicated the levels in Bq/kg) received with the information package from RRC-KI and assumed that all the radioactivity is homogeneously distributed within the upper 15 cm of the soil layer). The input ^{137}Cs and ^{90}Sr contamination maps used for the calculations are presented in *Figures 3.11* and *3.12*.

Soil–water partition coefficients

Experiments to measure the partition coefficients of ^{137}Cs and ^{90}Sr between contaminated soil and water were carried out specifically for samples of dry soil taken from the site.

A sample of dry soil was placed in distilled water at a weight ratio of 1:2, respectively, and the mix was agitated. Almost immediately after the agitation (i.e., after sedimentation of the macro-particles), the liquid phase was separated by filtration (using filter paper) and the radioactivity of the liquid phase and the deposit

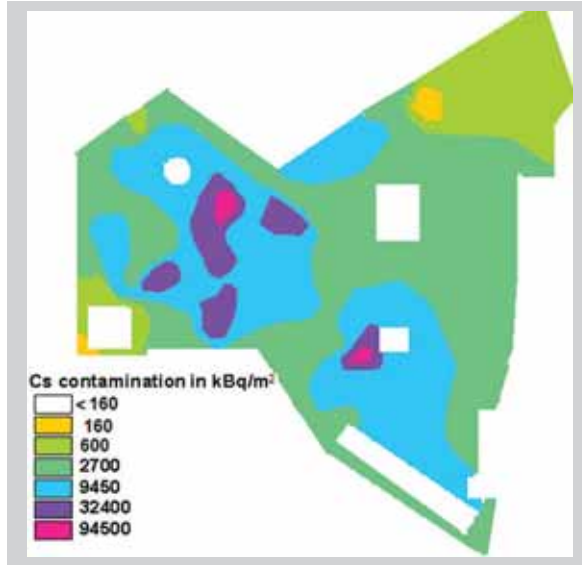


Figure 3.11. Initial ^{137}Cs contamination of the site in kBq/m², assuming that all the radioactivity is located within the top 15 cm of the soil layer.

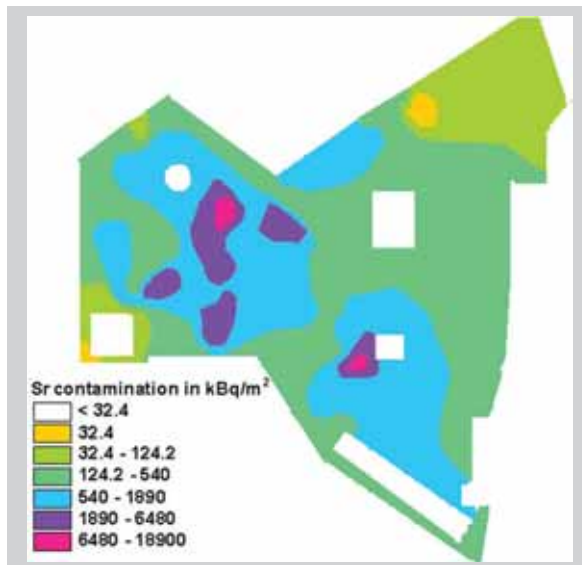


Figure 3.12. Initial ^{90}Sr contamination of the site in kBq/m², assuming that all the radioactivity is located within the top 15 cm of the soil layer.

Table 3.1. Results of experiments to determine the partition coefficients of ^{137}Cs and ^{90}Sr .

No	Nuclide	Weight of soil sample (g)	Weight of water (g)	Weight of deposits on filter (g)	Duration of contact of ground with water (minutes)	Radio-activity of soil sample (Bq)	Radio-activity in water (Bq)	Radio-activity of filter (Bq)
1	^{137}Cs	185	370	19.4	10	2.1×10^5	90.0	3.7×10^4
2		190	380	17.6	10	9.2×10^4	64.0	1.8×10^4
3		175	350	18.1	60	2.4×10^5	440.0	5.5×10^4
4		198	400	18.5	60	1.8×10^5	160.0	3.7×10^4
5	^{90}Sr	50	100	3.9	60	211	1.9	74.6
6		50	100	4.3	60	1121	4.3	296

on the filter were analyzed. ^{137}Cs radioactivity was measured with a Ge(Li) detector (DGDK-63B) of 63 cm³ volume and an analyzer (SBSA-40) connected to a personal computer. The resolution of the detector for gamma radiation from ^{60}Co was about 3 keV, with an error of $\pm 20\%$. The radioactivity of the radiochemically separated strontium was determined by a β -spectrometer. The accuracy of the measurements was $\pm 30\%$.

The results of the measurements of the soil–water partition coefficients for ^{137}Cs and ^{90}Sr are given in *Table 3.1*.

Contamination of underground medium at the site

Radiation monitoring of soil and groundwater was performed using 92 observation boreholes sunk in 1975–1992 (Mosinzhproekt Institute, 1986; GSPI, 2002). The boreholes have a 10–40 m depth and cover the site (see *Figure 3.6*) and adjacent area.

The most representative monitoring data obtained in 1991–1992 confirm that underground soil contamination is primarily caused by ^{90}Sr and ^{137}Cs (*Figure 3.13*).

The dose rate of ^{137}Cs and ^{90}Sr at some points exceeded the background tens of times. The concentration of ^{137}Cs varied from 0.2 to 128,000 Bq/kg, and that of ^{90}Sr from 0.4 to 20,000 Bq/kg. There were local spots of contamination by ^{134}Cs , ^{60}Co , ^{152}Eu , and ^{241}Am , located down to a depth of 5 m.

Radioactive contamination of groundwater caused by the presence of ^{90}Sr was revealed. For the upper sub-horizon, concentrations of ^{90}Sr ranged from 0.4 to 814 Bq/l; for the lower sub-horizon, from 0.4 to 74 Bq/l. As the base of some of the tanks and repositories of solid radioactive waste are below the water table,

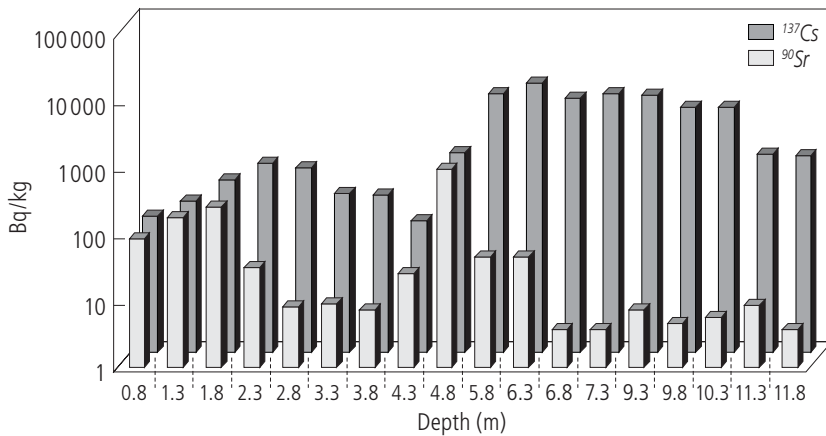


Figure 3.13. Distribution of ^{137}Cs and ^{90}Sr against depth of sampling.

it is quite possible that this contamination is caused by the inflow of groundwater through leaks and further leaching and by the radioactivity washing out.

3.3 Environmental characteristics of the radioactive waste storage site

The information presented in this section is based largely on the work conducted by the Russian team of experts that participated in the study; most of the information is presented in the Russian report (Gorlinsky, 2003). Data in this chapter are based on this report, which is therefore not cited unless there is a need to identify a specific source of information. In addition, a literature review was carried out to identify other possible sources of information and to compare the information reported previously with that made available during the study and detailed in the Russian report (Gorlinsky, 2003). Information derived from the other sources is referenced when used.

3.3.1 Topography and mechanical barriers to water drainage from the site

A general view of the radioactive waste site and its adjacent municipal area are presented in *Figure 3.14*; this is taken from the Russian report (Gorlinsky, 2003). *Figures 3.15–3.16* give an illustration of several vertical cross-sections. The illustrations presented in *Figures 3.18* and *3.19* are digital elevation maps based on these data and provided to the project by RRC-KI experts. The topography of the site and nearby territory was obtained using altitude measurements at a set of key points at

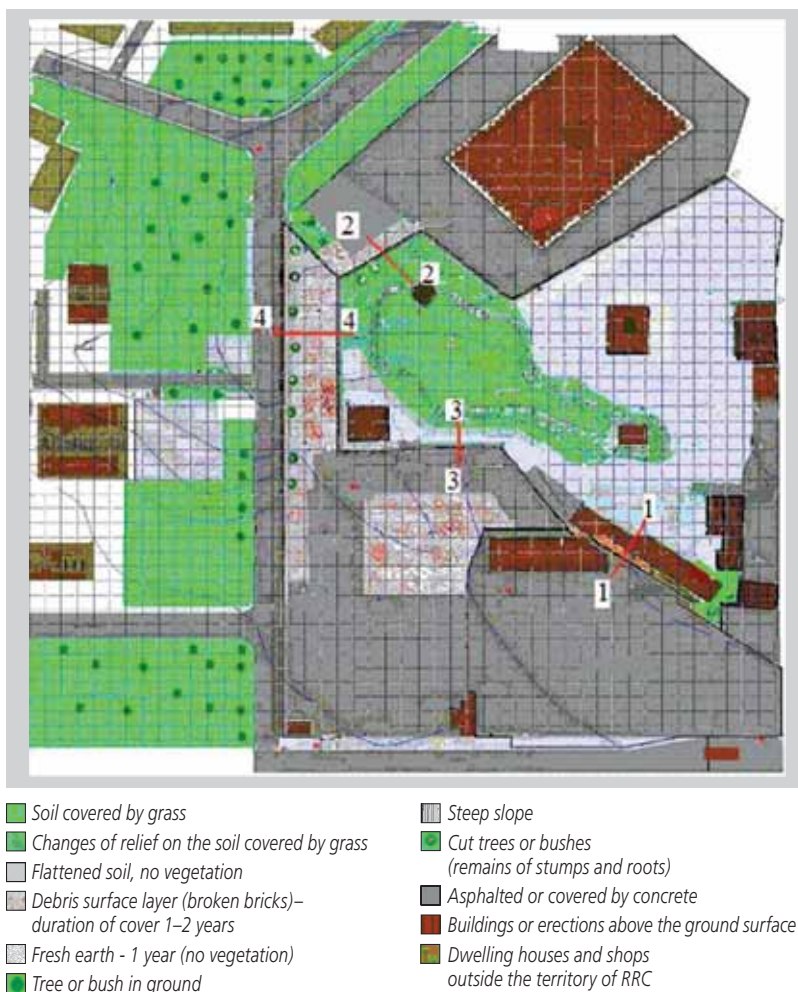


Figure 3.14. General view of the radioactive waste storage site and its municipal surroundings. Lines 1–1, 2–2, 3–3, and 4–4 designate the cross-sections represented in *Figures 3.15* and *3.16*.

the site, expert evaluation of the results, and computer interpolation. As is clear from the figures, the area of the waste storage site is quite small, about 11,500 m². The highest elevation point is 149 m and the lowest is 144.6 m.

The closest residential building area is only 100m from the site. Moreover, the territory within the contour MLKJIH (see *Figure 3.17*) is occupied by a municipal car park. Though access to this is limited to those using the area for car parking, public access is not really restricted. Thus, a high degree of precision is needed in

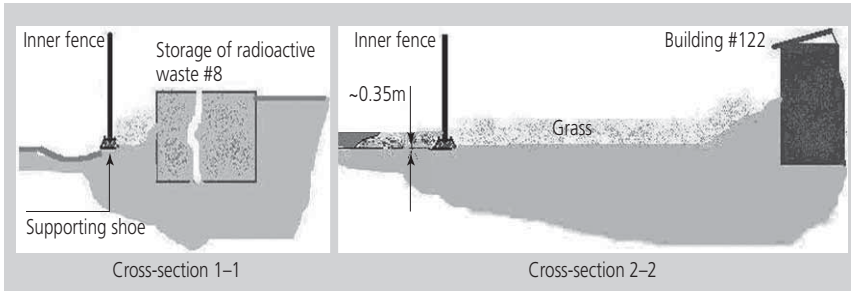


Figure 3.15. Vertical cross-sections 1-1 and 1-2 (see *Figure 3.14*) around the inner concrete wall of the storage site.

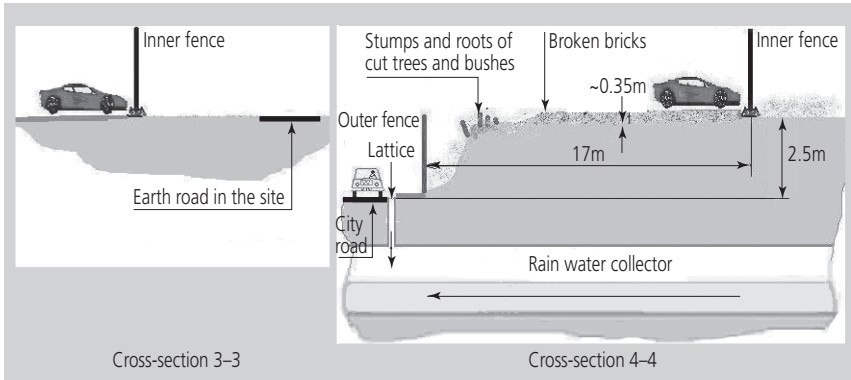


Figure 3.16. Vertical cross-sections 3-3 and 4-4 (see *Figure 3.14*) around the inner wall of the storage site.

calculating the redistribution of radionuclides in order to evaluate the impact on the local population of leaching pollutants.

The inner wall that currently surrounds the radioactive waste storage site is not a perfectly watertight barrier. There are holes of about 5–10 mm within each 2 m concrete section of the wall in sector CBAKJIHG (see *Figure 3.17*). The actual absence of a wall at the eastern part could result in water run-off toward the area of KI and radionuclide washout from the waste storage site (*Figure 3.19*). There is an opening built into the lower part of the outer brick wall for the discharge of run-off water toward the nearby municipal road. This opening (about 3 dm²) is marked as point “O” in *Figure 3.17*.

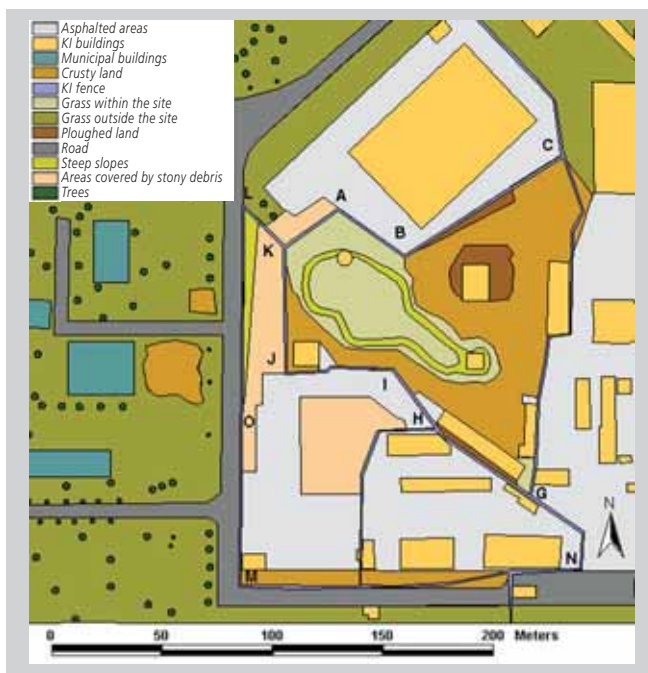


Figure 3.17. Area of the waste storage site of RRC-KI and its neighborhood. The contour CBAKJIHG is the inner wall around the waste storage site, which obstructs the formation of run-off from the site and the radionuclide washout by surface water.

3.3.2 Soil characteristics

The basic features of the ground and its surface are given in the scheme and explanations in *Figure 3.14*.

Components of the soil

The original natural relief is no longer present. It began to disappear when the topography of the area was restructured during the economic development of the site; this includes an original ravine being filled in. The absolute height of the surface of the ground ranges from 145 to 149 m.

Almost all the natural soil in the area of interest has been destroyed. Where it remains, it resembles the sod-podsolic type or urban soil (*Table 3.2*).

A layer of development debris (technogenic ground), which has been formed over several decades, covers the whole area of the site. In some cases it differs sharply from the natural bedrock that lies below; in others it does not. This ground is extraordinarily non-uniform in its structure, comprising 10–20% (and in some

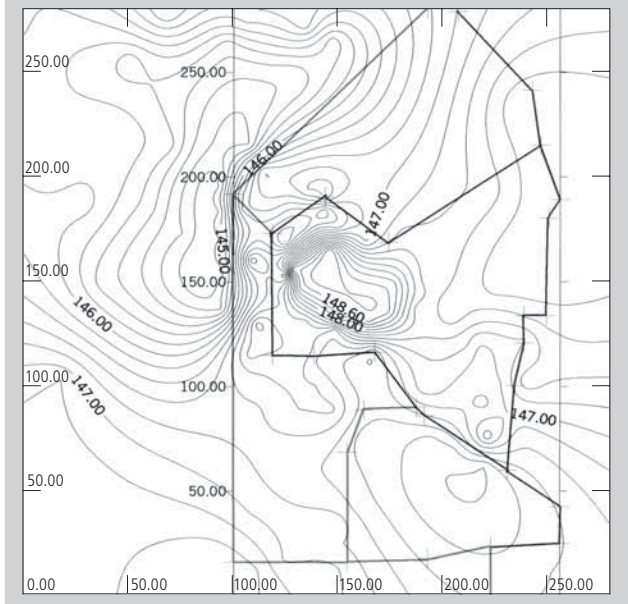


Figure 3.18. Relief of the RRC-KI radioactive waste storage site and adjacent area, and contours of the inner and the outer walls; axes X and Y are in meters; numbers on the isolines show the elevation in meters.

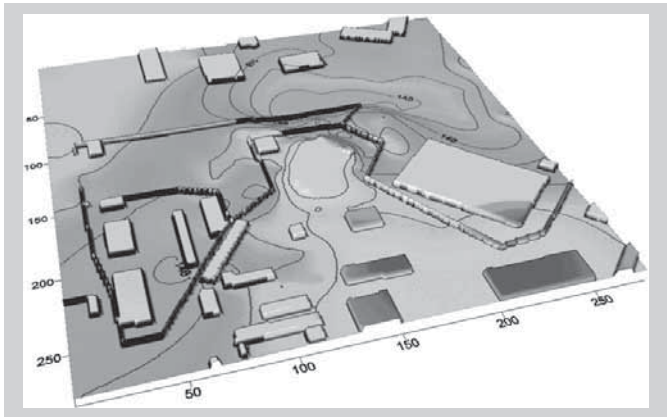


Figure 3.19. Isometric drawing of the digital elevation map, showing walls, buildings, and other constructions. The X and Y axes are in meters.

Table 3.2. Physical properties of the soil.

Physical properties	Urban soil (lawn)	Sod-podsolic
Granulometric structure, content (%) of fraction (diameter of particles <0.01 mm)	5–20	10–50
Hardness of ground (kg/cm ²)	40–45	20–25
Porosity (%)	30–40	50
Density of composition (g/cm ³)	Up to 1.8	0.9–1.2
Field moisture capacity (%)	5–14	14–20

places 30%) various artificial materials, such as broken bricks, wood, fragments of concrete and ferro-concrete items, pieces of metal hardware, and pieces of asphalt. The thickness of the technogenic layer varies widely—from several centimeters to several meters, depending on the relief and other factors.

The technogenic ground needs to be investigated thoroughly, as its composition, condition, and properties have not been quantified. For most of the area, the technogenic ground and soil areas are covered by buildings, constructions, concrete, and asphalt.

Granulometric structure of the soil

Among the basic parameters of an engineering and geological assessment of sandy bedrocks are heterogeneity and characteristics of water penetration. In most cases, the technogenic ground is composed of natural soil and rocks that were dug out of the trenches and foundation ditches when the construction and planning works were being carried out. It is thus fair to assume that its condition and properties are similar to those of the natural ground beneath it.

The natural ground comprises alluvial sand that formed the top layer of an above-floodplain terrace. The water permeability of the sand, whose particles mostly exceed 0.1 mm, is characterized by an infiltration coefficient of greater than 1 m per day. Sand with particles that are predominantly less than 0.1 mm have an infiltration coefficient of less than 1 m per day.

In *Table 3.3* data are given for the granulometric structure and infiltration factor that summarize the bulk ground bedding in a sublayer of alluvial sands of average dimension. The contents of the humus and the porosity of the urbanized soil are given in accordance with literature values.

Table 3.3. Granulometric structure of the soil.

Depth (cm)	Granulometric structure of ground						Humus (%)	Porosity (%)	Infiltration factor K_f (m/day)			
	<i>Diameter of particles (mm)</i>											
	>10	10–5	2–1	0.25–0.1	0.05–0.01	<0.005						
	5	2	1	0.25	0.1	0.05	0.01	0.005				
	<i>Urbanized soils similar to bulk ground of the site, summarized (%)</i>											
0–22	0.2–1.8	0.6–4.0	1.5–7.8	5.2–17.2	25.9–58.2	13.6–39.1	1.2–8.1	2.1–5.7	0.4–5.7	1.3	30–40	1–4
22–40										0.4		
40–50										0.4		
	<i>Natural sod–average podsollic sandy ground literature data (%)</i>											
0–20	27	50	7	2	13	2.3						
20–28	27	51	7	4	10	1.9						
28–35	56	26	8	2	7	0.2						
	<i>Natural sod–semipodsolic sandy ground literature data (%)</i>											
3–8	91	4	2	0	3	3.7						
45–55	92	3	1	1	3	0.4						
85–95	91	7	0	0	3	not present						
210–220	86	9	2	0	5	not defined						

Table 3.4a. Infiltration rate from field and laboratory studies.

Parameter	Method of calculation of infiltration factor K_f (m/day)			
	From laboratory data	Using Hazena's formula	According to restoration of the water level	From data on pumping out water*
Number of measurements	10	10	4	4
Spread of values	1.8–13.8	5.38–32.97	1.61–6.43	0.2–13.63 0.76–62.57
Average value of K_f	6.78	17.86	4.25	5.21 23.54

*Data for two boreholes shown.

Table 3.4b. Infiltration rate from literature search.

Ground	Permeability coefficient K_f (m/day)
Sands of average fineness	10–25
Fine Sand	2–10
Sandy loam	0.61–0.67
Loam	0.005–0.4

Organic content in surface soil layer

There is practically no soil cover in the area concerned. There is no layer of soil buried under the technogenic deposits. No studies of what remains of the soil have been carried out.

Whether there were organic compounds in the technogenic soil was not systematically determined. The presence of wood remains has sometimes been noted in descriptions of the technogenic deposits over boreholes.

Porosity

The porosity of sod–podsolc soil is about 50% and that of urban soil is 30–40% (Jakubov, 1999). The porosity of the technogenic deposits was not determined, nor was that of the alluvial sand bedding beneath them.

Permeability of soil surface layer

The water permeability of the technogenic deposits was not studied. The infiltration coefficients of the alluvial sand bedding beneath them vary from 1.8 to 13.8 according to laboratory data and from 1.61 to 6.43 according to data obtained by pumping out water (*Table 3.4a*). The results of the literature search for this soil property are given in *Table 3.4b*.

Moisture of the soil

The moisture of the soil was determined qualitatively by analysis of soil samples taken from the wells at the site. According to reference data (Stroganova *et al.*, 2000), the following three categories of soil moisture were used depending on the degree of moisture content (S_r):

Low	$0.0 < S_r < 0.5$
Normal	$0.5 < S_r < 0.8$
Saturated	$0.8 < S_r < 1.0$

3.3.3 Vegetation cover

Figures 3.14, 3.16, and 3.17 present a general scheme of the distribution of vegetation cover at the radioactive waste storage site and adjoining area. At the time of the case study (2003–2004) about 30% of the storage site was covered with grass. This was mostly over the waste burial places (spots) within the site. The rest of the general area is occupied by earth roads, buildings, asphalted sites, and storehouses.

Height of vegetation

The overall height of the grass at the site is low (about 20 cm). The grass areas have a grass coverage of around 70% (see also Figure 3.7). About 20% of the grassed area is covered with tansy to a height of about 40 cm.

Trees, reaching 4 m in height, were cut down in 2002. Their stumps and the bushes that have grown up to 2 m occupy the remaining 10% of the vegetated area.

The height of the trees growing on the adjoining city area vary from 4 to 8 m. The grass cover there is quite poor and of various types, with a height of 15–30 cm.

3.3.4 Geology and groundwaters

The basic mechanism for the spread of radioactive contaminants through an underground medium is radionuclide transport via groundwater (Laverov *et al.*, 1994). Hence, the analysis of water-permeable structures in the enclosing strata is of special importance to an assessment of the ecological hazard caused by the transport of radioactive contaminants in the underground medium.

As discussed above, the upper layer of the ground below the site was disturbed during the original urbanization of the area—for instance, the rainwater pipe constructed in the thalweg of Sobolevsky Creek (see Figure 3.4) that crosses the site from east to west and carries the rainwater accumulated from 400 ha of the neighboring area of the city. As also mentioned, failure of the pipe at the site or below it could cause heavy flooding of the site.

Geological characteristics of the site

As discussed, almost the whole of the top layer of the site is technogenic. Its thickness varies from several centimeters to several meters. Embedded in these technogenic deposits is an aeration zone through which atmospheric precipitation from rain and snow thaw percolates into the subsoil aquifer. As shown in *Figure 3.20*, the bottom of the technogenic deposits actually lies within the water-bearing horizon.

The underlying Quaternary strata clearly comprises three parts (*Figure 3.20*). The top part consists of alluvial sandy formations of the third floodplain terrace, the middle part of moraine loams of the Dnieper glaciation, and the lower part of alluvial–fluvioglacial (fluvioglacial) sandy, argillaceous formations. The sands of Quaternary age are predominantly quartz with feldspar and carbonates. In thin, powder-like fractions, glauconite is found as rounded grains, and ore minerals are also found in small quantities. The clay fraction of the sands consists of montmorillonite, hydromica, admixtures of magnesian silicates, halloysite, and oxides of iron. Moraine loams are spread insularly. In the ground below RRC-KI, the thickness of the loam layer varies from 0.6 to 5.8 m. Loams are brownish, fine-grained sand, and include up to 20% pebbles and detritus. They are hard, supple, wet, and dense.

Beneath the Quaternary strata are Jurassic deposits, namely, clays of the Oxford and Callovian layers. In general, the thickness of the Jurassic rocks is 16 m and more, but at some spots there are no Jurassic deposits.

Below the Jurassic sandy argillaceous deposits (or the Quaternary strata where there are no Jurassic deposits), there are coal-bearing deposits, represented by formations of the Upper Carboniferous. These are the Ratmirovsky limestones, which have been reduced to a condition of gruss (fragmented pieces) and clumps (bed depth is 6–8 m), and Voskresensky clays (bed depth is about 5 m). Below these are limestones and dolomites of the Podolsk–Myachkov horizon of the Middle Carboniferous. They are strongly karstic and broken in their upper zone.

Subsoil aquifers are confined to the Quaternary deposits; in the Carboniferous limestones there are pressurized, interstitial karstic waters.

Groundwater

The results of experimental studies obtained with the help of wells bored in the 1990s confirm that there are three aquifers under the territory of the site: above the moraine, beneath the moraine (above the Jurassic deposits), and in the Upper Carboniferous (GSPI, 2002).

The layer of moraine loams splits the Quaternary horizon into two water-bearing subhorizons. First, the upper subhorizon, which is found at 4–6 m depths

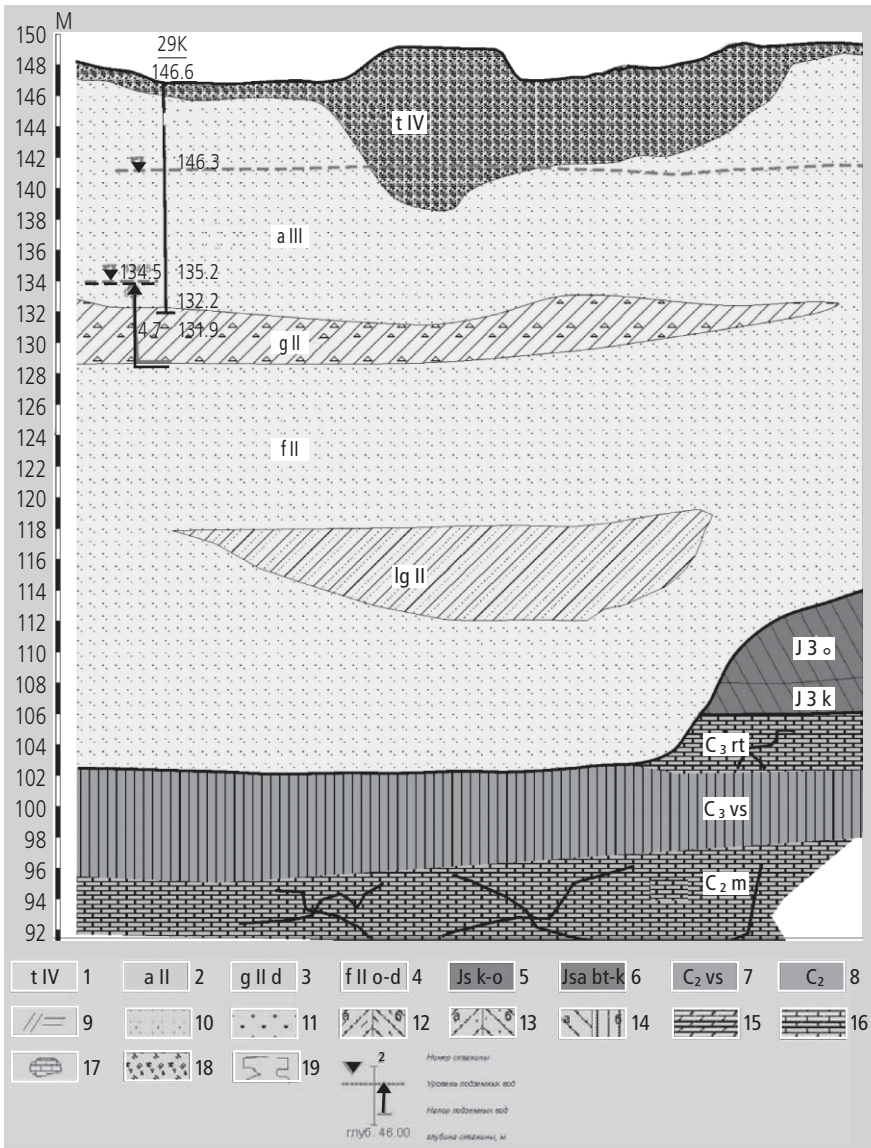


Figure 3.20. A diagrammatic geological section of the site. *Quaternary system:* 1, technogenic deposits; 2, alluvium of the third floodplain terrace; 3, moraine of the Dnieper glaciation; 4, fluvioglacial sediments. *Jurassic system:* 5, Callovian and Oxford deposits of malm; 6, Bath and Callovian deposits of malm and dogger. *Upper Carboniferous system, Kasimov layer, Krevyakin horizon:* 7, Voskresensky, thick. 8, Middle Carboniferous system. *Lithology:* 9, bank; 10, sands; 11, gravel chippings. 12, Loams: a, Quaternary; b, Jurassic. 13, Sandy loams: a, Quaternary; b, coal. 14, Clays: a, Jurassic; b, coal; 15, marl; 16, limestone; 17, limestone (disrupted); 18, gravel chippings, gruss, limestone flour; 19, loams with the clays resized by secondary processes.

below the surface and within which there is a water-bearing formation with a 6–10 m waterhead. Second, the lower horizon, which is found at 11–20 m depths, has a water-bearing formation with a water head up to 20 m and is thicker.

The uppermost aquifer, above the moraine, is free-flow and widespread beneath the whole area. Moraine loams constitute the water-confining layer. The chemical composition of this water changes over a wide range from very sweet water with mineralization of 0.2 g/l to a brackish kind with mineralization up to 2 g/l and more. Waters at this horizon contain nitrates, chlorides, phosphates, sulfates, and other substances that indicate contamination. Non-contaminated waters routinely have mineralization of 0.3–0.4 g/l, which is hydrocarbonaceous calcium.

The presence of the second aquifer—below the moraine and above the Jurassic deposits—was found in only one-fifth of all the boreholes. This horizon is a head-pressure one. Moraine loams provide the upper aquiclude, while the Jurassic clays provide the lower aquiclude, except in sectors where the Jurassic is absent, where clays of the Upper Carboniferous form the lower aquiclude. The water head in the horizon changes from 0.1 to 11.5 m. The chemical composition of these waters depends on their feed sources and is close either to the composition of the surface horizon or to the composition of the Upper Carboniferous aquifer.

The Upper Carboniferous aquifer is characterized by a high water head that amounts to between 24.4 and 25.2 m. The chemical composition of these waters was defined as hydrocarbonate–sulfate or calcium–sodium–magnesium. The degree of mineralization ranges from 0.37 to 0.7 g/l, and the temperature of the water ranges between 0 and 20°C.

Groundwater table

The ground surface is an upper boundary to the upper aquifer, and its relief is shown in *Figure 3.18*. The roof of the moraine loam is the lower boundary to the aquifer, and the base of the moraine loam is an upper boundary to the next horizon.

The permeability of the moraine loam that separates these aquifers is low. The velocities of the groundwater flow in the upper aquifer are such that contaminated waters flow outside the area where the moraine loam thins (to the northwest of it). Hence, it can be assumed that the main transfer of contaminants by underground waters occurs only in this moraine horizon. Thus, the migration of radionuclides is bounded below by a roof of moraine loams and above by the so-called depression surface, on which the water head is equal to the atmospheric pressure. The groundwater table, averaged over time, is shown in *Figure 3.20* (dashed line).

That the upper aquifer is open to the atmosphere enables a considerable fluctuation in levels of underground water to take place. The scale of the fluctuation can be estimated from long-term regular measurements of the water levels taken at the observation boreholes of the federal system for groundwater monitoring. The



Figure 3.21. Position of the nearest observation wells of the federal system for groundwater monitoring: 1, street name; 2, subway station; 3, logging area; 4, open water reservoir; 5, area covered with grass, bushes, and trees; 6, observation wells; 7, storage site for the radioactive waste at RRC-KI.

positions of the two nearest federal boreholes are shown in *Figure 3.21*. Registered changes of water level are illustrated in *Figure 3.22*.

These data indicate quite considerable changes in the groundwater table over time. The causes of this variation could be seasonal (such as the perennial cycling of the amount of atmospheric precipitation), changes in the area of watertight road coverage, and/or the activities of industrial enterprises and municipal services. However, comparison of the water level variation in two neighboring wells shows that, qualitatively, the variations coincide and that the quantitative differences are not that large. Note, though, that the distance between these two boreholes is about twice the size of the site. Thus, in any case, the bottom of the contaminated technogenic soil at the site is within the water-bearing horizon.

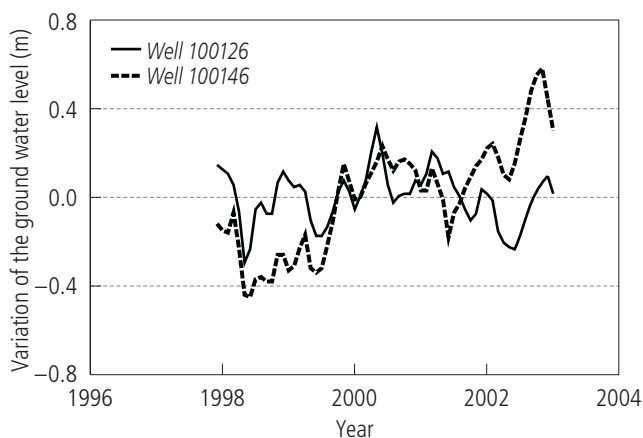


Figure 3.22. Variation in groundwater table in two federal monitoring wells near the site.

3.3.5 Weather patterns

Precipitation

Historical data on atmospheric precipitation in the Moscow area are taken from records of the Timiryazev Agriculture Academy in Moscow. Data for the period 1961–1997 are illustrated below.

Maximum accumulation of water by snow cover

Starting from the maximum height of snow cover, which in some years is up to 0.7 m before the spring thaw, and taking the density of snow to be 0.3 t/m^3 , the maximum height of the water level by the beginning of the thaw can be estimated at about 230 mm.

Maximum air temperature during the thaw

During the thaw, the maximum air temperature can reach 16°C .

Wind

Information on wind patterns in Moscow is taken from data provided by the Moscow Center for Hydrometeorology and Monitoring (see *Figure 3.23*). As part of the Russian Federal Service of Hydrometeorology and Environmental Monitoring, it regularly produces records of measurements at meteorological stations (Moscow Center for Hydrometeorology and Monitoring, 2002).

<i>Daily maximum precipitation (mm)</i>												
Jan	Feb	Mar	Apr	May	June	July	Aug	Sept	Oct	Nov	Dec	Year
19	35	19	29	34	62	100	45	47	40	27	26	100

<i>Average daily maximum precipitation (mm)</i>												
Jan	Feb	Mar	Apr	May	June	July	Aug	Sept	Oct	Nov	Dec	Year
8	9	9	12	14	24	27	21	17	16	13	10	37

<i>Number of days with various amounts of precipitation</i>										
Month	Amount of precipitation (mm)									
	≥0	≥0.1	≥0.5	≥1.0	≥5.0	≥10	≥20	≥30	≥50	≥80
Jan	26.4	20.2	14.6	10.9	2.7	0.3				
Feb	22.1	15.4	11.9	8.9	1.9	0.4	0.1	0.03		
Mar	19.5	13.8	10.6	8.3	2.0	0.4				
April	17.0	12.1	9.9	8.2	2.6	0.9	0.1			
May	16.2	12.3	10.3	8.5	3.6	1.4	0.3	0.03		
June	17.4	13.7	12.3	10.6	4.7	2.3	1.0	0.3	0.03	
July	17.6	14.2	12.6	11.0	5.0	2.6	1.0	0.4	0.06	0.03
Aug	17.4	14.3	12.0	10.5	4.9	2.4	0.7	0.3		
Sept	18.6	14.2	12.4	10.6	4.5	2.2	0.4	0.1		
Oct	19.9	15.1	12.3	10.4	4.2	1.9	0.4	0.1		
Nov	24.3	17.8	14.2	11.3	3.9	1.1	0.1			
Dec	27.6	21.6	16.0	11.9	3.4	0.7	0.03			
Year	244	185	149	121	43	17	4	1	0.1	0.03

<i>Monthly average duration of precipitation (hours)</i>												
Jan	Feb	Mar	Apr	May	June	July	Aug	Sept	Oct	Nov	Dec	Year
291	217	161	100	70	77	75	74	99	137	219	295	1816

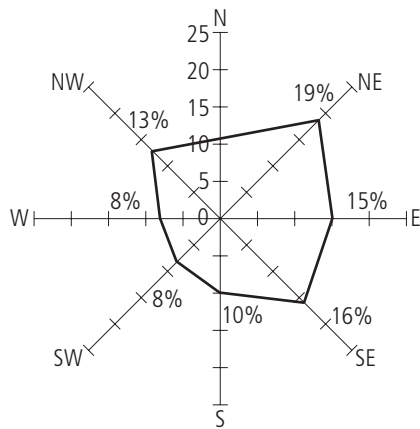


Figure 3.23. Rose diagram of wind patterns in Moscow (% of total observations).

Table 3.5. Variations in weather conditions, atmospheric stability, and velocity of wind. (Source: the “Podmoskovnaya” meteorologic station; see, for instance, Radon, 1999).

Parameter	Categories of atmospheric stability*						
	A	B	C	D	E	F	G
Recurrence of weather conditions (%)	0.86	7.37	12.72	48.76	3.74	1.61	3.13
Average wind velocity (m/s)	1.2	2.35	2.58	2.54	1.54	1.2	0.91
Calm (%)	1.36	1.31	1.51	10.86	2.09	1.02	3.63

*A to G from least to most stable (Energoatomizdat, 2002).

The predominant wind directions are southeasterly (16%), mainly during winter, and northeasterly (19%) during summer.

The variation between these weather conditions is shown in *Table 3.5*. These data do not include extreme wind events, for instance, a whirlwind that passed over the east side of RRC-KI in 1999 (fortunately over an area opposite the radioactive waste site) that resulted in many trees and branches coming down in the RRC-KI park zone.

3.4 Human patterns near to RRC-KI

3.4.1 Spatial density of the population around RRC-KI

The average density of the population in the Schukino municipality (RRC-KI is located in the central part of this area, see *Figure 3.1*) is about 10,000 persons/km². The perimeter of the area is approximately circular with a radius of about 1.5 km (Moscow Fund, 2001). The population distribution around RRC-KI is given in *Table 3.6*.

3.4.2 Age groups of the population

The age distribution of the local population is given in *Figure 3.24*.

3.4.3 Average time spent outdoors

The district neighboring RRC-KI (see *Figure 3.1*) can be considered a zone of potential pollution because of, for example, run-off transfer of radioactivity from the RRC-KI radioactive waste storage site. The district includes buildings located within 100 m of the boundaries of the site, namely, 14–16 Maksimova Street, 1, 2,

Table 3.6a. Distribution of the population within a 5 km radius of RRC-KI.

Radial zone (m)	No.	Sectors of wind direction															
		I N	II NNE	III NE	IV ENE	V E	VI ESE	VII SE	VIII SSE	IX S	X SSW	XI SW	XII WSW	XIII W	XIV WNW	XV NW	XVI NNW
100-150	1	0	0	0	0	0	0	0	0	0	0	0	0	0	163	0	0
150-200	2	0	0	0	0	0	0	0	0	0	0	593	99	65	0	0	0
200-250	3	104	0	0	0	0	0	0	0	0	0	0	0	0	0	140	221
250-300	4	100	0	0	0	0	0	0	0	0	0	0	100	0	94	0	0
300-350	5	106	0	0	0	0	0	0	0	0	323	0	106	475	62	0	0
350-400	6	0	0	0	0	0	0	0	0	0	0	364	166	0	90	0	0
400-450	7	0	0	0	0	0	0	0	0	0	333	0	0	0	0	0	0
450-500	8	0	52	0	0	0	0	0	0	0	0	0	344	98	6	0	0
500-550	9	0	44	0	0	0	0	0	0	0	0	286	168	288	0	0	0
550-600	10	0	0	0	0	0	0	0	0	0	401	255	0	81	0	0	0
600-650	11	0	0	0	0	0	0	0	0	0	0	388	0	61	0	0	0
650-700	12	66	267	0	0	0	0	0	0	0	0	273	0	0	0	0	0
700-750	13	282	0	0	0	0	0	0	0	0	0	0	105	0	0	96	0
750-800	14	109	0	0	0	0	315	0	0	0	145	311	0	0	0	229	0
800-850	15	130	0	0	0	0	0	0	0	0	110	255	0	0	0	0	0
850-900	16	400	455	0	0	0	0	0	0	0	465	263	0	00	0	258	0
900-950	17	162	0	0	0	0	0	0	0	0	222	137	0	0	0	86	0
950-1000	18	0	0	0	0	0	0	0	0	146	0	0	0	622	0	258	0
1000-1050	19	0	0	0	473	0	0	0	0	0	473	473	473	473	473	473	473
1050-1100	20	0	0	0	496	0	0	0	0	0	496	496	496	496	496	496	496
1100-1150	21	0	0	0	519	519	0	0	0	0	519	519	519	519	519	519	519
1150-1200	22	0	0	0	541	541	0	0	0	0	541	541	541	541	541	541	541
1200-1250	23	0	0	0	564	564	0	0	0	0	564	0	0	564	564	564	564
1250-1300	24	0	0	0	586	586	0	0	0	0	586	0	0	586	586	586	586
1300-1350	25	0	0	0	609	609	609	0	0	0	609	0	0	609	609	609	609
1350-1400	26	0	0	0	631	631	631	0	0	0	631	0	0	631	631	631	631
1400-1450	27	0	0	654	654	654	654	0	0	654	654	0	0	654	654	654	654
1450-1500	28	0	0	677	677	677	677	0	0	677	677	0	0	677	677	677	677
1500-1550	29	699	0	699	699	699	699	699	699	699	699	0	0	699	699	699	699
1550-1600	30	722	0	722	722	722	722	722	722	722	722	0	0	722	722	722	722
1600-1650	31	744	0	744	744	744	744	744	744	744	744	0	0	744	744	744	744
1650-1700	32	767	0	767	767	767	767	767	767	767	767	0	0	767	767	767	767
1700-1750	33	0	0	789	789	789	789	789	789	789	789	0	0	789	789	789	789

Table 3.6b. Distribution of the population within a 5 km radius of RRC-KI (continued).

Radial zone (m)	No.	Sectors of wind direction																
		I N	II NNE	III NE	IV ENE	V E	VI ESE	VII SE	VIII SSE	IX S	X SSW	XI SW	XII WSW	XIII W	XIV WNW	XV NW	XVI NNW	
1750-1800	34	0	0	812	812	812	812	812	812	812	812	812	812	812	0	0	812	812
1800-1850	35	0	0	835	835	835	835	835	835	835	835	835	835	835	0	0	835	835
1850-1900	36	0	0	857	857	857	857	857	857	857	857	857	857	857	0	0	857	857
1900-1950	37	0	0	880	880	880	880	880	880	880	880	880	880	880	0	0	880	880
1950-2000	38	0	0	902	902	902	902	902	902	902	902	902	902	902	0	0	902	902
2000-2050	39	0	0	925	925	925	925	925	925	925	925	925	925	925	925	925	925	925
2050-2100	40	0	0	947	947	947	947	947	947	947	947	947	947	947	947	947	947	947
2100-2150	41	0	0	970	970	970	970	970	970	970	970	970	970	970	0	0	970	970
2150-2200	42	0	0	993	993	993	993	993	993	993	993	993	993	993	0	0	993	993
2200-2250	43	0	1015	1015	1015	1015	1015	1015	1015	1015	1015	1015	1015	1015	0	0	1015	1015
2250-2300	44	0	1038	1038	1038	1038	1038	1038	1038	1038	1038	1038	1038	1038	0	0	1038	1038
2300-2350	45	0	1060	1060	1060	1060	1060	1060	1060	1060	1060	1060	1060	1060	0	0	1060	1060
2350-2400	46	0	1083	1083	1083	1083	1083	1083	1083	1083	1083	1083	1083	1083	0	0	1083	1083
2400-2450	47	0	1105	1105	1105	1105	1105	1105	1105	1105	1105	1105	1105	1105	0	0	1105	1105
2450-2500	48	0	1128	1128	1128	1128	1128	1128	1128	1128	1128	1128	1128	1128	0	0	1128	1128
2500-2550	49	0	1151	1151	1151	1151	1151	1151	1151	1151	1151	1151	1151	1151	0	0	1151	1151
2550-2600	50	0	1173	1173	1173	1173	1173	1173	1173	1173	1173	1173	1173	1173	0	0	1173	1173
2600-2650	51	0	1196	1196	1196	1196	1196	1196	1196	1196	1196	1196	1196	1196	0	0	1196	1196
2650-2700	52	0	1218	1218	1218	1218	1218	1218	1218	1218	1218	1218	1218	1218	0	0	1218	1218
2700-2750	53	0	1241	1241	1241	1241	1241	1241	1241	1241	1241	1241	1241	1241	0	0	1241	1241
2750-2800	54	0	1263	1263	1263	1263	1263	1263	1263	1263	1263	1263	1263	1263	0	0	1263	1263
2800-2850	55	0	1286	1286	1286	1286	1286	1286	1286	1286	1286	1286	1286	1286	0	0	1286	1286
2850-2900	56	0	1308	1308	1308	1308	1308	1308	1308	1308	1308	1308	1308	1308	0	0	1308	1308
2900-2950	57	0	1331	1331	1331	1331	1331	1331	1331	1331	1331	1331	1331	1331	0	0	1331	1331
2950-3000	58	0	1354	1354	1354	1354	1354	1354	1354	1354	1354	1354	1354	1354	0	0	1354	1354
3000-3050	59	0	1376	1376	1376	1376	1376	1376	1376	1376	1376	1376	1376	1376	0	0	1376	1376
3050-3100	60	0	1399	1399	1399	1399	1399	1399	1399	1399	1399	1399	1399	1399	0	0	1399	1399
3100-3150	61	0	1421	1421	1421	1421	1421	1421	1421	1421	1421	1421	1421	1421	0	0	1421	1421
3150-3200	62	0	1444	1444	1444	1444	1444	1444	1444	1444	1444	1444	1444	1444	0	0	1444	1444
3200-3250	63	0	1466	1466	1466	1466	1466	1466	1466	1466	1466	1466	1466	1466	0	0	1466	1466
3250-3300	64	0	1489	1489	1489	1489	1489	1489	1489	1489	1489	1489	1489	1489	0	0	1489	1489
3300-3350	65	0	1512	1512	1512	1512	1512	1512	1512	1512	1512	1512	1512	1512	0	0	1512	1512
3350-3400	66	0	1534	1534	1534	1534	1534	1534	1534	1534	1534	1534	1534	1534	0	0	1534	1534

Table 3.6c. Distribution of the population within a 5 km radius of RRC-KI (continued).

Radial zone (m)	No.	Sectors of wind direction															
		I	II	III	IV	V	VI	VII	VIII	IX	X	XI	XII	XIII	XIV	XV	XVI
		N	NNE	NE	ENE	E	ESE	SE	SSE	S	SSW	SW	WSW	W	WNW	NW	NNW
3400-3450	67	0	1557	1557	1557	1557	1557	1557	0	0	0	0	0	1557	0	0	1557
3450-3500	68	0	1579	1579	1579	1579	1579	1579	0	0	0	0	0	1579	0	0	1579
3500-3550	69	0	1602	1602	1602	1602	1602	1602	0	0	0	0	0	1602	0	0	1602
3550-3600	70	0	1624	1624	1624	1624	1624	1624	0	0	0	0	0	1624	0	0	1624
3600-3650	71	0	1647	1647	1647	1647	1647	1647	0	0	0	0	0	1647	0	0	1647
3650-3700	72	0	1670	1670	1670	1670	1670	1670	0	0	0	0	0	1670	0	0	1670
3700-3750	73	0	1692	1692	1692	1692	1692	1692	0	0	0	0	0	1692	0	0	1692
3750-3800	74	0	1715	1715	1715	1715	1715	1715	0	0	0	0	0	1715	0	0	1715
3800-3850	75	0	1737	1737	1737	1737	1737	1737	0	0	0	0	0	1737	0	0	1737
3850-3900	76	0	1760	1760	1760	1760	1760	1760	0	0	0	0	0	1760	0	0	1760
3900-3950	77	0	1782	1782	1782	1782	1782	1782	0	0	0	0	0	1782	0	1782	1782
3950-4000	78	0	1805	1805	1805	1805	1805	1805	0	0	0	0	0	1805	0	1805	1805
4000-4050	79	0	1828	1828	1828	1828	1828	1828	0	0	0	0	0	1828	0	1828	1828
4050-4100	80	0	1850	1850	1850	1850	1850	1850	0	0	0	0	0	1850	0	1850	1850
4100-4150	81	0	0	1873	1873	1873	1873	1873	0	0	0	0	0	1873	0	1873	1873
4150-4200	82	0	0	1895	1895	1895	1895	1895	0	0	0	0	0	1895	0	1895	1895
4200-4250	83	0	0	1918	1918	1918	1918	1918	0	0	0	0	1918	1918	0	1918	1918
4250-4300	84	0	0	1940	1940	1940	1940	1940	0	0	0	0	1940	1940	0	1940	1940
4300-4350	85	0	0	1963	1963	1963	1963	1963	0	0	0	0	1963	1963	0	1963	1963
4350-4400	86	0	0	1986	1986	1986	1986	1986	0	0	0	0	1986	1986	0	1986	1986
4400-4450	87	0	0	2008	2008	2008	2008	2008	0	0	0	0	2008	2008	0	2008	2008
4450-4500	88	0	0	2031	2031	2031	2031	2031	0	0	0	0	2031	2031	0	2031	2031
4500-4550	89	0	0	2053	2053	2053	2053	2053	0	0	0	0	2053	2053	0	2053	2053
4550-4600	90	0	0	2076	2076	2076	2076	2076	0	0	0	0	2076	2076	0	2076	2076
4600-4650	91	0	2098	2098	2098	2098	2098	2098	0	0	0	0	2098	2098	0	2098	2098
4650-4700	92	0	2121	2121	2121	2121	2121	2121	0	0	0	0	2121	2121	0	2121	2121
4700-4750	93	0	2144	2144	2144	2144	2144	2144	0	0	0	0	2144	2144	0	2144	2144
4750-4800	94	0	2166	2166	2166	2166	2166	2166	0	0	0	0	2166	2166	0	2166	2166
4800-4850	95	0	2189	2189	2189	2189	2189	2189	0	0	0	0	2189	2189	0	2189	2189
4850-4900	96	0	2211	2211	2211	2211	2211	2211	0	0	0	0	2211	2211	0	2211	2211
4900-4950	97	0	2234	2234	2234	2234	2234	2234	0	0	0	0	2234	2234	0	2234	2234
4950-5000	98	0	2256	2256	2256	2256	2256	2256	0	0	0	0	2256	2256	0	2256	2256

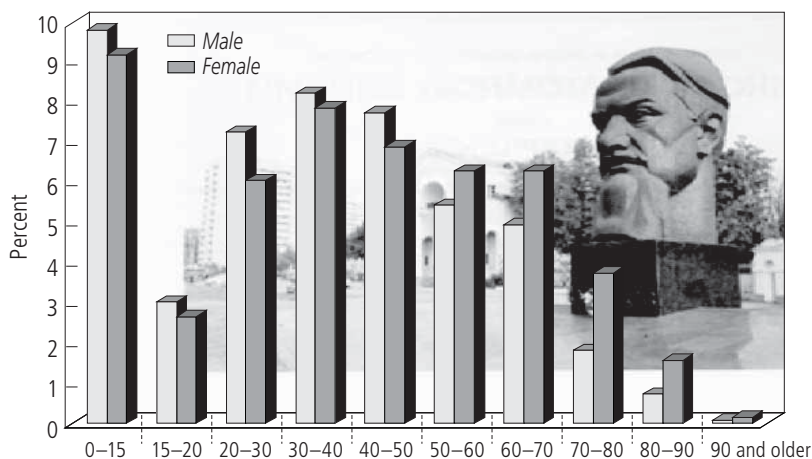


Figure 3.24. Age distribution of the local population.

and 4 Gamaley Street, and 2 Rogova Street. The aggregate number of inhabitants in these buildings was 1,447 as of March 2003, according to the Municipal Council of Schukino.

The following factors define the average time spent by the local population outdoors and in the area neighboring the RRC-KI radioactive waste storage site:

- Age structure of the inhabitants of the neighboring houses ;
- Ratio of adults to children, which is about five;
- Proximity of three restoration areas located outside the zone that could be polluted, namely:
 1. October stadium located 0.8 km to the west,
 2. Park around the RRC-KI palace of culture located 0.2 km to the south,
 2. Park zone located 0.3 km to the north behind 14–16 Maksimova Street.

The average time spent by the local population outdoors in the potentially polluted area neighboring the RRC-KI radioactive waste storage site is about 1.5 hours/day. The distribution of this period with age is given in *Table 3.7*.

An assessment of the above data shows that most of the groups that spend time walking (7–17 years of age and some of the over-60 group) spend their free time in recreational areas (e.g., outside the potentially polluted zone).

Table 3.7. Time spent outdoors by age groups.

Age (years)	Younger						
	than 1	1–2	2–7	7–12	12–17	17–60	Over 60
Time spent outdoors (hours)	1.5	2	3	1	0.5	0.3	1.5

3.4.4 Traffic intensity

In rush hours, up to 3,000 vehicles per hour use the city roads (Maksimova Street and Gamaley Street) adjoining the RRC-KI radioactive waste storage site. According to Russian municipal experts, 3,000 would be the maximum number, while around 700 vehicles per hour would be the average number in daytime (between 7 A.M. and 9 P.M.).

3.5 Run-off modeling

3.5.1 Choice of main scenarios for modeling

The environmental and radiological characteristics of the RRC-KI radioactive waste storage site, collected and collated within the TACIS and ISTC projects and presented above, are far from comprehensive—a reflection of the fact that the exploratory studies of site characteristics were insufficient. Also contributing to uncertainties in the data used as a basis for modeling the run-off transfer of radioactivity within the site and the washout of radioactivity from the site are 1) the incompleteness of the historical records as to what was buried at the site and the condition it was in and 2) disturbance from the recently started site-rehabilitation program.

In these circumstances modeling needs to be oriented toward a scoping analysis rather than a site-specific analysis. The scoping analysis should focus on the evaluation of the scale and possible limits of the redistribution and washout phenomenon; it should thus provide a first insight into the seriousness of the situation regarding run-off transfer. It should also produce recommendations for any further experimental studies needed to reduce uncertainties.

This approach defined the choice of run-off scenarios that were examined within the Moscow case study. The choice was made on the basis of the analysis of three main factors with an impact on the outcome of the modeling, namely:

- Precipitation rate;
- Soil properties within the site;

- Effectiveness of the inner wall of the site as a mechanical barrier against run-off transfer of radioactive waste to outside the storage site.

Precipitation rate

As shown by the meteorological records for the Moscow area presented in Section 3.3.5 on weather patterns, the heaviest rain to occur in Moscow during the past 37 years resulted in 100 mm/day precipitation. This figure was taken as an upper limit to characterize any “heavy rain or downpour” that might occur over the site.

The average maximum daily precipitation over a year presented in the same section is 37 mm/day. Thus, 35 mm of precipitation was taken as the lower limit of rain considered in the simulation of run-off.

Soil properties within the site

The rate of soil erosion as a result of run-off depends on the role of water infiltration of the ground. A crucial parameter for estimating the infiltration processes is saturated hydraulic conductivity. The range of values for this parameter in the Russian report (Gorlinsky, 2003) is extremely wide—the minimum value given is 0.2m/day, while the highest value is 62 m/day.

After careful discussion of that uncertainty, it was decided to apply an expert judgment that the site soil covered by grass resembles the “urbanosem” soil type. According to the data given in Section 3.3.2 on soil characteristics (see *Table 3.3*), the range for simulations of the run-off from this part of the site was defined as 150 mm/hour (high hydraulic conductivity) to 40 mm/hour (low hydraulic conductivity).

According to the land-use maps provided in the Russian report (Gorlinsky, 2003), the rest of the site is characterized by increased human activity that has resulted in soil compaction and a decrease in hydraulic conductivity. Thus, the hydraulic conductivity in these areas was assumed to be equal to the minimum of the considered range, 40 mm/hour, for all scenarios. In *Figure 3.17* these areas are shown as “hard land.”

Saturated soil moisture within the site was defined as being 35% (Gorlinsky, 2003). The preliminary analysis showed that the amount of radioactivity washed out from the site is strongly related to the initial soil moisture. A higher initial soil moisture might result in a lower infiltration and correspondingly higher rate of surface run-off. Thus, to explore the impact of the initial soil moisture on radioactivity washout from the site, two limits were considered: a low initial soil moisture (“dry soil”) and a high initial soil moisture (“wet soil”). The former can occur naturally when there is rain after a long period of drought. The latter refers to the

opposite situation in which heavy rain occurs after a lengthy period of drizzle. In this situation the increased soil moisture should result in decreased infiltration and consequently increased surface water run-off and increased radioactivity washout and redistribution. Taking into account the physical impossibility for the water to fill all the possible soil pores, the initial soil moisture for “wet soil” conditions was accepted as 80% of the saturated soil moisture.

Inner wall as a mechanical barrier to run-off transfer of radioactive waste outside the storage site

As discussed above, the inner wall (see *Figure 3.17*) that currently surrounds the radioactive waste storage site is not a perfect watertight barrier. The wall section CG is not an obstacle to surface run-off (Gorlinsky, 2003) or to radionuclide transport toward the area of the institute.

There are tiny holes up to 5–10 mm diameter within each 2 m concrete section of the wall on the contour KJIHG. However, such small perforations in the wall could not be considered in the frame of the available run-off codes. Instead, it was decided to simulate a situation in which a particular concrete section of the wall is removed, for instance, for repair or because the section bed is totally eroded and thus does not obstruct water flow at all.

A preliminary analysis of the storm-water run-off field on the site and its surroundings reveals that a few sections of the wall are subject to increased water erosion and, correspondingly, to a higher risk of being destroyed or repaired more often than other sections. The most vulnerable spots are represented by the letters “K” and “I” on *Figure 3.25*. *Figure 3.26* also shows the water run-off field over the digital elevation map. Thus, it was decided to consider two scenarios in which there is a 1 m gap in the inner wall at either point K or I (the “K” scenario and the “I” scenario).

The case in which the wall on the contour KJIHG is considered watertight is called the “No hole” scenario. However, the actual absence of the wall on the eastern part of the wall (sector CG) could result in water run-off toward the area of RRC-KI and radionuclide washout from the waste storage site area.

Finally, to examine the role of the wall as a simple mechanical barrier the “No fence” scenario was included in the simulations. This scenario also represents the case of “no effective wall,” when the wall basement is severely eroded and thus does not block run-off water.

A scheme of the combination of different features in the full set of scenarios used for the simulations is presented in *Figure 3.27*.

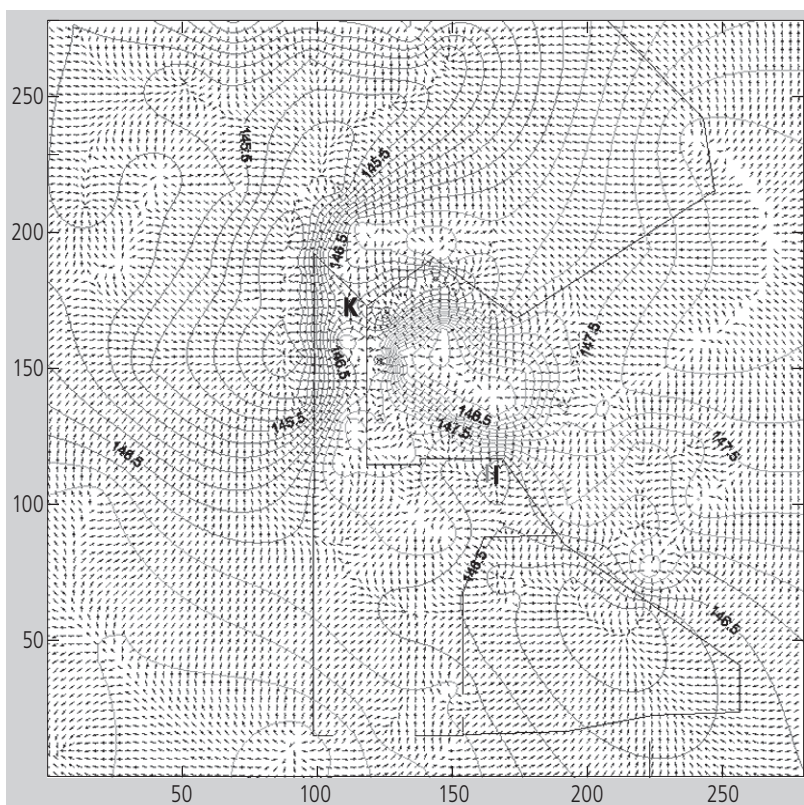


Figure 3.25. Storm-water run-off field for the waste storage site of RRC-KI and its surroundings. Walls around the site are shown as black lines. Letters K and I indicate the holes in the inner wall for scenarios “K” and “I,” correspondingly.

3.5.2 State of the art of soil erosion modeling and contaminant redistribution

The pathways of radionuclide distribution in the environment are relatively well studied and described in the literature. The number of software packages and models that describe these processes is already high and constantly increasing. However, the particular problem of radionuclide redistribution from nuclear waste sites within the urban environment has not been studied.

The vast majority of the models developed are devoted to the redistribution of radionuclides within large natural catchments and ecosystems. This is because these models are basically modifications of the models that describe soil erosion processes for large watersheds or tillage. Among the main soil erosion models widely recognized and used are EUROSEM, GLEAMS (CREAMS), (R)USLE, LISEM, WEPP, KINEROS, ANSWERS, AGNPS, MEDALUS, EPIC, etc.

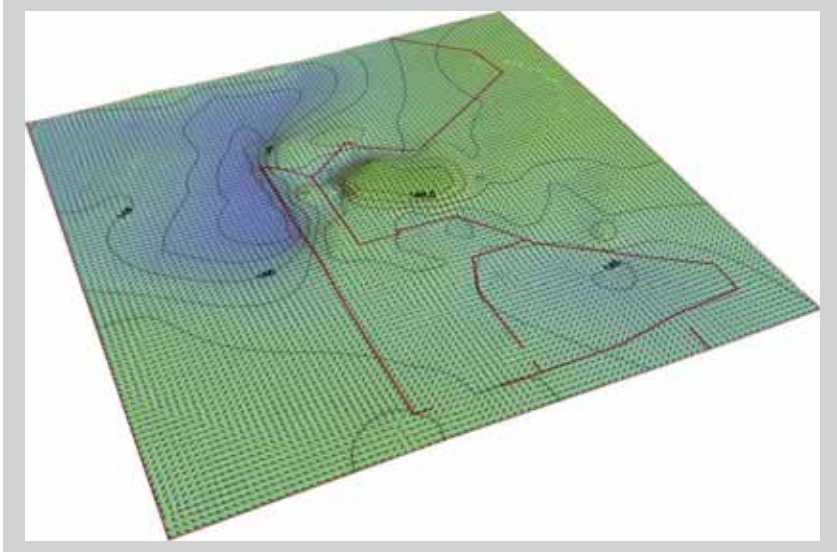


Figure 3.26. Water run-off fields over the digital elevation map. The red line over the landscape shows the location of the inner and outer RRC-KI walls.

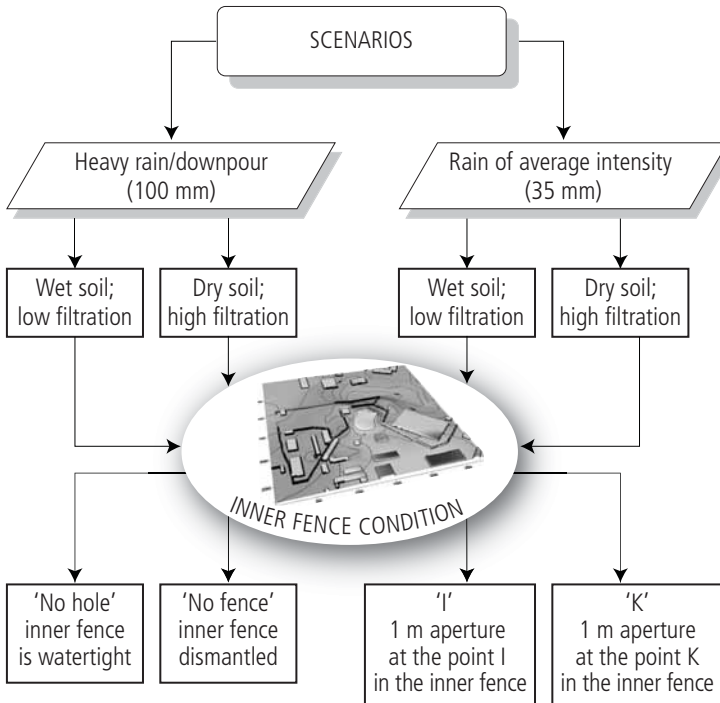


Figure 3.27. Illustration for chosen modeling scenarios.

Two general approaches to modeling soil erosion are known: empirical and physical. Models that follow an empirical approach (USLE and RUSLE) require only a small number of parameters and are easy to apply. However, these empirical models are lumped and oversimplify the erosion processes that occur at small scales (OCRWMA, 2000). Physically based models (LISEM, WEPP, EPIC, etc.) require many more parameters, but physically represent the processes in a more correct way.

There are two possible ways to model soil erosion over time: continuous and individual-based, within-storm modeling. Models such as CREAMS and WEPP use a continuous approach to model the daily seasonal changes in soil characteristics. In this way the conditions at the start of each rainstorm are predicted. The problem with continuous simulations is that they require a large amount of input data on the meteorology and land-use conditions over the year. Thus, they are used to model a large number of events that produce only small amounts of run-off and soil loss. Although they can sometimes be run for individual storms, they simulate the total storm soil loss only and assume a steady-flow profile along the surface. They do not model the peak sediment discharge or treat the pattern of events within a storm. On the contrary, within-storm modeling is more compatible with the equations used in process-based models to describe the mechanics of erosion. These equations cannot be applied to average conditions but require instantaneous conditions.

Many of the factors that influence erosion and sediment redistribution have considerable spatial variation and cannot be described by a single average value. Many models treat an area as a single unit or as a limited set of units with uniform characteristics. If the spatial variation is to be taken into account, a raster- (cell-) based model must be used. Using this approach the area is divided into a number of equal cells. Each cell has a number of characteristics, such as elevation, moisture, slope, etc., according to which the flow and sediment transportation is calculated.

As specified already, the aim of this study is to model the redistribution of radionuclides within the RRC-KI storage site, in both their soluble and particulate forms, and their washout to the municipal area as a result of extreme historical meteorological conditions, such as heavy rain. Taking into account the rather specific environment around the storage site, the scale and the location of the site, the necessity of tracing the fate of detached contaminated soil particles, and the need for high precision in the results, the range of applicable models shrinks drastically. For instance, many models (RUSLE, USLE, WEPP, etc.) account only for the average annual soil loss by particular watersheds, while others are not applicable to a single event or small-scale catchments.

Since the Chernobyl accident many models of radionuclide redistribution have been developed. However, most of these modeling efforts have focused on the

transfer from terrestrial to aquatic ecosystems (Monte, 1995; Schnoor, 1996; Bonniwell, 1999; etc.) or to their vertical redistribution within the soil (Chibowski and Mitura, 1995; Slavik, 2000; Panin, 2001). The former consider dissolved radionuclide transport only. Spatially distributed erosion and sedimentation models were not widely used to evaluate radionuclide transport from and within water catchments. Nevertheless, some radionuclides were widely used as tracers in many experimental soil erosion studies (Bonniwell, 1999; FAO/IAEA, 2001; Theocharopoulos, 2003; Walling *et al.*, 2003).

3.5.3 Model description

PCRaster

To combine a detailed spatial analysis with dynamic modeling of the soil erosion process and radionuclide redistribution, and also to meet the criteria given above, requires a geographic information system (GIS) software package that not only enables traditional spatial analysis, but also allows system behavior to be traced over time. There are two possible options to work with. First is the commonly recognized and widely used software package, ArcView. The special extension to this package, called Model Builder, allows a dynamic model using a GIS database (such as digital elevation map, land-cover map, etc.) to be constructed and run to observe the possible scenarios of radionuclide redistribution under different environmental conditions. However, this approach needs the existing mathematical models of radionuclide redistribution to be transcribed into the special ArcView script language.

The second choice is to use the raster GIS PCRaster software developed at the Department of Geographical Sciences of Utrecht University (Karssenbergh *et al.*, 2003). The PCRaster software is a GIS that consists of a set of computer tools to store, manipulate, analyze, and retrieve geographic information. PCRaster enables us to construct GIS-embedded environmental models by means of an easy-to-understand, high-level modeling language. The execution of the models within the raster GIS environment accomplishes a full integration between the geographic database and the various models and enables a flexible choice of submodels. There is a bank of existing routines and submodels developed for different environmental problems. One of the models developed that is appropriate for use within the current project is LISEM (Limburg Soil Erosion Model), along with a number of radionuclide redistribution submodels.

Taking into account the specific requirements for the model imposed by the site characteristics, LISEM was selected for the modeling stage, along with the extended data-analysis tools offered by ArcView software.

LISEM

LISEM is a physically based hydrologic and soil-erosion model that exists in two versions, one integrated within the PCRaster package and the other a user-friendly, stand-alone version. However, incorporation of the different submodels is possible only within the PCRaster version.

The ability of LISEM to cope with soil-erosion modeling has been tested against experimental data obtained by field measurements within the frameworks of many research projects all over the world (Takken *et al.*, 1999; van der Perk, 2000; Jetten, 2002; Hessel *et al.*, 2003a; Liu *et al.*, 2003). It has been accepted as giving adequately realistic results, although some limitations to its application were noticed (Roo and Jetten, 1999). LISEM is a raster-based model and can therefore simulate detailed spatial patterns of erosion.

LISEM accounts for rainfall, interception, surface storage in micro-depressions, infiltration, overland flow, splash erosion by rainfall, erosion by overland flow, and transport capacity of the flow. *Figure 3.28* gives a schematic overview of the processes considered.

Run-off formation in the model begins with raindrops reaching the soil surface. The initial stage of run-off formation includes modeling the kinetic energy of falling droplets of rain. From *Figure 3.28* it is clear that falling droplets are considered in two different ways: interception and direct throughfall to the surface. Interception is that part of the precipitation that wets or adheres to the surface of objects and vegetation above the ground. This variable in the model is calculated on the basis of information on vegetation cover and leaf area index that corresponds to the particular type of vegetation. Where vegetation cover is not present, the energy of falling raindrops detaches soil particles and collects both them and contaminants deposited on the surface. Soil aggregate stability is used to calculate the rate of rainfall detachment. The next stage that the falling water should pass through before it forms the surface run-off is to fill the micro-depressions in the local surface to form small puddles, which is called depression or surface storage. The final stage, which occurs at the same time as depression storage, is infiltration into the soil. The infiltration depends on the permeability characteristics of the soil (soil hydraulic conductivity) and the soil moisture content.

The flow erosion calculated in the model is divided into two parts: sheet over-flow (inter-rill) erosion and channel (rill) erosion. The network of possible rills formed during the rain simulation is calculated on the basis of the digital elevation map. The channels (or rills) formed can have their own flow and surface characteristics, such as flow resistance (Manning's N) or soil cohesion along the rill route.

Although it is possible to choose alternative equations to describe water infiltration into the soil, such as the Richardson, Green and Ampt, or Holton equations,

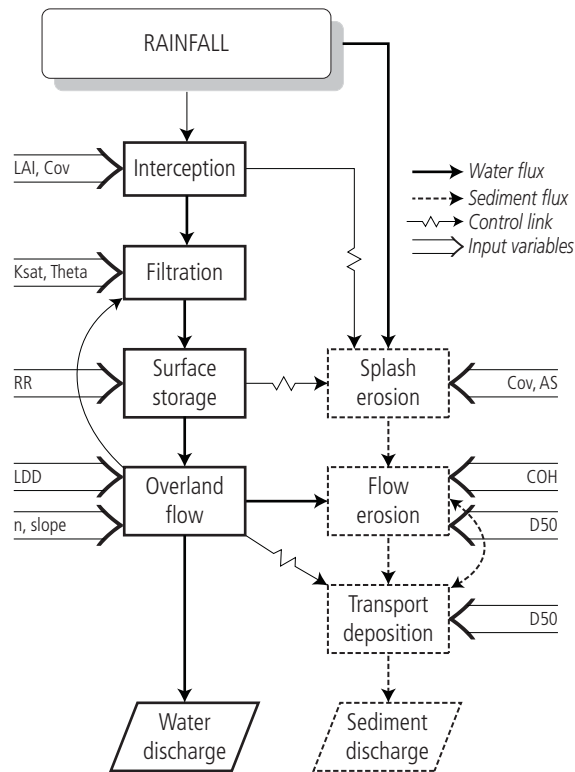


Figure 3.28. Simplified flowchart of LISEM (Jetten, 2002): LAI, leaf area index; Cov, fraction of the soil covered by vegetation; Ksat, saturated hydraulic conductivity; theta, initial soil moisture; RR, surface random roughness; LDD, local drain direction; n, Manning’s N, slope derived from the digital elevation map; AS, aggregate stability; COH, soil cohesion; D50, median value of diameter of soil particles in the top soil layer.

the infiltration model implemented in the radionuclide redistribution modification of LISEM is a one-layer Green and Ampt model. This does not limit the application of the model to the case under consideration, as, according to the opinions of RRC-KI experts, the artificial urban soil within the urban landscape in general and on the RRC-KI site in particular, is considered to be homogeneous within the first soil layer. This layer of artificial soil on the site has a depth of more than 2 m.

All the other basic equations that describe the processes of detachment and transport are identical to the equations used in the European Soil Erosion Model (EUROSEM), another well-known and widely recognized erosion model (Botterweg *et al.*, 1998; Klik, 1998; Morgan *et al.*, 1998).

The input for LISEM consists of a rainfall time-series and maps of catchment characteristics, such as vegetation cover, soil characteristics, etc. The total number of input maps required is 30. The output from the model is a few maps that present the erosion and deposition processes within the area under consideration and various time-series for the catchment, such as sediment concentration or water discharge.

A modification of LISEM to model the radionuclide redistribution exists only in the PCRaster version. This modification of the basic LISEM package was developed by the authors of LISEM, M. van der Perk and O. Slavik, at the Utrecht Center for Environment and Landscape Dynamics at Utrecht University, the Netherlands, in cooperation with a number of other European institutions within the framework of the SPARTACUS project founded by the INCO-COPERNICUS program (Kiviva and Zheleznyak 1999; van der Perk, 2000). It calculates radionuclide transport through a landscape based on sediment transport.

In addition to the basic initial data input for LISEM, the radionuclide modification requires a few parameters and maps to clarify the behavior of the radionuclide under consideration. In particular, maps of both the initial contamination and the radionuclide distribution coefficients should be provided. Furthermore, the set of output variables includes maps of deposited particulate activity and of soluble radioactivity in water bodies, along with a set of time-series, such as soluble and/or particulate radionuclide concentrations at the catchment outlet and/or suboutlets.

The Appendix contains the applied model code in PCRaster modeling language, as used for ^{137}Cs calculations. As all the erosion processes under consideration are exactly the same for both radionuclides, the simulation of ^{90}Sr washout is the same, except for different distribution coefficients and the map of initial contamination.

One of the characteristic features of any cell-based transport model is the special treatment of material movement from one cell to another. All these models consider this transfer on the basis of a digital elevation map. This leads to flow concentration within the cells that have the lowest elevation value and the formation of concentrated water streams. LISEM is not exclusive in this sense. There is only one possible outflow from a particular cell, which leads to the formation of a narrow (cell-wide) water flow and sedimentation redistribution path. *Figure 3.29* illustrates this principle.

A local drain-direction map is one of the inputs to LISEM that is derived from digital elevation maps. According to this map each cell is connected to its neighboring eight cells in only one way, and this defines the unique direction in which the material should flow out in the next time step. Outflow to a number of cells is not possible even if their characteristics are equal. As a result, moving material can be accumulated from a large catchment area and concentrated to within a narrow flow.

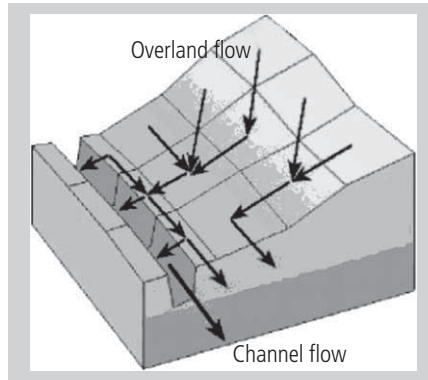


Figure 3.29. Overland and channel flow in LISEM based on the local drain-direction structure.

Uncertainties of the model applied

The selection of hydraulic conductivity as a parameter for sensitivity analysis is also justified by other authors. For example, Hessel *et al.* (2003b) claim that hydraulic conductivity is one of the most important calibration factors in LISEM.

It becomes clear that LISEM does not work well for environments with rather steep slopes within the digital elevation map—a specific feature of the model also mentioned by Hessel *et al.* (2003c). The reason for this shortcoming is that some processes described in LISEM were developed mainly with relatively low-grade slopes in mind. In particular, grid kinematics wave routing cannot cope with abrupt changes in flow conditions. For the uncertainties within both the digital elevation map and initial data, the effect of such an error is amplified. However, such a shortcoming is common for all the soil erosion models, as their main goal is to predict soil loss from fields.

One of the main problems with the model applied is the concentration of the flow accumulated from a large catchment area within a narrow flow, the maximum width of which cannot exceed the cell size. As the cell size in the model selected is equal to 1 m, the width of the rill formed is also equal to 1 m. This leads to increased rates of water discharge and, correspondingly, to higher soil erosion and radionuclide redistribution.

At the same time, the model cannot consider a pond in a local depression larger than 1 m in diameter. In other words, water accumulated within one cell cannot spread around other than in the one direction predefined by the local drain-direction map. As mentioned above, the local drain-direction map is calculated once prior to the simulation and remains unchanged throughout the simulation. Such an algorithm does not take into account the changes in local elevations caused by erosion

or the deposition of eroded material in some places. In terms of the simulation outputs, these features can result in an overestimated deposition within a particular cell. However, averaging over the adjacent area could significantly reduce this uncertainty. It was this approach that we applied in the study.

However, in principle, this situation can be radically improved only by modification of the initial code in a way that ensures recalculation of the local drain direction at each time step to incorporate changes in the digital elevation map during simulations. We hope that this will be done in further studies aimed at a more site-specific simulation.

3.5.4 Input data used

A physically based model always requires a wide range of initial data. The same applies to physically based soil-erosion models. LISEM alone requires at least 24 separate maps that describe catchments, vegetation, soil surface, infiltration, and erosion- and/or deposition-related characteristics.

The initial data should be supplied to LISEM in two different ways. The parameters that do not have spatial variation, such as soil bulk density, radionuclide distribution coefficients, or raindrop kinematic energy, are accounted for by changing values within the shell interface. The spatial input maps for LISEM have to be organized according to the PCRaster database structure and should be within the PCRaster GIS format only.

The information package received from RRC-KI experts (Gorlinsky, 2003) contained some maps with separated land-use categories, digital elevation maps, and contamination maps that were in MapInfo GIS format. The maps received were converted into ArcView format and a single land-use map was generated on the basis of the different maps. The derived map was used to create the set of initial maps for each of the 16 scenarios.

The values for the required parameters obtained either from the RRC-KI information package or from the available literature are shown in *Table 3.8*. The table also gives short explanations of the parameters used and their ranges, as suggested by the model authors.

One of the parameters that was not defined in the information package received from RRC-KI experts is Manning's N , which is used in the model to describe the resistance to flow. For a sheet flow (the flow over a plane surface), the friction value (Manning's N) is an effective roughness coefficient that also depends on obstacles, such as litter, crop ridges, and rocks, and the erosion and transportation of sediments, etc. Manning's N also varies with the depth flow.

The specific features of the site under consideration and the preliminary calculations enabled us to state that the depth of waterflow on most of the site can be considered as sheet flow. As Manning's N cannot be measured directly, expert

Table 3.8a. Parameters used to model the radioactive waste storage site.

Parameter	Definition	Range, units ^a	Values for different land-use categories ^b
Leaf area index	The total area of all leaves of plants relative to the ground surface within a given area	0–12, –	Grass, 1 Trees, 4 Other, 0
Fraction of soil covered by vegetation		0–1, –	Grass, 0.3 Trees, 1 Other, 0
Vegetation height	Height of vegetation cover on site and neighboring territory	0–30, m	Grass, 0.2 Trees, 5.2
Aggregate stability	Median number of drops to decrease the aggregate by 50%	0.00001–200 (for the ground that, in principle, is subject to erosion)	Hard land, 50 Non-erodible (road, asphalt), 9999 Grass, 10
Soil cohesion (COH)	COH is an index of soil resistance related to the ability to resist external forces	kPa Limitations: COH + COHADD \geq 0.196	Grass, ploughed land, 3 Steep, 2 Hard land, 50 Non-erodible (road, asphalt), 9999
Additional cohesion by vegetation roots (COHADD)	Additional resistance to external forces by vegetation roots	kPa Limitations: COH + COHADD \geq 0.196	Grass, steep, 1 Ploughed land, 0 Hard land, 0 Other, 0.02
Manning's N for the soil surface	Manning's N is a dimensionless number that defines the flow resistance of a unit of bed surface. Resistance is a function of particle size, bed shape, etc.	0.001–10, –	Varies from 0.02 (hard land on site) to 0.1 (lawn outside the site)

Table 3.8b. Parameters used to model the radioactive waste storage site (continued).

Parameter	Definition	Range, units ^a	Values for different land-use categories ^b
Random roughness for the soil surface	Standard deviation of the micro relief heights	0.05–20, cm	Road, 0.1 Other, 1
D50 value of the soil	Median of the texture of the soil	25–300, nm	50
Saturated hydraulic conductivity	The constant rate at which a saturated soil (or sand) is able to transmit water downward	0–1000, mm/h	Grass on the site low hydraulic conductivity, 40 high hydraulic conductivity, 150 Lawn outside the site, 40 Hard land on site, 40 Stone debris, 150 Roads, other, 0
Saturated volumetric soil moisture content	Volume of water in saturated soil divided by the total volume of the soil	0–1, –	0.35
Initial volumetric soil moisture content	Initial volume of water in soil divided by the total volume of the soil	0–1, –	Dry scenario, 0.14 Wet scenario, 0.28
Soil water tension at the wetting front	Soil water tension measures the force with which water is retained by the soil	0–1000, cm	17
Soil depth of first layer	Depth of the first soil layer (needed for infiltration calculations)	0–... , mm	Grass, land, 200 Stone debris, 100
Equilibrium distribution coefficient of Cs in water and in background soil	Relationship of the concentration of ¹³⁷ Cs in the water to the concentration of ¹³⁷ Cs in the background soil when in equilibrium	0.28–4.6, m ³ /kg	1.7

Table 3.8c. Parameters used to model the radioactive waste storage site (continued).

Parameter	Definition	Range, units ^a	Values for different land-use categories ^b
Equilibrium distribution coefficient of Cs in water and in suspended soil particles	Relationship of the concentration of ¹³⁷ Cs in the water to the concentration of ¹³⁷ Cs in the suspended soil particles when in equilibrium	0.28–4.6, m ³ /kg	3.7
Equilibrium distribution coefficient of Sr in water and in background soil	Relationship of the concentration of ⁹⁰ Sr in the water to the concentration of ⁹⁰ Sr in the background soil when in equilibrium	m ³ /kg	0.4
Equilibrium distribution coefficient of Sr in water and in suspended soil particles	Relationship of the concentration of ⁹⁰ Sr in the water to the concentration of ⁹⁰ Sr in suspended soil particles when in equilibrium	m ³ /kg	1.3
Thickness of active layer of interaction between run-off water and top soil		0–... , mm	5 (default value)
Soil density		kg/m ³	1800
Porosity	The total volume of voids per unit volume of porous material	0.01–0.60, cm ³ /cm ³	0.4

^a... for dimensionless parameter.

^b values for the parameters are given according to the land-use categories defined by RRC-KI experts (see *Figure 3.19*). If the specific map is not mentioned, the value is unique for the whole area.

estimates are needed. The literature available was used to define this value, but it gave a wide range of possible values. Moreover, in the manual for EUROSEM, Manning's N is considered to be a calibration parameter. In the StormSHED manual (BOSS International, 2001) the values for sheet flow over asphalt ranged from 0.011 to 0.05, while for short lawns the value is 0.15.

Calibrated values of Manning's N for LISEM are given in Takken (1999). According to this research, Manning's N values for asphalted roads and buildings should be about 0.01 and for grassland up to 0.2. While the urban lawn can be defined to some extent as a grassland, vegetation cover on the site is considered to be sparse and rare (Gorlinsky, 2003). Given the above considerations, Manning's N was accepted as within the range 0.01–0.1, with the minimum assigned to asphalted surfaces on the site and the maximum to areas covered with the grass outside the area of the site.

Another crucial parameter needed to estimate the infiltration processes is saturated hydraulic conductivity. The range of values for this parameter in the Russian report (Gorlinsky, 2003) is extremely wide. The minimum value presented is 0.2 m/day while the highest value is 62 m/day.

After careful discussion of the uncertainty it was recommended that expert judgment be applied, according to which the range for simulations should be from a high hydraulic conductivity of 150 mm/hour to a low one of 40 mm/hour.

Some site areas might have significant variation in hydraulic conductivity. These areas are characterized by grass cover and are hardly affected by human activity on the site. According to the land-use maps provided by KI, the rest of the site is characterized by increased human activity, which has resulted in soil compaction and a decrease in hydraulic conductivity. Thus, the hydraulic conductivity in such areas was assumed to be equal to the minimum of the considered range, 40 mm/hour, for all scenarios. In *Figure 3.17* these areas are presented as "Crusty Land."

Saturated soil moisture of the soil within the site was defined as 35% (Gorlinsky, 2003). The preliminary analysis showed that the amount of radioactivity washed out from the site is strongly related to the initial soil moisture. A higher initial soil moisture might result in a lower infiltration and, correspondingly, a higher rate of surface run-off. Thus, another set of scenarios has to be undertaken to enable a study of the influence of the initial soil moisture on the radioactivity washed out from the site. The first scenario corresponds to dry conditions with low initial soil moisture. Such a scenario applies when extremely heavy rain occurs after a long period of drought or lack of rain. A second scenario is for the situation in which heavy rain occurs after a period of continuous drizzle prior to the heavy rain. In this situation the increased soil moisture (wet conditions) should result in a decreased infiltration and, consequently, an increased surface-water run-off and increased radioactivity washout and redistribution. As it is physically impossible for the water

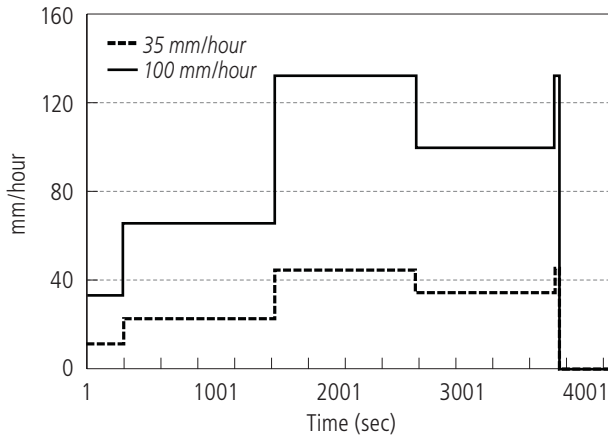


Figure 3.30. Time-series for rainfall intensities for two scenarios: heavy (100 mm/hour) and average (35 mm/hour) rain.

to fill all the possible soil pores, the initial soil moisture for wet soil conditions was accepted as 80% of that for saturated soil moisture.

As has already been mentioned, major soil erosion and corresponding radioactivity redistribution occur during single severe storms. Thus, the main set of scenarios developed simulates the redistribution of radionuclides caused by the most severe historically observed single storm in Moscow. According to past meteorological data, for the 37 years from 1961 to 1997 such a storm happened once and produced 100 mm of precipitation.

However, it was also decided to estimate radionuclide washout for rain of ordinary intensity, which is 35 mm for the region under consideration. On the basis of typical rain-intensity time-series for this region (Strauss *et al.*, 2001), an input time-series for rain (Figure 3.30) in the simulations was developed.

In both cases during the final 10 minutes there is no rainfall over the area (the rain intensity is 0 mm/hour). This is to allow all run-off over the area to end by reaching the outlet or by accumulating in local ponds.

As the area under consideration is relatively small in comparison to the typical input LISEM map that shows the different rain gauges, the rain gauge over the considered area is postulated as being homogeneous. This implies that the rain covers the whole area with the same intensity and duration.

As described above, for qualitative, physically based spatial modeling to be accurate, precise input information is required. One of the parameters that influences the final result the most is the digital elevation map. The whole set of initial maps, on the basis of which the level of erosion, direction of sediment transportation, and sedimentation rates are calculated, is derived solely from the digital elevation map.

To include the characteristic features of the site, such as buildings and other major obstacles to run-off formation and movement, the initial digital elevation map was modified by adding the buildings and wall. The corresponding isometric picture based on the actual digital elevation map used is presented in *Figure 3.19*.

3.5.5 Output of run-off modeling

The PCRaster software used to model the radionuclide redistribution not only enables a numerical estimate of the amount of radionuclide washout from the site to be obtained, but also shows the spatial redistribution pattern of washed-out contaminants. However, the output format for the results of the simulations should be treated further to obtain the final picture of redistribution. Also, the PCRaster environment does not enable a quantitative representation of the results obtained. Thus, the output maps were converted into the ArcView format and the spatial statistics for these maps calculated. The database that contains the results of the simulations, the final maps in the PCRaster and ArcView formats, and the time-series is archived on a CD-Rom. Results of the simulations carried out are given in *Table 3.9*.

The left side of *Table 3.9* describes the scenarios considered during the modeling and described above in Section 3.5.1 on the choice of main scenarios for modeling. The first column defines the different rain intensities, and the second column the soil condition in accordance with the initial soil moisture (“dry,” 0.14; “wet,” 0.28) and hydraulic conductivity for the site areas that do not have a compacted soil surface (40 mm/hour and 150 mm/hour). The third column clarifies the wall condition defined in the same section and assumed within the particular scenario. Additional details of the scenarios are given in Section 3.5.4 on input data used.

The amount of radionuclides washed out from the site was calculated by integration of the contaminants discharged through predefined points, called suboutlets in the LISEM environment. The “No fence” scenario (which is the same as “no effective wall,” as discussed above) presents the radionuclide discharge through the whole perimeter of the site. Thus, it is not possible to calculate the amount of radionuclides washed out in soluble form from the site. The particulate radionuclide contamination in this scenario was calculated on the basis of the map of contaminant redistribution in the GIS package ArcView.

The same technique was used to calculate the sedimentation of contaminated particles along their pathway in the scenario “No hole.” The territory outside the site along the redistribution pathway was divided into three subareas. This subdivision is determined by the different possible radiological implications of the deposited radionuclides. Area I is that part of the RRC-KI grounds between the storage site for the radioactive waste and the nearest checkpoint. Area II is the road between the checkpoint and municipal car park. Area III is the municipal car park, actually located between the inner and outer walls of RRC-KI. The borders

Table 3.9. Simulation results for radioactivity washout from the RRC-KI radioactive waste storage site. Shaded cells stand for the parameters in the "No fence" scenario when there is no code checkpoint indicated on the wall and, correspondingly, no calculation of washed-out material or activity is possible.

Rain intensity (mm)	Soil condition	¹³⁷ Cs activity						⁹⁰ Sr activity						Soil	
		Wall condition	Deposition at Area I (Bq)	Deposition at Area II (Bq)	Deposition at Area III		Washed in soluble form to outside the inner wall (Bq)	Deposition at Area I (Bq)	Deposition at Area II (Bq)	Deposition at Area III		Washed in soluble form to outside the inner wall (Bq)	Washout from the site (kg)		
					(Bq)	(kBq/m ²)				(Bq)	(kBq/m ²)				
100	Wet 40	"No hole"	2.2e+07	7.2e+05	6.3e+07	10.1	3.2e+07	4.3e+06	1.4e+05	1.3e+07	2.0	1.8e+06	1.1e+04		
		"No fence"	0	0	7.8e+07	12.5		0	0	1.5e+07	2.5				
	dry 150	"I"	0	0	4.2e+08	67.0	8.2e+06	0	0	8.3e+07	13.4	4.6e+06	1.9e+04		
		"K"	0	0	5.0e+08	80.8	7.0e+06	0	0	1.0e+08	16.3	4.0e+06	2.7e+04		
	35	Wet 40	"No hole"	6.3e+04	0	0	0.0	6.2e+05	9.1e+03	0	0	0.0	3.5e+05	9.0e+00	
			"No fence"	0	0	5.6e+07	9.1		0	0	1.1e+07	1.8			
		dry 150	"I"	0	0	1.1e+08	17.1	3.9e+06	0	0	2.1e+07	3.4	2.2e+06	8.5e+03	
			"K"	0	0	2.4e+08	38.3	3.7e+06	0	0	4.7e+07	7.6	2.1e+06	2.0e+04	
		dry 150	"No hole"	0	0	0	0.0	0	0	0	0	0.0	0	0	
			"No fence"	0	0	2.7e+07	4.3		0	0	5.4e+06	0.9			
35	Wet 40	"I"	0	0	1.1e+07	1.8	8.3e+05	0	0	2.2e+06	0.4	4.7e+05	1.1e+03		
		"K"	0	0	8.0e+07	13.0	8.4e+05	0	0	1.6e+07	2.6	4.8e+05	7.8e+03		
	dry 150	"No hole"	0	0	0	0.0	0	0	0	0	0.0	0	0		
		"No fence"	0	0	2.7e+07	4.3		0	0	5.4e+06	0.9				
dry 150	"I"	0	0	1.1e+07	1.8	8.2e+05	0	0	2.2e+06	0.4	4.7e+05	1.1e+03			
	"K"	0	0	8.0e+07	13.0	8.4e+05	0	0	1.6e+07	2.6	4.8e+05	7.8e+03			

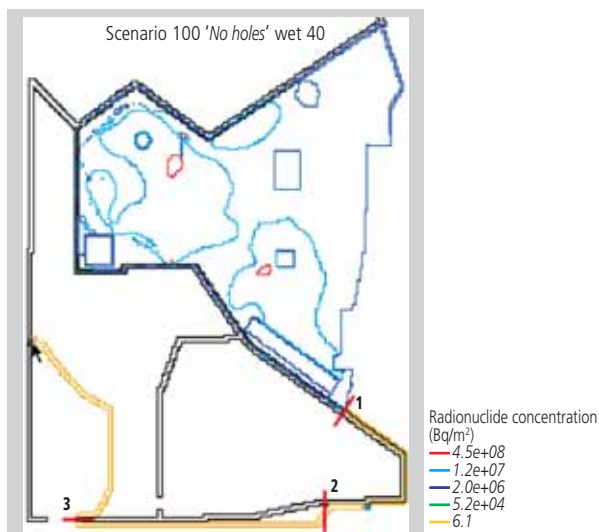


Figure 3.31. The radionuclide washout path for the “No hole” scenario with hydraulic conductivity 40 mm/hour, rain intensity 100 mm/hour, and initial soil moisture 0.28, and the areas of radionuclide deposition (1, site border; 2, Institute checkpoint; 3, municipal car park). Arrow shows the maximum deposition outside the radioactive waste storage site.

of the selected areas are shown in *Figure 3.31*: line 1 shows the border between the southwestern part of the waste storage site and the rest of the RRC-KI grounds. Line 2 separates the grounds of RRC-KI from the road that leads to the RRC-KI checkpoint, and line 3 shows the border between the road and the car park.

Comparison of *Figures 3.31* and *3.32* shows that contamination of the municipal car park can occur in the “No hole” scenario only with heavy rain and unfavorable soil conditions. The water discharge for scenario “dry 150” is not large enough to transport the contaminated sediments through the landscape.

From *Table 3.9* it is clear that the highest radionuclide washout occurs when the hole is located near the point “K.” This result is explained by the higher concentration of radionuclides in the catchment area near point “K” and also by the much lower soil cohesion in this part of the site. Moreover, the local elevation in the middle of the site that faces this (northern) part of the wall has a steep slope. According to the simulation, the waterflow out through hole “K” can have a speed of up to a few meters per second for the heavy rain scenario. Thus, the deposition rate near the inner wall is not high (*Figures 3.33* and *3.34*).

The higher deposition rate and correspondingly higher radioactivity concentration may be observed near the outer wall close to point “O” (see *Figure 3.17*). As described in Section 3.3.1 on topography and engineering barriers to water drainage

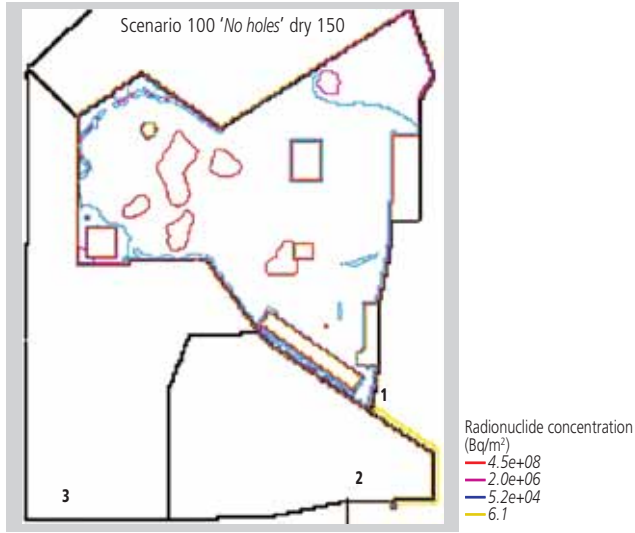


Figure 3.32. ^{137}Cs redistribution for the “No hole” scenario with hydraulic conductivity 150 mm/hour, rain intensity 100 mm/hour; and initial soil moisture 0.14, and the areas of radionuclide deposition outside the radioactive waste storage site.

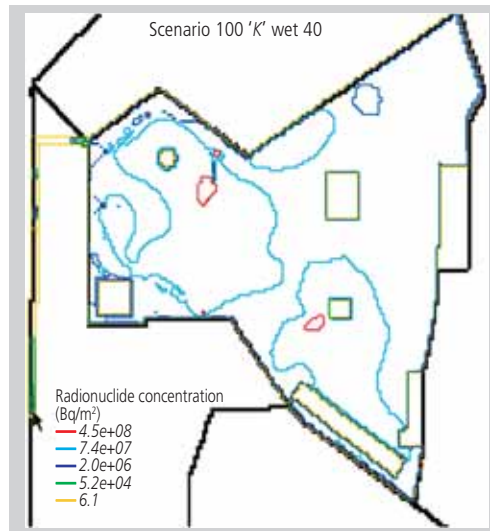


Figure 3.33. ^{137}Cs redistribution for scenario “K” with hydraulic conductivity 40 mm/hour, rain intensity 100 mm/hour, and initial soil moisture 0.28 (80% saturated). Arrow shows the maximum deposition outside the radioactive waste storage site.

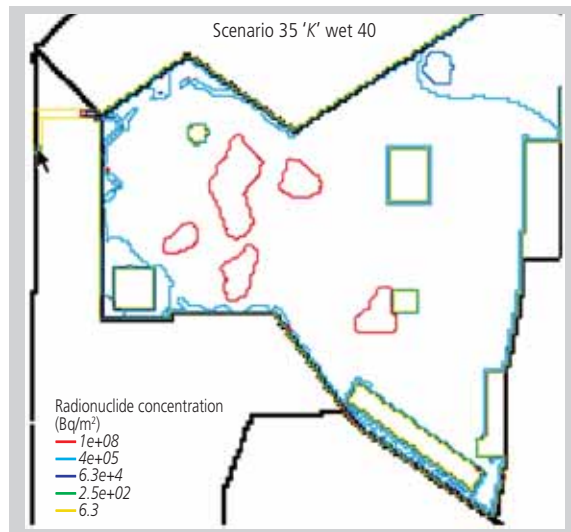


Figure 3.34. ^{137}Cs redistribution for scenario “K” with hydraulic conductivity 40 mm/hour, rain intensity 35 mm/hour, and initial soil moisture 0.28 (80% saturated). Arrow shows the maximum deposition outside the radioactive waste storage site.

from the site, the size of the drainage storm-water outlet in the outer wall can accommodate a water discharge of up to 100 l/s only. At the same time, the simulations show that the volume of incoming water is more than 1000 l/s. According to the digital elevation map, water that enters the car park will accumulate along the outer wall. This causes a significant decrease in the flow speed and, consequently, increases the sedimentation rate of contaminated particles.

Washout from the hole in the wall located at point “I” is also significant because of the direct water run-off from the top point in the center of the site. Unlike point “K,” there is no local elevation depression before the hole that provides some space for water to accumulate and thus increased sedimentation. Moreover, the surface around hole “I” along the redistribution route is flatter than that at “K.” Thus, the sedimentation rate is higher along the stream. ^{137}Cs redistributions for scenario “I, wet 40” for different rain intensities are shown in *Figure 3.35* and *Figure 3.36*.

The spatial patterns of radionuclide redistribution for the “No fence” scenario for heavy and average rain are presented in *Figures 3.37* and *3.38*. The areas contaminated with ^{137}Cs and ^{90}Sr within a particular scenario are identical. Thus, only one contaminant, either ^{137}Cs or ^{90}Sr , is presented here.

Figure 3.39 compares water discharges through the hole in the inner wall for scenario “I” for both rain intensities and both soil conditions. It can be concluded that variations in the soil characteristics within the specified ranges and the location

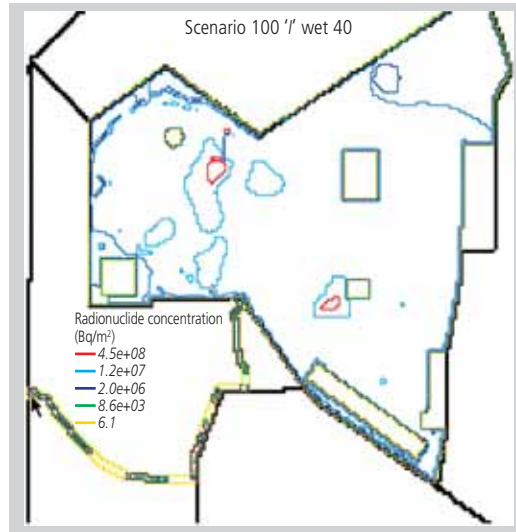


Figure 3.35. Radionuclide redistribution path for scenario “I” with hydraulic conductivity 40 mm/hour, rain intensity 100 mm/hour, and initial soil moisture 0.28 (80% saturated). Arrow shows the maximum deposition outside the radioactive waste storage site.

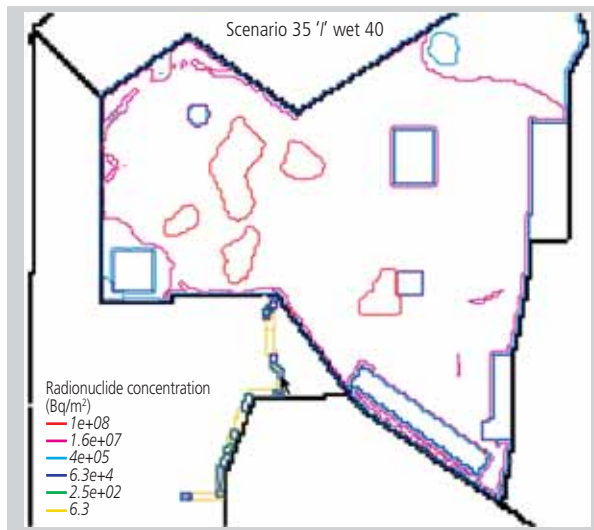


Figure 3.36. ¹³⁷Cs redistribution for scenario “I” with hydraulic conductivity 40 mm/hour, rain intensity 35 mm/hour, and initial soil moisture 0.28 (80% of saturated). Arrow shows the maximum deposition outside the radioactive waste storage site.

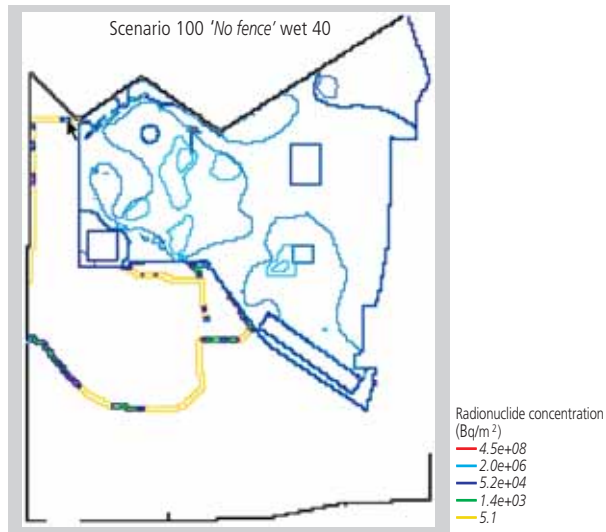


Figure 3.37. ^{137}Cs redistribution for the “No fence” scenario with hydraulic conductivity 40 mm/hour, rain intensity 100 mm/hour, and initial soil moisture 0.28 (80% of saturated). Arrow shows the maximum deposition outside the storage site for radioactive waste.

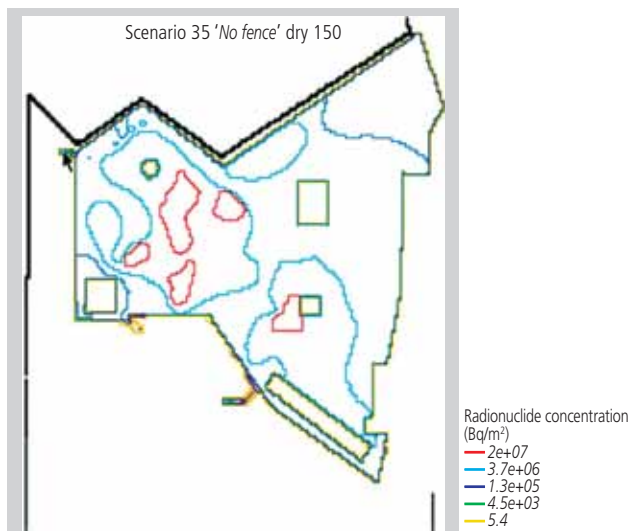


Figure 3.38. ^{90}Sr redistribution for the “No fence” scenario with hydraulic conductivity 150 mm/hour, rain intensity 35 mm/hour, and initial soil moisture 0.14 (40% saturated). Arrow shows the maximum deposition outside the radioactive waste storage site.

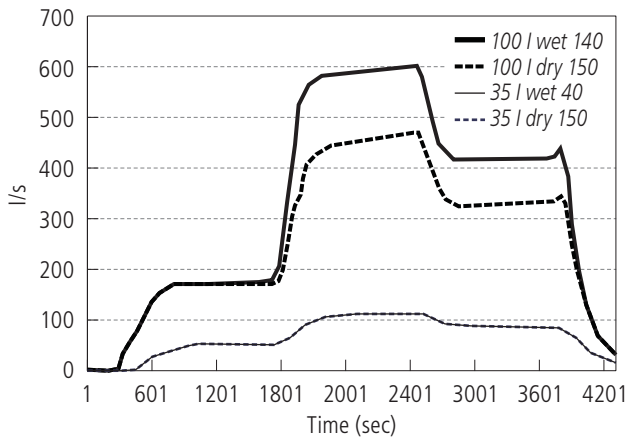


Figure 3.39. Comparison of water discharges through the hole in the inner wall for scenario “I.”

of the hole do not seriously influence water discharge from the site for rain of average intensity. Moreover, the catchment area for this outlet is covered mainly by “hard” (compacted) land. This result is in congruence with simulation results for the amount of leached radioactivity (see *Table 3.9*). The difference between scenarios “wet 40” and “dry 150” in terms of washed out radioactivity is negligible for average rain.

Radionuclide washout in the soluble form was calculated with suboutlet checkpoints provided by the LISEM code. In scenarios “I,” “K,” and “No hole” the local suboutlet is indicated at the hole within the wall for the first two scenarios or on the rill body at the eastern border of the site close to point N (*Figures 3.40–3.43*). This technique is possible for scenario “No hole” because the preliminary analysis of the formed rill structure showed only one water channel that flowed out from the area of the site along the southern wall through point “N” (see *Figure 3.17*).

In the process of run-off redistribution of the contamination within the site, the contaminated particles are eroded mainly from the hill slopes in the middle of the site and deposited along the wall in places where the rills are formed. However, such a deposition occurs only where the sediment concentration in the run-off water body becomes greater than the flow transport capacity. As the transport capacity is a function of flow velocity, which is in turn a function of the flow bed resistance and slope gradient, deposition occurs mainly in local depressions or on the land areas characterized by an increased resistance to flow.

Radionuclide redistribution within the waste storage site was calculated on the basis of the ArcView GIS package. The output maps from the PCRaster software were imported into the ArcView format and statistics for them calculated.

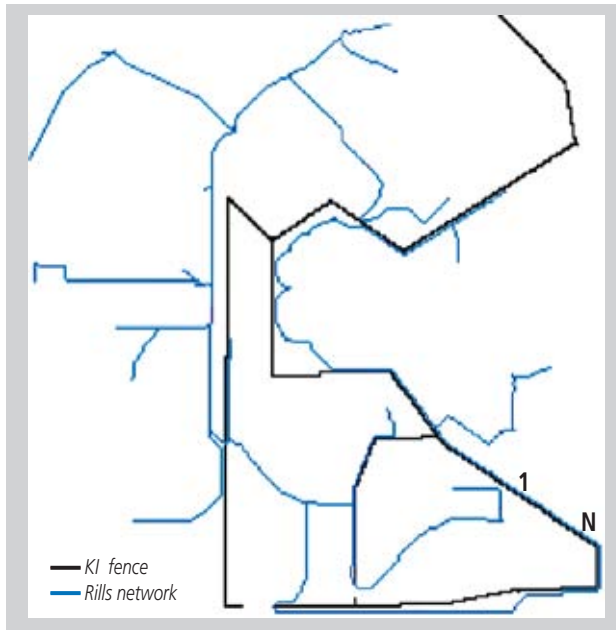


Figure 3.40. Rills network formed when it rains in the “No hole” scenario. The suboutlet specified to calculate the outflow is labeled with the number 1.

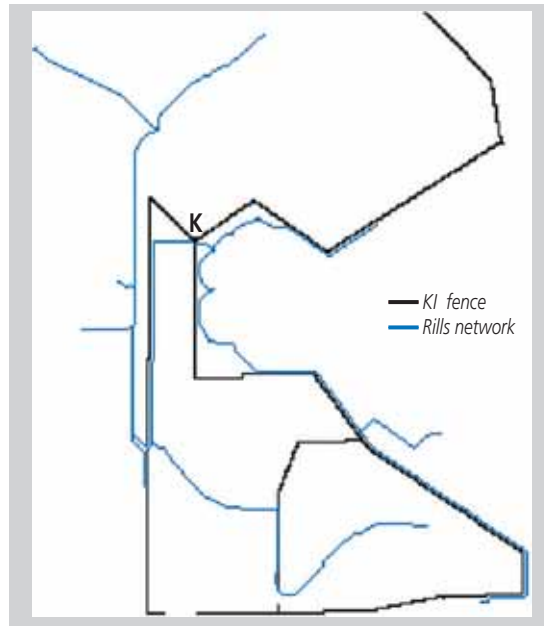


Figure 3.41. Rills network in scenario “K.”

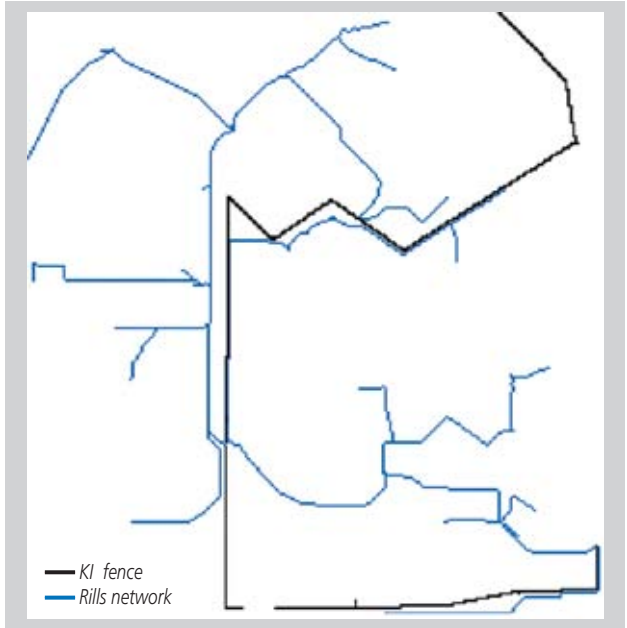


Figure 3.42. Rills network in the “No fence” scenario.

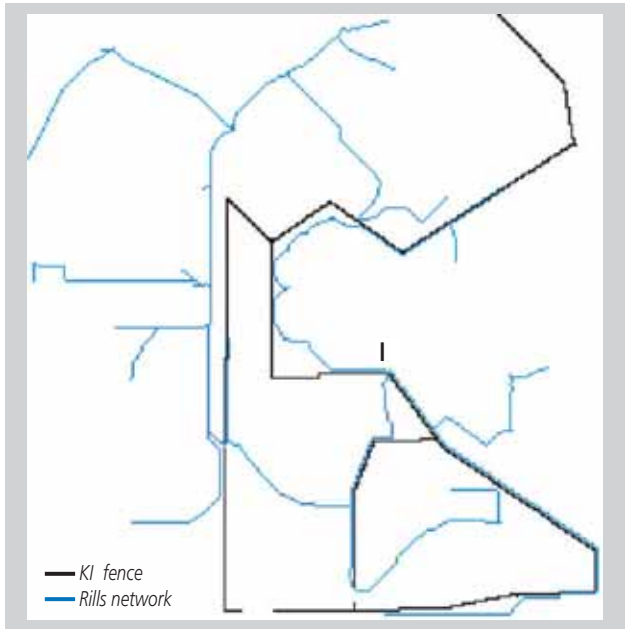


Figure 3.43. Rills network in scenario “I.”



Figure 3.44. ^{137}Cs redistribution within the site for scenario “100, “I,” wet 40.” d is the ratio between the final and initial activity of ^{137}Cs within the cell.

Table 3.10. The redistribution of radionuclides within the site for scenario “100, “I,” wet 40,” where d is the ratio between the final and initial activity of ^{137}Cs within the cell.

d intervals	Area (m^2)	Area/total site area
$d < 0.9$	330	0.033
$0.9 < d < 1.1$	9600	0.95
$1.1 < d < 2$	80	0.008
$2 < d < 10$	50	0.005
$10 < d$	7	0.0007

Table 3.10 shows the characteristics of redistribution of ^{137}Cs for the scenario “100, “I,” wet 40” and the corresponding redistribution of ^{137}Cs is presented in Figure 3.44.

3.5.6 Contamination of local area and public exposure

Public exposure to run-off from the RRC-KI radioactive waste storage site is based on the results of run-off modeling presented in the previous section. To simplify this section, the scenarios considered are briefly summarized below. Two rates of precipitation and two sets of conditions for the site soil are considered:

- Run-off from the radioactive waste site caused by heavy rain (downpour) with an intensity of 100 mm, the highest measured in Moscow for 40 years. The conditions of the soil on the radioactive waste site before the rain were considered as wet (case wet 40) or dry (case dry 150). The numbers in parenthesis indicate soil infiltration rate in mm/h.
- Run-off caused by a rain of average intensity (35 mm), cases wet 40 and dry 150.

Several hypothetical scenarios for the barrier capacity of the inner wall that surrounds the radioactive waste site were considered, in particular:

- “No hole” scenario: a watertight wall around the site, with the exception of the east perimeter, where the wall is “transparent” to run-off;
- “No fence” scenario: the wall around the radioactive waste site has no resistance to run-off waters;
- Scenarios “I” and “K” assume a watertight wall around the site with the exception of one aperture 1 m wide at points “I” and “K,” respectively; the locations of these points are on the run-off water flows (see *Figure 3.18*).

The “heavy rain” run-off scenario supposes flooding of the radioactive waste site with large amounts of rainwater and subsequent run-off from the site. It is assumed that the flow of contaminated water will reach the wall of the site and release it to the neighboring area between the wall of the site and the outer wall of RRC-KI; this area is used as a municipal car park. In addition, contaminated waters partially ooze out to the city street that adjoins the outer wall of RRC-KI; this flow runs along the street to the lowest local point, which is usually flooded during rainy periods. The run-off waters reach the flooded part (*Figure 3.45*) and disperse across the whole area. After the water has dried up, the flooded area is contaminated with radionuclides. The scenarios of contamination considered assume that the run-off event will be followed by dry weather, and thus new rains will not wash the radionuclides out from the contaminated ground or redistribute them further.

Contamination of local urban area according to run-off modeling results

According to the results of run-off scenarios, the local areas outside the RRC-KI boundaries that may be contaminated by run-off waters from the storage site are:

- Municipal car park;
- Part of the street flooded by the run-off waters during a rainy period.

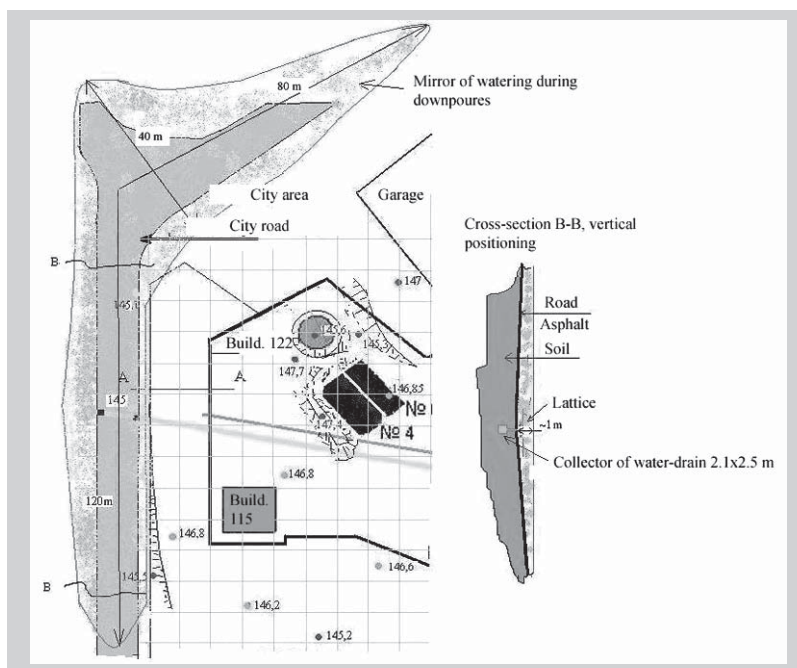


Figure 3.45. Flooded area near to the boundaries of the RRC-KI radioactive waste storage site during downpours that occurred from 1998 to 2000.

The area of the municipal car park is about $6,200 \text{ m}^2$ and the flooded area in the street about $3,500 \text{ m}^2$. The volume of the flooded part in rainy periods is about $2,500\text{--}2,700 \text{ m}^3$. According to the run-off scenarios, contamination of the car park forms by sedimentation of the radionuclides in particulate form: the contamination levels were calculated directly by LISEM (*Table 3.11*). In contrast, contamination of the street forms by radionuclides that ooze in soluble form through the hole in the outer wall (point “O” in *Figure 3.17*). The residual contamination of the street area after the contaminated water has entered the sewer via a drain was calculated on the assumption that the flooding waters remain in the street for several hours (up to 1 day) before drainage, so that radionuclides are adsorbed into the bottom soils. With conservative values for the partitioning coefficients (K_d) for ^{137}Cs and ^{90}Sr of 1800 and 110 l/kg, respectively (Thibault, 1990), and a sediment thickness of 1 cm, the estimated residual amounts of radionuclides in the street after the flooded area has dried are: ^{137}Cs up to 95% and ^{90}Sr about 70% of the initial contamination. The average densities of surface soil contamination across the flooded area in the street are given in *Table 3.11*.

Table 3.11. Surface activity of radionuclides in some local areas contaminated by run-off from the RRC-KI radioactive waste site. Local areas considered: (i) car park situated between the wall of the radioactive waste site and the outer wall of RRC-KI and (ii) local flooded area along the street adjacent to the outer wall of RRC-KI.

Scenario	Soil conditions before rain	Surface activity of ^{137}Cs at the car park (Bq/m^2)	Surface activity of ^{90}Sr at the car park (Bq/m^2)	Surface activity of ^{137}Cs at the flooded area in the street (Bq/m^2)	Surface activity of ^{90}Sr at the flooded area in the street (Bq/m^2)
<i>Heavy rain, downpour (100 mm)</i>					
"No hole"	Wet 40	1.01e(+4)	2.01e(+3)	8.9e(+3)	3.7e(+2)
	Dry 150	0	0	1.7e(+2)	70
"No fence"	Wet 40	1.25e(+4)	2.47e(+3)	not calculated	not calculated
	Dry 150	9.1e(+3)	1.8e(+3)	not calculated	not calculated
"I"	Wet 40	6.7e(+4)	1.34e(+4)	2.2e(+3)	9.3e(+2)
	Dry 150	1.71e(+4)	3.4e(+3)	1e(+3)	4.4e(+2)
"K"	Wet 40	8.08e(+4)	1.63e(+4)	1.9e(+3)	7.9e(+2)
	Dry 150	3.83e(+4)	7.6e(+3)	1e(+3)	4.2e(+2)
<i>Rain of average intensity (35 mm)</i>					
"No hole"	Wet 40	0	0	0	0
	Wet 40	4.3e(+3)	0.87e(+3)	not calculated	not calculated
"I"	Wet 40	1.8e(+3)	0.36e(+3)	2.3e(+2)	9.4e(+1)
	Wet 40	1.3e(+4)	2.6e(+3)	2.3e(+2)	9.6e(+1)

Estimation of public exposure

In urban conditions, the principal pathways for exposure of members of the public to radiation are:

- External gamma ray exposure from contaminated ground;
- Exposure from inhalation of resuspended radionuclides.

The local people living in the buildings nearest to the radioactive waste site and those who use the car park are considered to be critical groups that could potentially receive higher radiation exposures.

There are different approaches to evaluating the risk caused by radioactivity transfer outside an allotted area, such as comparison with the acceptable annual dose limit currently fixed in the official legislative and/or normative documents, estimation of the excess lifetime-risk through exposure, etc. As indicated above, run-off modeling was oriented to a scoping analysis. We thus decided not to become involved in a discussion as to which criterion is better and whether a dose limit is likely to change in the future, but to choose the simplest approach: comparison with the current official dose-rate limit. The data obtained and presented in this report on radionuclide contamination allow specialists to recalculate the risk in other terms, if they wish.

External exposure of local critical groups of citizens to gamma radiation

External exposures of members of the public to gamma radiation were calculated for two contaminated local areas: the car park and the contaminated local area in the street. The exposure from groundshine was associated with a surface contamination of the ground by ^{137}Cs . The effective dose coefficient for this (5.51e^{-16} Sv/s per Bq/m^2) used in the calculations includes contributions from progeny, assuming secular equilibrium; this value is recommended as the best value available to date for groundshine assessment (Eckerman and Leggett, 1996; ICRP, 1996a). A similar value for the groundshine dose conversion factor for ^{137}Cs was used in Energoatomizdat (1984). The estimated effective dose rates from groundshine received by members of the public are summarized in *Table 3.12*.

The scenarios of run-off from heavy rain indicate the following effects of groundshine external exposure on members of the public:

- At the car park, the effective dose rates from groundshine received by car drivers when outside their cars vary from about $0.02 \mu\text{Sv}/\text{h}$ to $0.12\text{--}0.15 \mu\text{Sv}/\text{h}$, depending on the run-off scenario. At present, the average measured value of

Table 3.12. External exposure received by members of the public from groundshine in some local areas contaminated after run-off from the RRC-KI radioactive waste site. Local areas considered are given in *Table 3.11*.

Scenario	Soil conditions before rain	Effective dose rate of external exposure to contaminated ground at the car park (Sv/h)	Effective dose rate of external exposure to contaminated ground in the flooded area in the street (Sv/h)
<i>Heavy rain, storm (100 mm)</i>			
"No hole"	Wet 40	0.019e(-6)	1.7e(-8)
	Dry 150	0	3.2e(-10)
"No fence"	Wet 40	0.024e(-6)	not calculated
	Dry 150	0.017e(-6)	not calculated
"I"	Wet 40	0.128(-6)	4.2e(-9)
	Dry 150	0.033e(-6)	2e(-9)
"K"	Wet 40	0.154e(-6)	3.6e(-9)
	Dry 150	0.073e(-6)	1.9e(-9)
<i>Rain of average intensity (35 mm)</i>			
"No hole"	Wet 40	0	0
"No fence"	Wet 40	8.2e(-9)	not calculated
"I"	Wet 40	3.4e(-9)	4.5e(-10)
"K"	Wet 40	2.4e(-8)	4.5e(-10)

external exposure is about 13.7 $\mu\text{R/h}$ at the car park. Maximum values can easily be detected by dosimetric control because the additional gamma irradiation practically doubles the existing radiation background here. The existing background at the car park is already somewhat higher (by 5 $\mu\text{R/h}$) than the normal background in the city. The increased levels of external exposure within the initial period are expected to continue after the run-off event; in subsequent periods, weathering and intensive traffic will lead to a gradual decrease in contamination at the car park. Moreover, car drivers usually spend only a short time at the car park. The highest doses of external exposure will be associated with the permanent personnel responsible for cleaning and guarding the car park.

- In the street, the effective external dose rates received by members of the public within the contaminated local area are very low and hardly detectable by dosimetric control. The maximum value is about 0.017 $\mu\text{Sv/h}$ (*Table 3.12*).

The scenarios of run-off from rain of average intensity indicate the following effects of external exposure of members of the public to groundshine (*Table 3.12*):

- Rain of average intensity can lead to a small increase in external exposure at the car park, with a maximum value of $0.02 \mu\text{Sv/h}$ (scenario “K”);
- Normal rain has practically no effect on the external exposure received by the public within the local area flooded with rainwater.

Inhalation pathway of exposure of local critical groups of inhabitants

After rainfall, run-off from the radioactive waste site will lead to local areas being contaminated with dried radioactive sediments. The dried solutions form deposits of very fine particles with an active median aerodynamic diameter (AMAD) of about 1 μm and less. These particles are easily suspended in the air to form fine radioactive dust (see, for instance, Gavrillov *et al.*, 1995; Hollander and Garger, 1996; Garger *et al.*, 1999).

The concentration of radioactivity in the air, C_{air} (1 m above surface), is estimated by the formula (Nickholson, 1988; Makhonko, 1992; Goscomecology, 1999):

$$C_{air}(Bq/m^3) = K_{susp}(t)C_{ground}(Bq/m^2),$$

where

C_{ground} is the surface density of the radionuclide on the ground;

$K_{susp}(t)$ is the resuspension factor (m^{-1}).

Several expressions exist for $K_{susp}(t)$ as a function of time t (Sehmel, 1980; Nickholson, 1988; Makhonko, 1992; Goscomecology, 1999). For an urban area disturbed by traffic and pedestrians, the initial resuspension factors of about $10^{-5} m^{-1}$ for fresh atmospheric deposits tend to decrease with time, even when downward migration is inhibited, as on asphalt road (Sehmel, 1980; Till and Meyer, 1983; Nickholson, 1988). Usually, the resuspension factor drops by two or three orders of magnitude within 1 month of deposition. In Goscomecology (1999), the recommendation is to estimate the resuspension factor using the formula

$$K_{susp}(t) = 10^{-5}\exp[-(\lambda_1 + \lambda_2 + \lambda)t] + 10^{-9}\exp[-(\lambda_2 + \lambda)t],$$

where $\lambda_1 = 1.26 \times 10^{-2}/\text{day}$, which is the decrease in the rate of resuspension with time ($t_{1/2} = 55$ days for the initial “rapid” phase of resuspension decrease), λ_2 is the decrease in the rate of residual long-term resuspension with time, and

λ is the radioactive decay constant for a given radionuclide. Given the initial phase of resuspension from a contaminated dried flooded area and the long-lived radionuclides (^{90}Sr and ^{137}Cs), a reasonable value for K_{susp} from dried deposits would be 10^{-5} m^{-1} . However, since the depositions are originally wet and cannot suspend easily, a more realistic value for the resuspension factor during the initial period after the run-off is 10^{-6} m^{-1} . This value decreases to $2 \times 10^{-8} \text{ m}^{-1}$, an average experimental value under normal conditions over this area. Inhalation dose rates (E_{inh}) for members of local critical groups of inhabitants are estimated using the formula (Moiseev and Ivanov, 1990; Goscomecology, 1999):

$$E_{inh} = DF_{inh} \times \text{inhalation of radioactive dust (Bq/h)}$$

Inhalation of radioactive dust was calculated by multiplying the activity in the air (in the street or building) by breathing rate and period of breathing. Breathing rates for typical men, women, and children of different ages (both at rest and when active) are given in Goscomecology (1999) and Moiseev and Ivanov (1990). Dose conversion factors for inhalation (DF_{inh} , in Sv/Bq) were taken from ICRP (1996b) and IAEA (1996).

The calculated concentrations of resuspended radionuclides in the air and the effective dose rates by inhalation of ^{137}Cs and ^{90}Sr are given in *Tables 3.13* and *3.14*. The run-off scenarios for heavy rain indicate the following effects on air contamination and corresponding inhalation dose rates to members of the public:

- At the car park, the contamination of the air (1 m above ground) caused by resuspension of dried deposits varies within the ranges $0.01\text{--}0.08 \text{ Bq/m}^3$ for ^{137}Cs and $0.002\text{--}0.016 \text{ Bq/m}^3$ for ^{90}Sr (*Table 3.13*). These values are higher than the typical observed activity concentrations in air within the KI boundaries, which are reported to be about 1×10^{-4} to $2 \times 10^{-4} \text{ Bq/m}^3$. The calculated values show the maximum levels of air contamination, which are expected to decrease to normal within a few months. The effective inhalation dose rates for drivers when outside their cars vary within the ranges 5×10^{-11} to $44 \times 10^{-11} \text{ Sv/h}$ for ^{137}Cs and 7.8×10^{-11} to $69 \times 10^{-11} \text{ Sv/h}$ for ^{90}Sr , depending on the run-off scenario. All these dose rates are very low compared with the dose limit.
- In the street, contamination of the air (1 m above contaminated ground) through resuspension of dried deposits varies within the ranges 1.7×10^{-4} to $8.9 \times 10^{-3} \text{ Bq/m}^3$ for ^{137}Cs , and 7×10^{-5} to $9.3 \times 10^{-4} \text{ Bq/m}^3$ for ^{90}Sr (*Table 3.14*). In the street, the effective inhalation dose rates received by adult members of the public within the contaminated local area are very low, varying within the ranges 1×10^{-12} to $4.9 \times 10^{-11} \text{ Sv/h}$ for ^{137}Cs and 3×10^{-12} to $4 \times 10^{-11} \text{ Sv/h}$ for ^{90}Sr (*Table 3.14*).

Table 3.13. Exposure received by members of the public from inhalation of resuspended radionuclides at the municipal car park.

Scenario	Soil conditions before rain	Activity concentration of ^{137}Cs in the air at the car park (Bq/m^3)		Effective inhalation dose rate received by adults from resuspended ^{137}Cs at the car park (Sv/h)		Effective inhalation dose rate received by adults from resuspended ^{90}Sr at the car park (Sv/h)	
		Activity concentration of ^{137}Cs in the air at the car park (Bq/m^3)	Activity concentration of ^{137}Cs in the air at the car park (Bq/m^3)	Effective inhalation dose rate received by adults from resuspended ^{137}Cs at the car park (Sv/h)	Effective inhalation dose rate received by adults from resuspended ^{137}Cs at the car park (Sv/h)	Activity concentration of ^{90}Sr in the air at the car park (Bq/m^3)	Effective inhalation dose rate received by adults from resuspended ^{90}Sr at the car park (Sv/h)
<i>Heavy rain, storm (100 mm)</i>							
"No hole"	Wet 40	0.01	0	5.5e(-11)	2e(-3)	8.7e(-11)	0
	Dry 150	0	0	0	0	0	0
"No fence"	Wet 40	0.012	0	5.5e(-11)	2.5e(-3)	1.1e(-10)	1.1e(-10)
	Dry 150	0.009	0	5e(-11)	1.8e(-3)	7.8e(-11)	7.8e(-11)
"I"	Wet 40	0.067	0	3.8e(-10)	1.3e(-2)	5.6e(-10)	5.6e(-10)
	Dry 150	0.017	0	9e(-11)	3.4e(-3)	1.46e(-10)	1.46e(-10)
"K"	Wet 40	0.08	0	4.4e(-10)	1.6e(-2)	6.9e(-10)	6.9e(-10)
	Dry 150	0.04	0	2.2e(-10)	7.6e(-3)	3.3e(-10)	3.3e(-10)
<i>Rain of average intensity (35 mm)</i>							
"No fence"	Wet 40	4.3e(-3)	0	2.4e(-11)	8.7e(-4)	3.8e(-11)	3.8e(-11)
	Wet 40	1.8e(-3)	0	1e(-11)	3.6e(-4)	1.6e(-11)	1.6e(-11)
"K"	Wet 40	0.013	0	7e(-11)	2.6e(-3)	1.1e(-10)	1.1e(-10)

Table 3.14. Exposure received by members of the public from inhalation of resuspended radionuclides at the flooded area in the street adjacent to the outer wall of RRC-KI.

Scenario	Soil conditions before rain	Activity concentration of		Inhalation dose rate received by adults from resuspended		Inhalation dose rate received by adults from resuspended	
		^{137}Cs in air over flooded street (Bq/m^3)	^{137}Cs in air over flooded street (Bq/m^3)	^{90}Sr in air over flooded street (Bq/m^3)	^{90}Sr in air over flooded street (Bq/m^3)	^{90}Sr in air over flooded street (Sv/h)	^{90}Sr in air over flooded street (Sv/h)
<i>Heavy rain, storm (100 mm)</i>							
"No hole"	Wet 40	8.9e(-3)	4.9e(-11)	3.7e(-4)	1.6e(-11)		
	Dry 150	1.7e(-4)	1e(-12)	7e(-5)	3e(-12)		
"No fence"	Wet 40	not calculated		not calculated			
	Dry 150	not calculated		not calculated			
"I"	Wet 40	2.2e(-3)	1.2e(-11)	9.3e(-4)	4e(-11)		
	Dry 150	1e(-3)	5.5e(-12)	4.4e(-4)	1.9e(-11)		
"K"	Wet 40	1.9e(-3)	1e(-11)	7.9e(-4)	3.4e(-11)		
	Dry 150	1e(-3)	5.5e(-12)	4.2e(-4)	1.8e(-11)		
<i>Rain of average intensity (35 mm)</i>							
"No hole"	Wet 40	0	0	0	0		
	Wet 40	not calculated		not calculated			
"I"	Wet 40	2.3e(-4)	1.3e(-12)	9.4e(-5)	4.1e(-12)		
	Wet 40	2.3e(-4)	1.3e(-12)	9.6e(-5)	4.1e(-12)		

The scenarios for run-off from rain of average intensity indicate no effects from inhalation exposure received by the public in the street. At the car park, the maximum increase in ^{137}Cs concentration in air was 0.013 Bq/m^3 and that of ^{90}Sr was 0.0026 Bq/m^3 during the first period of resuspension (“K” scenario); the corresponding inhalation dose rates do not exceed $1.8 \times 10^{-10} \text{ Sv/h}^{-1}$.

Annual doses of exposure at contaminated places

The hypothetical annual doses received by members of the public were calculated based on the pessimistic assumption that the maximum exposure levels at the contaminated sites are maintained for a year after the run-off event. In other words, it was supposed that run-off deposits of radionuclide outside the restricted area would not be removed nor the contaminated area cleaned within 1 year of the event. Therefore, the total dose is numerically equal to the total dose rate.

It was assumed that a car driver spends 1 hour per day in the car park throughout the year, that car park personnel spend 4 working hours per day without protection, and that pedestrians spend 1 hour per day at the contaminated local spot in the street. The calculated annual doses to members of critical groups of the public are given in *Table 3.15*. These are compared with the annual dose limit for members of the public in general (1 mSv/year). Car park personnel are expected to receive the maximum annual doses, that is 1.8–13.3% of the annual dose limit in the “heavy rain” scenarios and up to 1.7% of the dose limit in the “ordinary rain” scenarios. External exposure is the dominant pathway in all the scenarios. Car drivers are expected to receive 0.7–5.4% and up to 0.7% of the annual dose limits in the “heavy rain” and “ordinary rain” scenarios, respectively. Pedestrians who use the contaminated area in the street may receive up to 0.62% of the annual dose limit in the “heavy rain” scenarios or about 0.017% of the annual limit in the “ordinary rain” scenarios.

Discussion of the results and their uncertainty

Assessment of the dose uptakes by the critical population groups after the run-off scenarios from the radioactive waste site shows that natural events, such as average or heavy rain, are unlikely to cause considerable reduction in environmental safety.

We repeat here the uncertainties in the dose calculation, which are predominantly caused by uncertainties in the run-off erosion calculation. The run-off model LISEM used in the study is a physically based simulation model, but, of course, it applies some empirical relationships to describe the physical processes that underlie the model. All the papers we referred to found that the LISEM discharge estimate agrees with measured estimates to within 15% and that uncertainties in the input parameters are the most important in terms of assessing the final results.

Table 3.15. Annual doses received by the critical local groups of inhabitants from contact with the areas contaminated by run-off from the radioactive waste site of RRC-KI.

Members of local critical groups	Annual dose from external exposure (Sv/year)	Annual dose from inhalation (Sv/year)	Total annual dose (Sv/year)	Share of the annual dose limit of 1 mSv/year (%)
<i>Heavy rain scenarios</i>				
Car drivers at the car park	7–55e(-6)	0.046–0.41e(-6)	7.1–54.4e(-6)	0.7–5.4
Personnel at the car park	17.6–132e(-6)	0.11–1e(-6)	17.7–133e(-6)	1.8–13.3
Pedestrians in the street	Up to 6.2e(-6)	0.15–3.3e(-8)	Up to 6.24e(-6)	Up to 0.62
<i>Scenarios with rain of average intensity</i>				
Car drivers at the car park	Up to 7.3e(-6)	1–6e(-8)	Up to 7.4e(-6)	Up to 0.7
Personnel at the car park	Up to 17.6e(-6)	2.3–16e(-8)	Up to 17.8e(-6)	Up to 1.7
Pedestrians in the street	1.64e(-7)	2e(-9)	1.7e(-7)	0.017

Hence, we intentionally give the results of modeling 16 different scenarios, which include variation of the major parameters within their uncertainty range, evaluated by expert interpretation. Actually, these 16 scenarios constitute a kind of sensitivity analysis and produce a feeling for the range of variation in the output data. Therefore, the maximum calculated dose should be considered as an upper limit obtained within the scoping analysis. In other words, the approach is intentionally skewed toward overstating the exposure and dose.

The calculated dose rates for the hypothetical exposure of members of the public vary from 0.02 to 13.3% of the annual dose limit, established at a level of 1 mSv/year. However, the results from the run-off scenarios show that radionuclides can be washed off outside the radioactive waste site and even reach the city street, which may in itself be a psychological factor that contributes to public anxiety. The radiation background in local areas adjacent to the radioactive waste site can be elevated noticeably by the run-off events. These local areas need to be kept under systematic dosimetric control. The possibility of the gradual accumulation of radionuclides through repeated wash-off events over long periods is a subject for further consideration. Besides natural run-off events, there are several other pathways of radionuclide migration from the radioactive waste site to the city areas, such as migration with groundwaters, direct resuspension of dust from the site,

and so on. The contribution of these processes to the exposure of critical groups of inhabitants is a subject for further analysis. In addition, the effects of possible infrastructural failures (e.g., heavy run-off that results from failure of the rainwater pipe) are worthy of special study.

Conclusions and Recommendations

Attention has been drawn to the consequences of the recent significant growth in urbanization throughout the world that has resulted in the de facto siting of waste disposal facilities in densely populated urban areas. In some cases the expanded residential areas actually surround these waste disposal facilities. This represents a global problem as waste management practices previously located in the outer suburbs of the city could now seriously affect the public. These past waste disposal sites could be of chemical, industrial, municipal, or mixed origin. The nuclear legacy, particularly that of storage sites for radioactive waste in what are now urban areas, is an extreme example of this phenomenon.

For a number of reasons, the nuclear legacy in the urban environment has only recently come to the attention of environmental specialists and the population. The first reason is that in countries with developed nuclear industries this urban nuclear legacy is less than 1% of the total nuclear legacy. After the end of the Cold War, studies of the global nuclear legacy mainly focused on nuclear weapons production sites, which contain the vast majority of the accumulated radioactive waste. These sites were commissioned in scarcely populated areas for secrecy reasons and most remain in relatively underpopulated areas. However, it has now become widely recognized that, though the nuclear legacy in the urban environment is a small fraction of the total, other factors, such as urban population density and its proximity to operational or obsolete nuclear facilities, increase the importance of this legacy and even give it priority in social terms.

Section 1, on generic problems of the nuclear legacy in urbanized areas, describes the nuclear legacy in the urban environment as having mainly been created by nuclear facilities built in the past, such as experimental nuclear reactors in research, testing, and educational centers constructed between the 1940s and 1970s. These centers were largely in the vicinity of big cities but now are within the city limits. After decades of operation the research reactors at the nuclear centers have produced millions of Curies of radioactivity in spent nuclear fuel and radioactive waste. As the spent fuel is, in many cases, non-standard, it cannot be reprocessed by the usual technologies and even requires special storage conditions. As a result, this spent nuclear fuel is often stored at the nuclear center site itself, that is, in the host city.

An additional input to this legacy is the radioactive waste generated during the operation of the research reactors, their decommissioning, etc. The radioactive

waste was often placed in “temporary” storage at the nuclear center sites. The radiation protection norms at the time these were created were not always as strict as they are now and also, in many cases, they were not even properly implemented, either because of the nuclear arms race or just through negligence.

Such nuclear facilities are not only a source of radioactive waste, often stored under inadequate conditions at the site, but they also create dangerous targets as they have no protection against plane crashes or missile attacks. Recent terrorist attacks on the Russia, Spain, the United Kingdom, and the United States highlight the risk posed by urban facilities that contain radioactive waste or spent nuclear fuel that may be targeted in future attacks. This topic is the focus of increased attention from the nuclear scientific community.

The report analyzes world statistics concerning nuclear research reactors and concludes that 60% of these are more than 30 years old. Furthermore, many are in, or rapidly approaching, crisis conditions. It states that there is a lack of interest in decommissioning by political decision makers that often results in passive decommissioning strategies and, in the longer term, various safety concerns.

The former practice of building nuclear centers in or near to large cities can be easily traced around the world (Berlin, Budapest, Grenoble, London, Paris, San Diego, Sofia, etc.). However, the Moscow case seems to be, to some extent, extraordinary, because of the rush nuclear program that started in Moscow after the nuclear bombing of Hiroshima to gain nuclear parity with the United States.

Section 3, on the Moscow case study of the nuclear legacy, compiles and generalizes the results of the Moscow case study carried out by IIASA and the Central European University in cooperation with three Russian institutions: the Federal Agency for Atomic Energy, the Russian Academy of Sciences, and the Russian Research Center-Kurchatov Institute.

Analysis of the statistics of nuclear facilities in Moscow and the Moscow Region shows that priority should be given to the nuclear legacy at RRC-KI because of the amount of radioactivity that has accumulated at the site and because of its proximity to the densely populated areas of downtown Moscow. Data on the nuclear facilities of RRC-KI responsible for this nuclear legacy show that the stores of spent nuclear fuel now contain over 1,300 spent fuel assemblies of various designs with a total radioactivity of about 2 MCi.

The spent fuel at RRC-KI differs in terms of its chemical composition, its degree of uranium enrichment, and its protective cladding. As for this type of nuclear legacy in general (see above), in many cases it cannot be reprocessed by standard technology and requires special storage conditions. Another important feature is that a high fraction of the experimental fuel elements were damaged during testing, which also means that this fuel cannot be reprocessed at the existing reprocessing plants in Russia.

Non-standard spent nuclear fuel constitutes 60% of the total amount at RRC-KI, of which 10% has varying degrees of damage. The time necessary to transport the spent nuclear fuel from RRC-KI to the Urals or Krasnoyarsk Mining and Chemical Combine is estimated as not less than 7 years, all conditions being favorable, which is questionable.

Another important component of the nuclear legacy at RRC-KI is the radioactive waste placed in temporary storage. Most of the waste was stored in the 1950s and 1960s without due attention to the possible environmental consequences. This has resulted in contamination of the surface layer of the site and the groundwater.

Living close to such a “neighbor” inevitably causes concern for Moscow inhabitants and visitors about the environmental security of their situation. Indeed:

1. The closest residential building area is only about 100 m from the radioactive waste storage site.
2. The area between the inner wall of the storage site and the nearest section of the outer wall (see *Figure 3.16*) is occupied by a municipal car park. Though access to this is limited to people who use the area to park their cars, public access to the area is not really restricted..
3. The municipal road along the outer wall of RRC-KI passes at a distance of several meters. At peak times up to 3,000 vehicles per hour use this road.

The report includes the results of the collection, analysis, and collation of currently available data regarding the radioactive source term at the disposal area for the radioactive waste within the main boundaries of RRC-KI. It also gives the environmental characteristics and human patterns necessary for modeling radionuclide migration within and out of the site.

Analysis of the environmental and radiological characteristics of the site shows that these data are far from being comprehensive. This reflects the real situation, as:

- Data from the early years of the site are incomplete and inconsistent;
- Insufficient experimental studies have been undertaken to explore the site characteristics that have to be used in this study;
- The recently begun site-rehabilitation program has introduced further uncertainties into the input data regarding surface contamination.

The basis of the information on surface contamination at the storage site applied in the study is the gamma radiation survey of the site surface made in 10 m steps to a distance of 1–1.5 m from the surface. This provided the exposure dose rates, which typically vary from 30 $\mu\text{R/h}$ to 3000 $\mu\text{R/h}$, and at some places are even higher than 3000 $\mu\text{R/h}$.

The maps of surface contamination by ^{137}Cs and ^{90}Sr were created by recalculating the exposure dose rates under the supposition of a 15 cm surface soil layer that is homogeneously contaminated. The recalculation procedure was based on the following:

- The actual measurements of the exposure dose rate at nine points on the site were compared with the exposure dose rates calculated from the measurement of ^{137}Cs concentrations in samples taken from those nine points. This comparison showed reasonable agreement with the supposition that the exposure dose rate is mainly caused by ^{137}Cs contamination at the surface layer.
- The average ratio between ^{137}Cs and ^{90}Sr concentration measured in seven samples taken from different parts of the site. This ratio was used to create a ^{90}Sr contamination map.

Though these statistics are not sufficient for a very heterogeneously contaminated site, they may still serve as a first approximation.

Another uncertain parameter is the soil hydraulic conductivity, for which the range of values now available is extremely wide. These data, however, are based on different methodologies: laboratory sample testing, field study of water pumping from observation wells, rate of restoration of a created depression zone, etc. No cross-comparison of these results was possible because of the limited information available on the details of the measurements. After careful discussion of this uncertainty, it was decided to use an expert judgment that the site soil covered by grass is similar to the so-called urbanosem type of soil.

In these circumstances, the run-off model was oriented toward a scoping analysis rather than a site-specific analysis. The scoping analysis focused on an evaluation of the scale of and possible limits to the redistribution and washout phenomenon and thus provided a first insight into the seriousness of run-off transfer; it recommended that further experimental studies were needed to reduce the uncertainties. Consequently, the study, while hopefully scientifically rigorous, was based more upon consequence analysis and general principles than on exact site-specific features.

As the run-off model was, in essence, a scoping analysis, we did not analyze which criteria are best for evaluating the risk or whether the dose rate limit currently fixed in the official legislative and/or normative documents is likely to change in the future. Instead, we chose the simplest approach: comparison with the current official dose rate limit. The data on radionuclide contamination obtained and presented in the report allow specialists to recalculate the risk in other terms, if they wish.

Uncertainty in the dose calculation is predominantly caused by uncertainties in the run-off erosion calculation. The run-off model LISEM used in the study is a physically based simulation model. However, of course, it applies some empirical

relationships to describe the physical processes that underlie it. The literature we refer to agrees that the LISEM discharge estimate is within 15% of that observed and that, in assessing the final results, it is the uncertainties in the input parameters that are the most significant. Hence, we intentionally give the results of modeling 16 different scenarios, which include variations of the major parameters within their uncertainty, evaluated through expert discussion. These 16 scenarios provide, in effect, an approximate sensitivity analysis and give a feel for the range in the variation of the output data. Therefore, the maximum calculated dose should be considered as an upper limit obtained within the scoping analysis. In other words, this shows that the approach intentionally overstates both exposure and dose.

Despite all the limitations introduced in modeling the potential implications of the run-off transfer of radioactivity from the RRC-KI waste storage site, the analysis indicates that the potential run-off transfer of radioactivity cannot be ignored because:

- Given the current condition of the inner wall around the storage site, which acts as a physical barrier to the path of the run-off water, and given the lack of any specific drainage system at the site, the site topography does not prevent run-off washout from the site.
- The model results show that under unfavorable meteorological conditions (periods of lengthy drizzle followed by a downpour of the maximum intensity observed in Moscow), run-off water could transfer contaminated soil particles outside the perimeter of the storage site and further down to the municipal car park located between the inner wall of the storage site and the adjacent section of the outer wall of RRC-KI. This would result in surface contamination of dozens of kBq/m².
- Though such radioactivity washout will not significantly increase the dose uptake by critical population groups, even in the most conservative scenario (up to 20% of the established dose limit), the increase in background radiation outside the RRC-KI boundaries may cause public anxiety, especially if washed-out radioactivity reaches the city street.
- Last, but not least, is the potential redistribution of soil contaminants within the storage site (about 100 m² could incur contamination twice that in existence before the run-off event). This should be taken into account when planning a site-rehabilitation program.

Thus, modeling the run-off transfer of radioactivity at the RRC-KI radioactive waste storage site shows that the way radioactive waste was managed in the past at nuclear centers in urban environments could result in radioactivity being washed out from the boundaries of the site now and in the future. Though, in this particular case, the natural events causing run-off, such as average or heavy rain, are unlikely

to substantially reduce environmental security, the potential run-off transfer outside the storage site could create a constant and growing concern for people living in nearby residential areas.

An outcome of this study is the recommendation that the role of the gradual accumulation of radionuclides through repeated wash-off events over a long period of time should be evaluated. This point could be of specific importance in planning a remediation program, as it is hardly possible and even less reasonable to remediate to a “zero” level of contamination. Thus, an acceptable level of residual contamination that should provide no “substantial” release from the site for a long period of time (say, hundreds of years) should be examined and defined.

Moreover, other contaminated areas that are part of RRC-KI but were not identified by the Russian partner for this study, like the enclave located on the bank of the Moscow River, deserve attention and analysis. Thus:

- Our first recommendation is to extend run-off studies to evaluate the cumulative, long-term consequences of run-off transfer from sites with residual contamination.
- Next, in order to reduce the uncertainty caused by incomplete knowledge of the source term and environmental characteristics, further experiments are advised to enable site-specific modeling.
- This study focused on the run-off caused by natural events, but beneath the storage site is a complicated network of different pipelines, including a municipal rainwater pipe that transmits rainwater accumulated from an area of about 400 ha. Hence, in addition to the modeling performed, the effects of possible infrastructure failures, such as heavy run-off from a failure of the rainwater pipe and consequent site flooding are worthy of a special study.
- As the background radiation in the areas adjacent to the storage site for the RRC-KI radioactive waste can be noticeably elevated by run-off events, these areas need to be under systematic dosimetric control.
- Besides natural run-off events, there are several pathways of radionuclide migration from the radioactive waste storage site to the city areas, namely, migration within groundwater, direct resuspension of dust from the site, and air transfer by strong winds. The contribution of these processes to the exposure of critical groups of inhabitants should be a subject for further analysis. This is particularly important because of the remediation measures that have already started at the site, which include excavation of the contaminated soil and its separation into fractions of different contamination levels. Such operations necessitate further study without delay.

The results of such an assessment make it possible to identify potential counter-measures, and their cost, and to minimize the radiological impact on the population and personnel involved in the remediation and/or stabilization of the site.

As for specific recommendations to reduce the potential run-off washout, the following points should be considered:

- First of all, the RRC-KI radioactive waste storage site should have a special drainage system designed to intercept and control run-off waters at the site.
- Should repair work of the inner wall around the storage site be deemed necessary, it is recommended that this be carried out during the winter months.
- A number of potential engineering methods to reduce the run-off transfer from the storage site should be evaluated carefully and choices made as to the optimum method or methods of achieving this. As an example we list below what is more or less obvious:
 - Compaction of the soil, for which there are a number of technical possibilities, to reduce the erosion rate;
 - Chemical stabilization, perhaps with cement and polymers, to keep the soil particles in place;
 - Reduction of the amount of precipitation that falls on the storage site using a cloud-seeding technique.¹
- The need to use international experience to solve problems caused by radioactive contamination is self-evident.

As for the social aspects of the problem, one of the first efforts recommended for coping with this situation is to set up “round table” meetings to improve the exchange of views between the RRC-KI administration and social groups living near RRC-KI. These meetings should also include communication with international experts as well as discussion of up-to-date information regarding the situation and of the solutions being used in other countries where contamination caused by activities at nuclear complexes in the urban environment has occurred. Such comparisons could help to identify common issues and differences in coping with the radiation

¹There are reservations in some publications about the reproducibility of this technique and its effectiveness in controlling rainfall, and the idea that it could work on a small area is even more questionable. However, we know at least two events in which cloud-seeding techniques were successfully used to reduce the amount of precipitation: in 1980 during the Olympic Games in Russia and in 1997 during the 850th anniversary of the founding of Moscow. In both cases cloud seeding forced precipitation outside the perimeter of the city of Moscow and provided good weather in the city. In principle, if necessary, the technique could be applied to an expanded area that includes the radioactive waste site and its environs.

legacy in large cities and to work out recommendations for future improvements. Timely and deeper attention to these aspects is recommended.

The report concludes that countries with similar problems of a nuclear legacy in the urban environment could benefit from sharing their experience and cooperating in this field.

Appendix: Initial Code for the Radionuclide Redistribution Model in PCRast Modeling Language

Example of Cs-137 redistribution

```
#####  
# Cs-137 REDISTRIBUTION MODEL Version 2.0A  
#  
# Version 19 July 2001  
#  
# by M. van der Perk,  
# Utrecht Centre for Environment and Landscape Dynamics - UCEL, Faculty of  
# Geographical Sciences, Utrecht University, Netherlands.  
# e-mail: m.vanderperk@geog.uu.nl  
#  
# and  
#  
# O. Slávik, VUJE Trnava a.s., Slovakia.  
# e-mail: slavik@vuje.sk  
#  
#  
# Runoff and Sediment transport model based on LISEM 5.1  
# original LISEM script by A.P.J. de Roo, V.G. Jetten, and B. Iversen  
# modified by M. van der Perk,  
# extended by a Cs-137 interaction and transport module by O. Slávik and M. van der  
# Perk  
#  
# MODEL FEATURES  
#  
#  
# Model calculates Cs-137 transport through a landscape based on sediment transport.  
# It accounts for soil detachment by splash erosion and flow detachment and  
# Deposition from overland flow. The Cs-137 module requires a Cs-137 soil  
# contamination map (Bq/m2).  
# Using a standardized depth distribution (negative exponential or part of Cs-137  
# equally distributed over top soil layer), the Cs-137 activity concentration of the  
# active topsoil layer is calculated. The dissolved Cs-137 activity concentration in  
# the runoff water (rainfall - interception) is calculated from the Cs-137 activity  
# concentration in the active layer of the top soil using a Kd distribution  
# coefficient and the suspended sediment concentration. The particulate Cs-137  
# activity concentration is also calculated using a distribution coefficient. It is  
# assumed that the equilibrium between Cs-137 in top soil, water and suspended  
# sediment is reached instantaneously. Subsequently, the water and sediment is mixed  
# with water and sediment from upstream cells.  
#####  
  
binding  
  
#*****  
#***** input maps *****  
#*****  
  
# drainage basin morphology maps  
RainGauge=id.map; # area covered by raingauges  
LDD=ldd.map; # LDD map
```

```

Gradient=grad.map;           # slope gradient
OutFlowPoints=outlet.map;    # Boolean map with outflow points
RoadWidth=roadwidt.map;     # width of roads

# soil and landuse maps;
LAI=lai.map;                 # leaf area index
VegetatFraction=per.map;     # fraction of soil covered by vegetation
RandomRoughness=rr.map;     # random roughness of the soil surface
CropHeight=ch.map;          # vegetation height
AggregateStab=aggrstab.map; # aggregate stability
SoilCohesion=coh.map;        # cohesion of bare soil
SoilAddCohesion=cohadd.map;  # additional cohesion by vegetation roots
N=n.map;                     # Manning's n for the soil surface
D50=d50.map;                 # d50 value of the soil
StoneFraction=stonefrc.map;  # fraction of soil covered by stones
WheelWidth=wheelwid.map;    # width of wheeltracks

# channel maps
ChannelGradient=changrad.map; # channel slope gradient
ChannelN=chanman.map;        # Manning's n for the channel
ChannelCohesion=chancoh.map;  # cohesion of the channel bed
ChannelWidth=chanwidt.map;   # width of channel

# infiltration maps
# 1 layer Green/AmpT

Ksat1=ksat1.map;            # saturated hydraulic conductivity
ThetaS1=thetas1.map;        # saturated volumetric soil moisture content
ThetaT1=thetait1.map;       # Initial volumetric soil moisture content
PSI1=psil.map;              # Soil water tension at the wetting front
SoilDepth1=soildepl.map;    # Soil depth of first layer (mm)

# Radiocaesium maps
Csinit=Csinit.map;          # Soil contamination by Cs-137 (Bq/m2)

#*****
#***** input timeseries *****
#*****

RainTSS=pre.tss;            # timeseries with rainintensity (mm/hour)

#*****
#***** constant *****
#*****

Fcumini=0;                  # initial cumulative infiltration
Beta=0.6;                   # kinematic wave parameter for sheet flow
Vmax=2.0;                   # maximum flow velocity (m/s) for
                             # transportcapacity calculation
CriticalStreamPower=0.4;    # critical unit stream power, in cm/s! = 0.4,
                             # according to Govers, 1990
SplashDelivery=0.1;         # splash delivery ratio determines the fraction
                             # of splash detachment on non-ponded sites that
                             # enters the overland flow (0-1)
DT=2;                       # duration of timestep (s)
F=0.92;                     # factor to limit the transport to F*cell length
                             # per time step

# Radiocaesium parameters

ActiveLayer=5.0;            # Thickness of active top soil layer of
                             # interaction between runoff water and top soil
                             # (mm)
BulkDens=1300;              # bulk density of the soil and top soil (kg/m3)
Porosity=0.4;               # porosity of the top soil (active layer) (-)

```

```

Mo=0.8; # Median coefficient (cm/sqrt(year)) for
# calculation of depth distribution
Ti=20; # days after deposition for calculation of depth
# distribution
Ploughed=boolean(0); # value does not matter if ploughed is 'true'
# soil ploughed (1) or not ploughed (0) after
# initial deposition
PloughDepth=0.25; # ploughing depth (m)
PartPlough=0.9; # part of Cs-137 that is in the plough layer if
# CsSoil = CsMax (areal maximum -Perk teraz
# vypnute)if CsSoil is below CSAverage then all
# Caesium is assumed to be in the plough layer
# the part of Cs-137 is scaled between the
# average CsSoil (part=1)and CsMax

(part=PartPlough)
Kdb=1; # equilibrium distribution coefficient CsWater
# and CsSoil (m3/kg)
Kds=3.0; # equilibrium distribution coefficient CsWater
# and CsSuspMat (m3/kg)

#*****
#***** reported maps *****
#*****

Erosion=eros.map; # reported map for produced
# erosion (tons/ha)
Deposition=dep.map; # reported map for produced
# deposition (tons/ha)

#*****
#***** reported timeseries *****
#*****

DischargeTSS=dischar.tss; # reported timeseries with discharge at
# basin outlet and suboutlets (l/s)
SedDischargeTSS=seddisch.tss; # report timeseries with Qsedout at
# basin outlet and suboutlets (kg/s)
Arrows=errorw.tss; # reported timeseries with water mass balance
error (%)
ErrorSTSS=errors.tss; # reported timeseries with sediment mass balance
error (%)
ErrorCTSS=errorc.tss; # reported timeseries with Cs-137 mass balance
error (%)
SedConcTSS=sedconc.tss; # reported timeseries with sediment
concentration (mg/l)
CsWConcTSS=Cswconc.tss; # reported timeseries with soluble Cs-137 act
concentration (Bq/l)
CsSConcTSS=Cssconc.tss; # reported timeseries with particulate Cs-137
act concentration(Bq/l)
CsTotConcTSS=Cstotcon.tss; # reported timeseries with total Cs-137 activity
concentration (Bq/l)
CsWDischTSS=Cswdisch.tss; # reported timeseries with soluble Cs-137
activity discharge (Bq/s)
CsSDischTSS=Cssdisch.tss; # reported timeseries with particulate Cs-137
act discharge (Bq/s)
CsTotDischTSS=Cstotdis.tss; # reported timeseries with total Cs-137 activity
discharge (Bq/s)

areamap
area.map;

timer
1 4300 1;
reportdefault = 200,600,900,1500,4000,5000,7200,12500..endtime;
# reportdefault = 20+20..1000,1001+1..1019,1020+20..endtime;

```

```

initial

# calculation of celllength (m)
DX =celllength();
DXL=max(downstreamdist(LDD),DX);

# width of stone surface (m)
StoneWidth=(DX-RoadWidth-WheelWidth)*StoneFraction;

# channel width
ChannelWidth = cover(ChannelWidth,0);

# map with outflow point 1 (basin outlet)
# remaining part of the map becomes 0
OutFlowPoint1= if(OutFlowPoints eq 1, scalar(1),0);

# map with outflow point 2 (suboutlet 1)
# remaining part of the map becomes MV
OutFlowPoint2= if(OutFlowPoints eq 2, scalar(1));

# map with outflow point 3 (suboutlet 2)
# remaining part of the map becomes MV
OutFlowPoint3= if(OutFlowPoints eq 3, scalar(1));

# replaces pixels of zero inclination by a standard low value
# (if not division by zero!)
Gradient=max(if(cover(ChannelGradient,0) gt 0,ChannelGradient, Gradient), 0.005);

*****
*****                W A T E R                *****
*****

# maximum interception (mm), Van Hoyningen-Huene (1981), p.46
InterceptionWHmax=0.935+(0.498*LAI)-(0.00575*sqr(LAI));

# maximum storage in micro-depressions (Onstad, 1984) (mm)
# cannot be less than 0
IsolatedWHmax=max(10*(0.112*RandomRoughness+0.031*sqr(RandomRoughness)
-0.012*RandomRoughness*(Gradient*100)),0);

# net rainfall needed to fill all micro-depressions (Onstad, 1984) (mm)
# cannot be less than 0
IsolatedWHrain=max(10*(0.329*RandomRoughness+0.073*sqr(RandomRoughness)
-0.018*RandomRoughness*(Gradient*100)),0);

# threshold net rainfall after which runoff starts (mm)
# runoff starts before all micro-depressions are filled
PotentialWHstart=max(IsolatedWHrain*(0.0527*RandomRoughness
-0.0049*(Gradient*100)),0);

# maximum fraction of surface covered with water (Onstad, 1984)
# is assumed not to be less than 0.10, lower values give mass balance error
# for steep slopes!
WaterFractionmax=max(0.152*RandomRoughness-0.008*sqr(RandomRoughness)-0.008
*RandomRoughness*(Gradient*100),0.10);

# initial accumulated rainfall (mm)
RainWHaccum = 0;

# initial actual fraction of surface covered with water
# needed her because used in infiltration
WaterFraction=0;

# initial total rainfall in total catchment area (m3)
RainVolttotal=0;

# initial stage of total interception in total catchment area (m3)

```

```

InterceptionVolttotal=0;

# initial stage of total accumulated infiltration (m3)
InfilVolttotal=0;

# initial surface water storage (m3)
IsolatedWH=0.;

#initial total catchment runoff
CatchmentRunoffVol=0;

# Constant factor in calculation of Alpha (Manning's equation)
AlphaFact = (if(cover(ChannelN,0) gt 0.001,ChannelN, N)/(sqrt(Gradient)))**Beta;

# Constant power of Alpha (Manning's equation)
AlphaPower = (2/3)*Beta;

# Initial waterheight (mm)
WH=0.00;

# Initial volume of water (m3)
Volold=0;
Vol=0;

# initial discharge (m3/s)
Qout=1e-9;
Qoutold=1e-9;

# Intitial flow velocity (m/s)
V=1e-7;

#####
##### initial conditions related to Green/Ampt#####
#####

# conversion of Ksat and SoilDepth to cm/h and cm
Ksat1=Ksat1/10;
SoilDepth1=SoilDepth1/10;

# cumulative infiltration in mm
Fcum=Fcumini;

#####
##### S E D I M E N T #####
#####

# total cohesion of soil (kPa)
SoilCohesionsTotal=if(cover(ChannelCohesion,0) gt
0,ChannelCohesion,SoilCohesion+SoilAddCohesion);

# Y is the flow detachment efficiency coefficient
# Ugmin = 1.0 cm/s (Rauws & Govers, 1988)
# Ugcrit = 0.89+0.56*(COH+COHADD)
# SoilCohesion is the soil cohesion (kPa),
# which is 9.806*Torvane value (kg/cm2)
# SoilAddCohesion is the extra cohesion provided by plant roots
# enter high cohesion values (9999) for non-erodible surfaces
# thus, Y becomes 0
Y=if(SoilCohesionsTotal<100,1/(0.89+0.56*SoilCohesionsTotal),0);
Y=min(Y,1);

#enter high ChannelCohesion (9999) for non-erodible surfaces
ChannelY=if(ChannelCohesion lt 100,1/(0.89+0.56*ChannelCohesion),0);
ChannelY=min(ChannelY,1);

Y = cover(ChannelY,Y);

```

```

# settling velocity of sediment at 20 C (m/s)
# 2650 = particle density kgm-3
# 1000 = density of water kgm-3
# 9.80 = acceleration of gravity
# 0.001 = viscosity of water
# Settling Velocity = 0.00080903 m/s for D50 = 30 mu at 20 C
# (Stokes' Law) from "Soil Physics" (Marshall & Holmes, '79; p.24/5)
SettlingVelocity=2*(2650-1000)*9.80*sqr(D50/2000000)/(9*0.001);

#experimentally derived coefficient
#depending on D50 (Govers, 1990; EUROSEM, 1992)
#CSS fit from EUROSEM manual data: r2=0.9979
#CGovers and DGOVERS are calculated from D50, and thus now spatial
CGovers=0.015061+exp(-2.33860-0.014059*D50);

#experimentally derived coefficient
#depending on D50 (Govers, 1990; EUROSEM, 1992)
#CSS fit from EUROSEM manual data: r2=0.979
DGovers=log10(2.431200+0.027716*D50);

# initial TransportCapacity
TransportCapacity = scalar(0);

# initial Sediment Concentration (kg/m3)
SedConc = scalar(0.00001);

#initial amount of sediment flow transport (kg/s) and storage (kg)
Sedflux=0;
Sedst=0;
Sedin=0;
Sedout=0;

# initial total erosion in catchment (kg)
Eros=0;

# initial total deposition in catchment (kg)
Dep=0;

# initial soil loss from catchment (kg)
CatchmentSoilLoss=0;

# initial transported sediment (kg)
SedTrtotal=0;

# initial total rainfall detachment (kg)
RainfallDetachmenttotal=0;

# initial stage of total flow detachment (kg)
FlowDetachmenttotal=0;

#*****
#*****          C s - 1 3 7          *****
#*****
CsSoil=Csinit;
Toter=0;
#Calculation of Initial Cs activity concentration in active layer (Bq/kg)

#1. Not ploughed soil
MedianDepth=10*Mo*sqr(Ti/365); #mm
B=ln(2)/MedianDepth;
CsTopSoil=CsSoil*(1-exp(-B*ActiveLayer))/BulkDens/(ActiveLayer/1000);
C_bgInit= B*Csinit*exp(-B*(ActiveLayer+Toter));
report Cbgini=C_bgInit;

#2. Ploughed soil
CsAverage=areaaverage(CsSoil,nominal(area.map));

```

```

CsMax=mapmaximum(CsSoil);
TopSoilFactor=1;
#TopSoilFactor=if(CsSoil le CsAverage,1,PartPlough+(1-PartPlough)*
# ((CsMax-CsSoil)/(CsMax-CsAverage)));
report CsTopSoil=if(Ploughed,TopSoilFactor*CsSoil/BulkDens/PloughDepth,CsTopSoil);
C_bs=CsTopSoil;
Cbs=C_bs;
C_bg=if(not Ploughed,C_bgInit,Cbs);
TotDep=0;
Actdep=0;
CsSuspMat=CsTopSoil;
CsWater=0;
Csst=0;
Cwst=0;
Csup=0;
CsTotalInit=maptotal(CsSoil*sqr(DX));
CatchmentCsLoss=0;
CsCatchmentLoss=0;
CsCatchmentLossQ=0;
CatchmentSoilLossQ=0;
CsWloss=0;
dynamic

```

```

#*****
#*****          W A T E R          *****
#*****

```

```

#*****
#***** rainfall & interception *****
#*****

```

```

# rainfall intensity (mm/h)
RainIntensity=timeinputscalar(RainTSS,RainGauge);

```

```

# amount of rainfall in each time interval (mm)
RainWH=RainIntensity*DT/3600;

```

```

# amount of rainfall in each time interval (m3)
RainVol=RainWH*DX*DX/1000;
RainVoltotal+=maptotal(RainVol);

```

```

# total rainfall amount in a point (mm)
RainWHaccum+=RainWH;

```

```

# amount of interception in each time interval (mm)
# according to Aston (1979), based on Merriam (1960/1973)
#  $0.046 * LAI = k = (1-p) \Leftrightarrow p = 1 - 0.046 * LAI$ 
# the cumulative interception at time = t-1 is subtracted
# from the cum. interception at time = t (RainWHaccum)
# note: LAI is not a pixel average, but the average for VegetatFraction!
InterceptionWH=VegetatFraction*(InterceptionWHmax*(exp(-(0.046*LAI)*
(RainWHaccum-RainWH)/InterceptionWHmax)-exp(-(0.046*LAI)*
RainWHaccum/InterceptionWHmax)));

```

```

# no interception on roads and channels
InterceptionWH = if (ChannelWidth != 0, 0, InterceptionWH);

```

```

# total interception (m3)
InterceptionVol = InterceptionWH*(DX-RoadWidth)* DX/1000;
InterceptionVoltotal+=maptotal(InterceptionVol);

```

```

# Waterheight after rainfall and Interception (mm)
WH = WH + RainWH - InterceptionWH*(1-RoadWidth/DX);

```

```

#*****
#***** infiltration *****
#*****

```

```

# depth of wetting front (cm)
# Fcum in mm, but needed in cm, therefore division by 10!
L1=if(ThetaI1 lt ThetaS1, (Fcum/10)/(ThetaS1-ThetaI1), SoilDepth1);

# (cm)
# ADR/VJ: included water height at the surface as positive pressure
Delta=(ThetaS1-ThetaI1)*(PSI1+WH/10);

#DeltaF is maximum infiltration in cm (from Li 1978: Modeling of Rivers)
#maximize is to obtain only the positive root: the negative root
#has no physical significance
DeltaF=max(-(2*Fcum/10-Ksat1*DT/3600)/2+((2*Fcum/10-Ksat1*DT/3600)**2
+8*Ksat1*(DT/3600)*(Delta+Fcum/10))**(0.5)/2,0);

# infiltration (mm) per time interval
# maximum infiltration is equal to WH
# no infiltration into stones, roads, and channels

FiltSize = if(ChannelWidth != 0,0, min(WH,DeltaF*10)*(DX-StoneWidth-RoadWidth)/DX);

# if wetting front depth is equal to the soil depth,
# infiltration is zero --> saturation overland flow
FiltSize = if(L1 lt SoilDepth1,FiltSize,0);

# Accumulated infiltration (mm)
Fcum+=FiltSize;

# Amount of infiltration (m3)
InfilVol = FiltSize*(DX-StoneWidth-RoadWidth)*DX/1000;
InfilVoltotal+=maptotal(InfilVol);

# Waterheight after infiltration
WH = max(WH-FiltSize*(DX-StoneWidth-RoadWidth)/DX,0);

#####
##### surface storage in micro-depressions #####
#####

# potential surface runoff (mm)
# equal to the sum of all water minus the storage in depressions
# WH is the available amount of water (mm)
# PotentialWHstart is the net amount of water needed
# for starting overland flow (mm)
# IsolatedWHrain is the total amount of net rainfall needed
# to fill all depressions (mm)
# IsolatedWHmax is the maximum amount of depression storage (mm)
# between PotentialWHstart and IsolatedWHrain
# a linear relationship is assumed

IsolatedWHold = IsolatedWH;

PotentialWHin=if(WH gt (PotentialWHstart) and ((IsolatedWHrain
-PotentialWHstart)*(IsolatedWHrain-IsolatedWHmax)) gt 0,
((WH-PotentialWHstart)/(IsolatedWHrain-PotentialWHstart)
*(IsolatedWHrain-IsolatedWHmax),0);
PotentialWHin=if(WH gt (IsolatedWHrain),(WH-IsolatedWHmax),PotentialWHin);

# isolated water storage in micro-depressions (mm)
IsolatedWH=max(WH-PotentialWHin,0);

# no isolated water in channels
IsolatedWH=if(ChannelWidth != 0,0,IsolatedWH);

# amount of water in isolated depressions (m3)
SurfaceStorageVol=(IsolatedWH-IsolatedWHold)*DX*(DX-RoadWidth)/1000;
SurfaceStorageVoltotal=maptotal(IsolatedWH*DX*(DX-RoadWidth)/1000);
Surfst =SurfaceStorageVol;

```

```

# width of overlandflow (m)
FlowWidth=if(WH gt 1e-9,DX*max((WH-IsolatedWH)/WH,0),0);
FlowWidth=if(ChannelWidth gt 0,ChannelWidth,FlowWidth);

# Waterheight after surface storage (mm)
WH = max(WH-IsolatedWH*(1-RoadWidth/DX),0);

#####
##### kinematic wave calculation for overland flow #####
#####

# calculation of alpha parameter from
# Manning's equation (Chow, 1988, p. 288)
Alpha=AlphaFact*((max(FlowWidth,DX/100)+2*WH/1000)**AlphaPower);

# additional runoff input from rainfall minus interception and surface storage
Voladd = RainVol-InterceptionVol-InfilVol-SurfaceStorageVol;
Qadd = Voladd/DT/DXL;

# numerical solution for kinematic wave for cell outflow (m3/s) and water level (mm)
report Qout = kinematic(LDD,Qout,Qadd,Alpha,Beta,DT,DXL);
WH = if(FlowWidth gt 0.0001,1000*(Alpha*(Qout**Beta))/FlowWidth,0);

# Volume of water in each cell (m3)
Vol=(Alpha*(Qout**Beta))*DX;

# flow velocity (m/s)
Vreal=if (Vol gt 1e-8 and WH gt 1e-7, Qout/(FlowWidth*WH/1000),0); #m/s
V=max(min(Vreal,Vmax),0);

#####
##### S E D I M E N T #####
#####

# volumetric transport capacity of sediment
# from overland flow (cm3 soil)/(cm3 water)
# V is flow rate in m/s; formula requires cm/s, thus factor 100
# condition Gradient*V*100>CriticalStreamPower
# is to prevent not allowed operation
TransportCapacity=if(Gradient*V*100 gt CriticalStreamPower,CGovers
*(Gradient*V*100-CriticalStreamPower)**(DGovers),0);

TransportCapacity=if(Vol gt 1e-8,TransportCapacity,0);
TransportCapacity=min(TransportCapacity,0.32);
TransportCapacity=TransportCapacity*2650;
# 2650 is the particle density in kg/m3
# the unit of TransportCapacity is now in kg/m3

# report TrCap=TransportCapacity;

#####
# Intermediate sediment calculation #
#####

# Sediment (kg) current input from upstream cells and output to downstream cells
Sedout=if(Vol gt 1e-8,if(Vreal*DT lt
F*DX,SedConc*Qout*DT,SedConc*(F*DX/DT)*FlowWidth*(WH/1000)*DT),0);
Sedin=upstream(LDD,Sedout);
# New sediment concentration in cell and upstream cell (kg/m3)
SedConc=if(Vol gt 1e-8,Sedst/Vol,0);

#####
##### Splash detachment #####
#####

```

```

# calculation of kinetic energy

# LeafDrainageKin is the kinetic energy from leaf drainage (J/m2/mm)
# CropHeight is the effective height of the plant canopy (m)
# cannot be less than 0
LeafDrainageKin=max(15.8*sqrt(CropHeight)-5.87,0);

# DirectThroughfallKin is the kinetic energy
# from direct throughfall (J/m2/mm)
# RainIntensity is the rainfall intensity (mm/h)
# cannot be less than 0
# prevent the case when RainIntensity equals 0: 10log(0)!!
DirectThroughfallKin=if(RainIntensity>0,max(8.95+8.44
    *log10(RainIntensity),0),0);

# splash detachment

# splash is calculated separately for ponded and non ponded areas;
# the Aggregate Stability map should contain 0 or negative values!
# /1000 is to go from grams per timestep to kg per timestep
# from Kin = 0 to Kin = 10 the relationship is linear!,
# based on field experiments
# these formulas are from EUROSEM, but modified and calibrated
# for the Limburg soils
# NO SPLASH ON STONE COVERED SOILS

# water height factor
WH0=exp(-1.48*WH);

# wet splash area (m2)
SplashArea=(WheelWidth+WaterFraction*DX)*DX/1000;

# direct rainfall on soil (mm)
RainDirectWH=RainWH*(1-VegetatFraction);

# factor 0.6 = stemflow 40% !
# this corresponds to an leaf to ground surface angle of 36.87 degrees
# the effect of leaf drainage is negligible when CropHeight<0.15 m.
# InterceptionWH is already taking VegetatFraction into account
ThroughfallWH=(RainWH*VegetatFraction-InterceptionWH)*0.6;

# 1) splash detachment on ponded areas from direct rainfall
DirectThroughfallDetach=if(DirectThroughfallKin gt 10 and AggregateStab gt 0,
    (2.82/AggregateStab*DirectThroughfallKin*WH0
    +2.96)*RainDirectWH*SplashArea,
    DirectThroughfallKin/10*(2.82/AggregateStab
    *10*WH0+2.96)*RainDirectWH*SplashArea);

DirectThroughfallDetach=if(DirectThroughfallKin gt 10 and AggregateStab le 0,
(0.1033/SoilCohesion*DirectThroughfallKin*WH0+3.58)*RainDirectWH*SplashArea,
    DirectThroughfallDetach);

DirectThroughfallDetach=if(DirectThroughfallKin le 10 and AggregateStab le 0,
DirectThroughfallKin/10*(0.1033/SoilCohesion*10*WH0+3.58)*RainDirectWH*SplashArea,
    DirectThroughfallDetach);

# 2) splash detachment on ponded areas from leaf drainage
LeafDrainageDetach=if(LeafDrainageKin gt 10 and AggregateStab gt 0,
    (2.82/AggregateStab*LeafDrainageKin*WH0+2.96)
    *ThroughfallWH*SplashArea,LeafDrainageKin/10
    *(2.82/AggregateStab*10*WH0+2.96)*ThroughfallWH
    *SplashArea);

LeafDrainageDetach=if(LeafDrainageKin gt 10 and AggregateStab le 0,
    (0.1033/SoilCohesion*LeafDrainageKin*WH0+3.58)
    *ThroughfallWH*SplashArea,LeafDrainageDetach);

```

```

LeafDrainageDetach=if(LeafDrainageKin le 10 and AggregateStab le 0,
    LeafDrainageKin/10*(0.1033/SoilCohesion*10*WH0+3.58)
    *ThroughfallWH*SplashArea,LeafDrainageDetach);

# the types of splash detachment are added
RainfallDetachment=DirectThroughfallDetach+LeafDrainageDetach;

# 3) splash detachment on non-ponded areas from direct rainfall: WH0 = 1
# dry area
SplashArea=(1-WaterFraction)*DX*DX/1000;

DirectThroughfallDetach=if(DirectThroughfallKin gt 10 and AggregateStab
    gt 0,(2.82/AggregateStab*DirectThroughfallKin+2.96)
    *RainDirectWH*SplashArea,DirectThroughfallKin/10
    *(2.82/AggregateStab*10+2.96)*RainDirectWH
    *SplashArea);

DirectThroughfallDetach=if(DirectThroughfallKin gt 10 and AggregateStab
    le 0,(0.1033/SoilCohesion*DirectThroughfallKin
    +3.58)*RainDirectWH*SplashArea,
    DirectThroughfallDetach);

DirectThroughfallDetach=if(DirectThroughfallKin le 10 and AggregateStab
    le 0,DirectThroughfallKin/10*(0.1033/SoilCohesion
    *10+3.58)*RainDirectWH*SplashArea,
    DirectThroughfallDetach);

# 4) splash detachment on non-ponded areas from leaf drainage: WH0 = 1

LeafDrainageDetach=if(LeafDrainageKin gt 10 and AggregateStab gt 0,
    (2.82/AggregateStab*LeafDrainageKin+2.96)*ThroughfallWH
    *SplashArea,LeafDrainageKin/10*(2.82/AggregateStab*10
    +2.96)*ThroughfallWH*SplashArea);

LeafDrainageDetach=if(LeafDrainageKin gt 10 and AggregateStab le 0,
    (0.1033/SoilCohesion*LeafDrainageKin+3.58)*ThroughfallWH
    *SplashArea,LeafDrainageDetach);

LeafDrainageDetach=if(LeafDrainageKin le 10 and AggregateStab le 0,
    LeafDrainageKin/10*(0.1033/SoilCohesion*10+3.58)
    *ThroughfallWH*SplashArea,LeafDrainageDetach);

# the types of splash detachment are added (kg)
RainfallDetachment+=SplashDelivery*(DirectThroughfallDetach
    +LeafDrainageDetach);
RainfallDetachment=if(Vol gt 1e-8,RainfallDetachment,0);

# report rainadd=RainfallDetachment;

#####
# Intermediate sediment calculation #
#####

# Additional Sediment (kg) input from detachment
Sedadd=RainfallDetachment;

# Sediment concentration (kg/m3)
SedConc=if(Vol gt 1e-8,max(Sedst+Sedin-Sedout+Sedadd,0)/Vol,0);

#####
#***** Flow detachment *****
#*****

# overland flow detachment

```

```

# settling velocity concept according to Stokes' Law and D50 dependent!
# SettlingVelocity*DT is max. distance travelled and is compared with WH/1000
# Old script linear: SettlingVelocityFactor=if(Vol gt 1e-
8,SettlingVelocity*DT/(WH/1000),1);

SettlingVelocityFactor=if(Vol gt 1e-8 and WH gt 1e-7,1-exp(-
DT*SettlingVelocity/(WH/1000)),1);
SettlingVelocityFactor=max(min(SettlingVelocityFactor,1),0);
# report SetF=SettlingVelocityFactor;

# roadwidthfactor: no flow detachment on roads
RoadWidthFactor=if(FlowWidth gt 0,1-RoadWidth/DX,0);

# detachment by overland flow (kg)
# cannot be larger than the remaining transport capacity
# corrected for roads
FlowDetachment=if(TransportCapacity gt SedConc and Vol gt 1e-8,
Y*(TransportCapacity-
SedConc)*Vol*SettlingVelocityFactor*RoadWidthFactor,0);
# report flowadd = FlowDetachment;

#####
# Intermediate sediment calculation #
#####

# Additional Sediment (kg) input from detachment
Sedadd=RainfallDetachment+FlowDetachment;

# Sediment concentration (kg/m3)
SedConc=if(Vol gt 1e-8,max(Sedst+Sedin-Sedout+Sedadd,0)/Vol,0);

#####
#***** Deposition from overland flow (kg) *****
#####

# (positive = supply to the flow; negative = deposition)
# deposition cannot be larger than the amount of available sediment
FlowDeposition=if(TransportCapacity lt SedConc,(TransportCapacity-
SedConc)*Vol*SettlingVelocityFactor,0);
FlowDeposition=if(Vol gt 1e-8,max(FlowDeposition,-Sedst),-Sedst);
# report flowdep = FlowDeposition;

#####
#***** Mass balance for sediment and Cs-137 *****
#####

E_b=if(FlowWidth gt 0.00001,1000*max(RainfallDetachment+FlowDetachment,0)/
BulkDens/DX/FlowWidth,1e-8); #erosion (mm)
#tu sa porovnavaj s Actdep z predchadz kroku
Totero=if(E_b gt Actdep, Totero+(E_b-Actdep),Totero);
C_bgInit=if(not Ploughed,B*Csinit*exp(-B*(ActiveLayer+Totero)),CsTopSoil);

# Cs-137 activity concentration in eroded soil layer
C_bg=if(Vol gt 1e-8 and E_b gt Actdep+.005 and not Ploughed,
(Cbs*Actdep/1000*BulkDens+ Csinit*exp(-B*(ActiveLayer+Totero))*
(1-exp(min(-B*(E_b-Actdep),0))))/(BulkDens*(E_b/1000)),
if(Vol lt 1e-8 and not Ploughed and Actdep lt ActiveLayer/100, C_bg, C_bs
));

#For avoiding dividing by small E_b
report C_bg=if(E_b lt ActiveLayer/100 and Actdep lt ActiveLayer/100,C_bgInit,
if(E_b gt ActiveLayer/100,C_bg, Cbs) );

# updating of active soil layer(C_bs)(Bq/kg) after leaching and topsoil mixing
interaction
report C_bs=(Cbs*ActiveLayer+ C_bg*E_b) / (ActiveLayer+E_b)/

```

```

      ( 1+ (Voladd/sqr(DX)*1000)/(Kdb*(ActiveLayer+E_b)*BulkDens) );

C_w=if(Vol gt 1e-8 and SedConc gt 1e-
8,C_bs/Kdb*(1+Kdb*SedConc)/(1+Kds*SedConc),C_bs/Kds);
report C_s=C_w*Kds;

D_b=if(FlowWidth gt 0, 1000*(-FlowDeposition)/BulkDens/DX/FlowWidth,0);
Actdep=max(0,Actdep-E_b)+ D_b; # #Actdep- celk hrubka sa o eroziu E_b
znizi -vid dalej

Totdep=Totdep+D_b;

#Sedadd=RainfallDetachment+FlowDetachment;
# Cs-137 activity concentration suspended solids (Bq) by mixing sediment sources
CsSuspMat=if(Vol gt 1e-8 and SedConc gt 1e-9,((Sedst-Sedout)* CsSuspMat+ Sedin*Csup+
Sedadd*C_bs)/(Sedst-Sedout+Sedin+Sedadd),CsSuspMat);#C_s

#Protection, CsSuspMat can be maximally equal to xKds/Kdb
#CsSuspMat=if(CsSuspMat gt CsTopSoil*Kds/Kdb,CsTopSoil*Kds/Kdb,CsSuspMat);
# Cs-137 activity concentration in sediment
report CsSS=CsSuspMat; #Bq/kg

CsWater=CsSuspMat/Kds;

#Cs-137 activity concentration in water (Bq/m3) by mixing water sources
#Voladd=RainVol-InterceptionVol-InfilVol;
#Volout=if(Vol gt 1e-8,if(Vreal*DT lt
F*DX,Qout*DT,(F*DX/DT)*FlowWidth*(WH/1000)*DT),0);
#Volin=upstream(LDD,Volout);
#Cswadd=Voladd*C_w;
#Cswout=if(Vol gt 1e-8,if(Vreal*DT lt
#F*DX,CsWater*Qout*DT,CsWater*(F*DX/DT)*FlowWidth*(WH/1000)*DT),0);
#Cswin=upstream(LDD,Cswout);
#CsWater=if(Vol gt 1e-8 and (Volold+Volin-Volout+Voladd) gt 1e-8,
# max(Cwst+Cswin-Cswout+Cswadd,0)/(Volold+Volin-Volout+Voladd),0);

report CsWflux=if(Vreal*DT lt F*DX,CsWater*Qout,CsWater*(F*DX/DT)*FlowWidth*WH/1000);
#Bq/s

# Additional Sediment (kg) and Cs-137 (Bq) input from detachment minus deposition
Sedadd=RainfallDetachment+FlowDetachment+FlowDeposition;

# Sediment concentration (kg/m3)
report SedConc=if(Vol gt 1e-8,max(Sedst+Sedin-Sedout+Sedadd,0)/Vol,0);

# Sediment in small water volumes is deposited
RestDeposition=SedConc*Vol-max(Sedst+Sedin-Sedout+Sedadd,0);

# Update Cs-137 concentration in soil layer (Bq/m2) after erosion and deposition
CsSoil=if(Vol gt 1e-8, max(CsSoil- (C_bs*(RainfallDetachment+FlowDetachment)+
C_bs/Kdb*Voladd + CsSuspMat*(FlowDeposition+RestDeposition)) /sqr(DX),0 ),
CsSoil);

#update of C_bs in top soil after deposition:
report Cbs= (C_bs*ActiveLayer+ CsSuspMat*D_b)/(ActiveLayer+ D_b);
report Cs_soil=CsSoil;
#report delC_bs =C_bs-Cbs;
#report delCSS= CsSS-C_bs;

CsConc=CsSuspMat*SedConc;
report CsSflux=if(Vreal*DT lt F*DX,CsConc*Qout,CsConc*(F*DX/DT)*FlowWidth*WH/1000);
#Bq/s
report CsConc+=CsWater; #Bq/m3

report Csflux=if(Vreal*DT lt F*DX,CsConc*Qout,CsConc*(F*DX/DT)*FlowWidth*WH/1000);
#Bq/s
# Sediment mass balance (kg)
Sedst=SedConc*Vol;

```

```

report Sedflux=if(Vreal*DT lt
F*DX,SedConc*Qout,SedConc*(F*DX/DT)*FlowWidth*WH/1000); #kg/s
Csst=C SuspMat*Sedst;
Cwst=C sWater*Vol;
# Cs-137 activity concentration on suspended sediment in upstream cells
Csup=if(Vol gt 1e-8 and upstream(LDD,Sedst) gt 1e-8,
upstream(LDD, Csst)/upstream(LDD,Sedst),0);
Volold=Vol;

#####
##### calculate totals & output #####
#####

# W A T E R

# report timeseries with total water discharge at basin outlet and suboutlets (l/s)
report DischargeTSS=timeoutput(nominal(OutFlowPoints),Qout*1000);

# water mass balance error (%)
CatchmentRunoffVol+=maptotal(if(boolean(OutFlowPoint1),Qout,0))*DT;
RunoffVolttotal=maptotal(Vol);
ErrorW=if(RainVolttotal gt 0,100*(RainVolttotal-InterceptionVolttotal-InfilVolttotal-
SurfaceStorageVolttotal-CatchmentRunoffVol-RunoffVolttotal)/RainVolttotal,0);
report ErrorWTSS=timeoutput(boolean(OutFlowPoint1),ErrorW);
report WatLoss.tss=CatchmentRunoffVol;#integral outflow from catchmnet, m3

# S E D I M E N T

# total erosion in catchment after last timestep
# conversion to tons/ha
Cf=sqr(100)/sqr(DX)/1000;
report Eros+=(RainfallDetachment+FlowDetachment)*Cf;
# total deposition in catchment after last timestep
# conversion to tons/ha
report Dep+=(FlowDeposition+RestDeposition)*Cf;

# sediment mass balance error (%)

CatchmentSoilLossQ+=maptotal(if(boolean(OutFlowPoint1),SedConc*Qout,0))*DT;#kg/catchme
nt
report SedlosQ.tss=CatchmentSoilLossQ; #time integral of sedConc*Qout from catchmnet,
kg/cat

CatchmentSoilLoss+=maptotal(if(boolean(OutFlowPoint1),Sedflux,0))*DT*Cf;
report SedlossF.tss=CatchmentSoilLoss; #time integral of sediment flux from
catchmnet, t/ha

SedTrtotal=maptotal(Sedst)*Cf;
ErrorS=if(maptotal(Eros) gt 0, 100*(maptotal(Eros)+maptotal(Dep)-
CatchmentSoilLoss-SedTrtotal)/maptotal(Eros),0);
report ErrorSTSS=timeoutput(boolean(OutFlowPoint1),ErrorS);

# report timeseries with total sediment load at basin outlet and suboutlets (kg/s)
report SedDischargeTSS=timeoutput(nominal(OutFlowPoints),SedConc*Qout);

# report timeseries with sediment concentration basin outlet and suboutlets (kg/m3)
report SedConcTSS=timeoutput(nominal(OutFlowPoints),SedConc);

# C s - 1 3 7

# report timeseries with soluble Cs-137 activity concentration (Bq/m3) at basin
outlet and suboutlets
report CsWConcTSS=timeoutput(nominal(OutFlowPoints),CsWater);
CsWloss+=maptotal(if(boolean(OutFlowPoint1),CsWater*Qout,0))*DT;#Bq
report CsWloss.tss=CsWloss;#integral Bq from catchmnet
# report timeseries with particulate Cs-137 activity concentration (Bq/kg) at basin
outlet and suboutlets

```

```

#report CsSConcTSS=timeoutput(nominal(OutFlowPoints),CsSuspMat);

# report timeseries with total Cs-137 activity concentration (Bq/m3) at basin outlet
and suboutlets
report CsTotConcTSS=timeoutput(nominal(OutFlowPoints),CsConc);
# report timeseries with soluble Cs-137 activity discharge (Bq/s) at basin outlet and
suboutlets
report CsWDischTSS=timeoutput(nominal(OutFlowPoints),CsWater*Qout);

# report timeseries with particulate Cs-137 activity discharge (Bq/s) at basin outlet
and suboutlets
#report CsSDischTSS=timeoutput(nominal(OutFlowPoints),CsSuspMat*SedConc*Qout);

# report timeseries with total Cs-137 activity discharge (Bq/s) at basin outlet and
suboutlets
report CsTotDischTSS=timeoutput(nominal(OutFlowPoints),CsConc*Qout);#Bq/s

CsCatchmentLossQ+=maptotal(if(boolean(OutFlowPoint1),CsConc*Qout,0))*DT;#Bq
report Cstotlos.tss =CsCatchmentLossQ;#integral Bq from catchmnet

# Cs-137 mass balance error (%)
CatchmentCsLoss+=maptotal(if(boolean(OutFlowPoint1),Csflux,0))*DT; #Bq

CsTotal=maptotal(CsSoil*sqr(DX)+Csst+Cwst); #Bq
ErrorCs=100* ((CsTotal+CatchmentCsLoss)/CsTotalInit -1);

#report CsFlloss.tss= CatchmentCsLoss;#time integral of Csflux from catchm Bq
report ErrorCTSS=timeoutput(boolean(OutFlowPoint1),ErrorCs);
# ratio of transported Cs 137 from catchment
report TraperCs.tss=100*CatchmentCsLoss/CsTotalInit;
report CsSorat.tss =100*maptotal(CsSoil*sqr(DX))/CsTotalInit;
#report CsRWrat.tss =100*maptotal(Csst+Cwst)/CsTotalInit;

```

References

- Amaev A., Ambartsumjan R., Goncharov V., *et al.* (1966), Tests and study of an experimental assembly of rods with cores from sintered uranium dioxide in claddings from the zirconium alloy, which has reached maximal burning out of 68000 MW day per t of U. Preprint, IAE-1181, M. Moscow: Kurchatov Institute.
- Bonniwell E. (1999), Determining times and distances of particle transit in a mountain stream using fallout radionuclides, *Geomorphology*, **27**, 75–92.
- Borohovich A., Bavrin V., Kuznetcova T., and Shishkin G. (1999), About radioecology of the Kurchatov Institute, *News of Academy of Industrial Ecology*, No. 2, page 107. Moscow: Kurchatov Institute.
- BOSS International, Inc. (2001) *Stormshed: Urban Hydrology Modelling*, Software Manual and Tutorial. London: BOSS International, Inc. and Engenious Systems.
- Botterweg P., Leek R., Romstad E., and Vatn A. (1998), The EUROSEM-GRIDSEM modeling system for erosion analyses under different natural and economic conditions, *Ecological Modeling*, **108**, 115–129.
- Chibowski S. and Mitura A. (1995), Studies of the rate of migration of radiocesium in some types of soil of Eastern Poland, *Science of the Total Environment*, **170**, 193–198.
- Eckerman K. and Leggett R. (1996), DCFPAK: Dose coefficient data file package for Sandia National Laboratory, Oak Ridge National Laboratory Report ORNL/TM-13347. Oak Ridge, TN: Oak Ridge National Laboratory.
- Egorov N., Novikov V., Parker F., and Popov V. (Eds.) (2000), *Radiation Legacy of the Soviet Nuclear Complex*, London: Earthscan Publications, pp. 236
- Energoatomizdat (1984), *Safety In Nuclear Power Engineering. Part 1. General conditions of safety of NPPs. Methods for calculating the dispersion of radioactivity from NPP and exposure of local population.* Appendixes. Normative-Technical Document 38.220.56-84, Vol. 1. Moscow: Energoatomizdat.
- Energoatomizdat (2002), *Methodical Maintenance of the Radiating Control at Enterprises*, Vol. 2, page 26. Moscow: Energoatomizdat.
- FAO/IAEA (2001), *Co-ordinated Research Project Assessment of Soil Erosion through the Use of Cs¹³⁷ and Related Techniques as a Basis for Soil Conservation, Sustainable Agricultural Production and Environmental Protection.* Final Report of the FAO/IAEA Co-ordinated Research Project. Vienna: FAO/IAEA.
- Ferguson C. and Potter W. (2003), *The Four Faces of Nuclear Terrorism.* Monterey: Center for Nonproliferation Studies, pp. 374.
- Garger E., Hoffman F., Thiessen K., *et al.* (1999), Test of existing mathematical models for atmospheric resuspension of radionuclides, *Journal of Environmental Radioactivity*, **42**, 157–175.

- Gavrilov V., Klepicova N., Troyanova N., and Rodean H. (1995), Stationary model for resuspension of radionuclides and assessment of Cs¹³⁷ concentration in the near-surface layer for the contaminated areas in the Bryansk Region of Russia and Belarus, *Atmospheric Environment*, **29**, No. 19, 2633–2650.
- Goncharov V., Rjazantsev E., Nikolaev J., *et al.* (1965), Creation of research reactor MP for tests fuel on rods and materials, *Proceedings of the of Third International Conferences on Peaceful Uses of Atomic Energy*, Geneva, Vol. 7, p. 314. Moscow: Fizmatgiz.
- Goncharov V. (1986), *Research Reactors*, Moscow: Nauka [in Russian].
- Gorlinsky Yu. (2003), *Data for Modeling Surface Transfer of Radionuclides: Summary Material*. Moscow: RRC-KI.
- Goscomecology (1999), *Guidebook for Evaluation of Permissible Levels of Radioactivity Releases in the Atmosphere*. Moscow: Minatom of Russian Federation.
- GSPI (2002), *Report on Boring and Equipping of Observational Holes in the Area Adjacent to the Territory of Aged Burial Sites*. No GSPI 215-0-IGF35. Moscow: GSPI.
- Gusev N., Kovalev E., Osanov D., and Popov V. (1961), *Protection from Radiation of Extended Sources*. Moscow: Gosatomizdat.
- Hessel R., Jetten V., and Zhang G. (2003a), Estimating Manning's N for steep slopes, *Catena*, **54**, 77–91.
- Hessel R., Jetten V., Baoyuan L., Yan Z., and Stolte J. (2003b), Calibration of the LISEM model for a small loess plateau catchment, *Catena*, **54**, 235–254.
- Hessel R., Messing I., Liding C., Ritsema C., and Stolte J. (2003c), Soil erosion simulations of land use scenarios for a small loess plateau catchment, *Catena*, **54**, 289–302.
- Hollander W. and Gargerl E. (1996), *Contamination of Surfaces by Resuspended Material*, Report of the European Commission, EUR 16527 EN, pp. 3–10. Brussels: European Commission.
- IAEA (1996). *International Basic Safety Standards for Protection against Ionizing Radiation and for the Safety of Radiation Sources*, IAEA, Safety Series No. 115. Vienna: International Atomic Energy Agency.
- IAEA Database (2004), World research reactors. See <http://www.iaea.org/worlddata>.
- ICRP (1996a), *Conversion Coefficients for Use in Radiological Protection against External Radiation*, ICRP Publication 74. Annals of the ICRP, Vol. 26/3. Oxford: Pergamon Press.
- ICRP (1996b), *Age-Dependent Doses to Members of the Public From Intake of Radionuclides: Part 5. Compilation Of Ingestion And Inhalation Dose Coefficients*, ICRP Publication 72, Annals of the ICRP, Vol. 26/1. Oxford: Pergamon Press.
- IIASA (1996), *Mayak Case Study*, Final Report of IAEA to DoE on Subcontract #4603510 (DE-AC03-76SF00098 – DoE, USA), September, 1996. Vienna: International Institute for Applied Systems Analysis.
- Jakubov H. (1999), *Condition of Green Plantations in Moscow, According to Monitoring Data in 1998: State Report*. Moscow: Prima Press, pp. 216.
- Jetten V. (2002), *Limburg Soil Erosion Model (LISEM)*, Manual. Utrecht: Utrecht Center for Environment and Landscape Dynamics.

- Karssenber D., Wesseling C., and van Deursen W. (2003), *PCRaster Version 2, Manual*. Utrecht, Utrecht University, pp. 380.
- Kiiva, S. and Zheleznyak M. (1999), *Spatial Redistribution of Radionuclides within Catchments: Development of GIS-based Models for Decision Support Systems*. Report for EU Inco-Copernicus Program, Project SPARTACUS. Kiev: Institute Of Mathematical Machines and Systems Problems.
- Kikoin I., Dmitrievsky V., Grigoriev I., *et al.* (1958), Gas core experimental nuclear reactor, *Atomnaya Energia*, **5**, No. 3, 294–300.
- Klik A., ed. (1998), Experiences with soil erosion models, *Proceedings of International Workshop on Soil Erosion*. Vienna: Institute of Hydraulics and Rural Water Management.
- Kosson D., Novikov V., and Parker F. (2004), *Proceedings of Workshop on Urban Radiological Security*. CD-Rom, published 2006. Nashville: Vanderbilt University.
- Kruzhilin, G. (1955), A reactor for physical and technical research, *Proceedings of the First International Conference On Peaceful Uses of Atomic Energy*, Geneva, Vol. 2, pp. 507–522. Moscow: Fizmatgiz.
- Kurchatov I., Goncharov V., Gurevich I., *et al.* (1955), Reactor for physical and engineering research, *Nuclear Energy*, Selected Works Series, Vol. 3, pp. 110–141. Moscow: Nauka.
- Laverov N., Omel'janenko B., and Velichkin V. (1994), Geologic aspects of the problem of burial of radioactive waste, *Geoecology*, Vol. 6., 3–20.
- Liu G., Xu M., and Ritsema C. (2003), Study of soil surface characteristics in a small watershed in the Hilly, gullied area on the Chinese loess plateau, *Catena*, **54**, No 1, 31–44.
- Makhonko K. (1992), Resuspension of radioactive dust from underlying surface, *Atomnaya Energia*, **72**, No. 5, 523–531.
- Moiseev A. and Ivanov V. (1990), *Handbook on Dosimetry and Radiation Hygiene*. Moscow: Energoatomizdat.
- Monte L. (1995), Evaluation of radionuclide transfer functions from drainage basins of fresh water systems, *Journal of Environmental Radioactivity*, **26**, 71–82.
- Morgan R., Quinton J., Smith R., *et al.* (1998) *The European Soil Erosion Model (EUROSEM)*, Documentation and User Guide. Silsoe: Cranfield University.
- Moscow Center for Hydrometeorology and Monitoring (2002), *V.A. Mihel'son Observatory*, Federal Service of Russia for Hydrometeorology and Monitoring of the Environment. Moscow: Moscow Centre on Hydrometeorology and Monitoring.
- Moscow Fund (2001), *Social Passport of the Region of Schukino*. Moscow: Moscow Fund of Development of Parliamentary and Social Information.
- Mosinzhprouekt Institute (1986), *Underground Communications on the Site of the Kurchatov Institute*, Order No 12628G/S. Moscow: Mosinzhprouekt Institute.
- Nickholson, K. (1988), A review of particle resuspension, *Atmospheric Environment*, **22**, 2639–2651.
- Novikov, V., Ignatjev V., Fedulov V., and Cherednikov V. (1990), *Molten Salt Nuclear Energy System: Prospects and Problems*, Moscow: Energoatomizdat, pp. 191.

- Novikov V., Parker F., Ponomarev-Stepnoy N., Ryazantsev E., and Gorlinsky Yu. (2003), Generic problems of the nuclear legacy in urbanized areas of megacities and the particularities of the Moscow case. *Proceedings of the International Conference on Safety of Mega Cities: Problems, Solutions, International Experience*, October 7–9, 2003, Moscow, Russia. CD-Rom published 2006.
- OCRWMA (2000), *Evaluate Soil/Radionuclide Removal by Erosion and Leaching*, Internal Report, Office of Civilian Radioactive Waste Management Analysis. Washington DC: US Department of Energy.
- Pan Ziqiang, Wang Zhibo, Chen Zhuzhou, Zhang Yongxing, and Xie Jianlun (1996), Radiological environmental impact assessment for the nuclear industry in China, *Health Physics*, **71**, No. 6, 847–862.
- Panin A. (2001), The role of soil erosion and fluvial processes in the post-fallout redistribution of Chernobyl-derived caesium-137: A case study of the Lapki catchment, Central Russia, *Geomorphology*, **40**, 185–204.
- Petrov E., Zabud'ko A., and Sadohin I. (1999), Results of all-round radiological investigation of personal subsidiary small-holdings in the polluted regions of Kaluga, *News of the Academy of Industrial Ecology*, **2**, 112–120.
- Ponomarev-Stepnoy N. and Gorlinsky Yu. (2004), The radiation legacy of the Kurchatov Institute: problems and solutions, *Proceedings of the Workshop on Urban Radiological Security* (Vanderbilt University, Nashville, November 14–16). Published as CD-Rom in 2006.
- Ponomarev-Stepnoy N. and Kukharkin N. (2000), The Reactor Converter Romashka, *Atomic Energy*, **88**, No. 3, 176–183.
- Ponomarev-Stepnoy N. Rjazantsev E., and Gorlinsky J. (2002a), *Radiation Legacy of the First Soviet Nuclear Center—Kurchatov Institute: How significant Are the Problems and What Is Necessary for a Decision?* Report at Session of Contact Experts Group, IIASA. Vienna: International Institute for Applied Systems Analysis.
- Ponomarev-Stepnoy N., Volkov V., Kukharkin N., *et al.* (2002b), *Rehabilitation of Radioactively Contaminated Objects and the Territory of RRC-KI*. Report at the 28th International Symposium on Radwaste Management (WM'02). CD-Rom. Tucson: University of Arizona.
- Radon (1999), *Manual for Ascertaining Admissible Releases of Radioactive Substances into the Atmosphere*. DV-98. Moscow: Radon.
- Roo A. and Jetten V. (1999), Calibrating and validating the LISEM model for two data sets from The Netherlands and South Africa, *Catena*, **37**, 477–493.
- Ryazantsev E., Koljadin V., Egorenkov P. *et al.* (1999a), Decommissioning nuclear and radioactive dangerous objects (NRDO) at RRC-KI, *Atomic Energy*, **87**, No. 3, 180–189.
- Ryazantsev E., Egorenkov P., Kolyadin V., *et al.* (1999b), The first results of the research reactor MR decommissioning. *Proceedings of the International Symposium on Research Reactor Utilization, Safety and Management, Lisbon, Portugal*. IAEA., SM-360-39P, p. 177–179. Vienna; International Atomic Energy Agency.

- Ryazantsev E., Kolyadin V., Bylkin B., Zverkov Yu., and Kuznetsova T. (2000), *On the Problems of Safety of Nuclear Installations in Big Cities*, Preprint, RRC-KI – 6184/7. Moscow: Russian Research Center – Kurchatov Institute.
- Schnoor J. (1996), *Environmental Modelling: Fate and Transport of Pollutants in Water, Air, and Soil*. Chichester: Wiley & Sons.
- Sehmel G. (1980), Particle resuspension: a review, *Atmospheric Environment*, **4**, 107–127.
- Slavik O. (2000), *Modelling of ^{137}Cs Interaction in Overland Flow after Chernobyl Accident Deposition*, Report for Spartacus Project. Trnava: VÚJE Trnava, Inc. (Engineering, Design and Research Organization).
- Stroganova M., Myagkova A., and Gubankov A. (2000), *Ecological Atlas of Moscow*. Moscow: ABF.
- Strauss P., Konecny F., and Zach S. (2001), *Raingen 1.0 Manual. A System for Generating Internal Rainfall Structure of Rainfall Events*. Petzenkirchen: Institute for Land and Water Management. Federal Agency for Water Management, and Vienna: Institute for Soil Science, University for Agricultural Sciences.
- Takken L., Beuselinck L., Nachtergaele J., Govers G., Poesen J., and Degraer G. (1999), Spatial evaluation of a physically-based distributed erosion model, LISEM, *Catena*, **37**, 431–447.
- Theocharopoulos S. (2003), Soil erosion and deposition rates in a cultivated catchment area in Central Greece, estimated using the ^{137}Cs technique, *Soil and Tillage Research*, **69**, 153–162.
- Thibault D., Sheppard M., and Smith P. (1990), *A Critical Compilation and Review of Default Solid/Liquid Partition Coefficients, K_d , for Use in Environmental Assessments*. AECL-10125. Pinawa: Whiteshell Nuclear Research Establishment.
- Till J. and Meyer H. (1983), *Radiological Assessment. A Textbook On Environmental Dose Analysis*. Washington DC: US Government Printing Office.
- US Department of Energy (1997), *Linking Legacies – Connecting the Cold War Nuclear Weapons Production Processes to their Environmental Consequences*. Office of Environmental Management, DOE/EM-0319, pp 227.
- van der Perk M. (2000), *Spatial Redistribution of Radionuclides within Catchments: Development of GIS-Based Models for Decision Support Systems*, Spartacus Project, Final Report. Utrecht: Utrecht University.
- Walling D., He Q., and Whelan P. (2003), Using ^{137}Cs measurements to validate the application of the AGNPS and ANSWERS erosion and sediment yield models in two small Devon catchments, *Soil and Tillage Research*, **69**, 27–43.
- Warner Sir F. and Harrison R. (1993), *Radioecology after Chernobyl: Biogeochemical pathways of artificial radionuclides, Scope 50*. Chichester: Wiley & Sons.



International Institute for Applied Systems Analysis
Schlossplatz 1, A-2361 Laxenburg, Austria
Tel: +43 2236 807 Fax: +43 2236 71313
www.iiasa.ac.at

The Nuclear Legacy in Urbanized Areas

Editor: Vladimir Novikov

RR-07-001

ISBN 978-3-7045-0146-2